Anomalies and Tensions in Cosmological Data: Challenges and Insights

September 9th 2024
The Dark Side of the Universe - DSU2024
Corfu

Eleonora Di Valentino
Royal Society Dorothy Hodgkin Research Fellow
School of Mathematics and Statistics
University of Sheffield (UK)

University of Sheffield

THE ROYAL SOCIETY

The ΛCDM model

The Lambda Cold Dark Matter (ΛCDM) model
has been chosen as the standard cosmological model due to its simplicity
and its ability to accurately describe a wide range of observations.
However, it has theoretical limitations and relies on three main components which are inferred from observations rather than theoretical principles or laboratory experiments:

- Inflation is modeled by a slow-rolling scalar field.
- Dark matter is considered cold, pressureless, and interacts only through gravity
- Dark energy is represented by the cosmological constant.

Despite accurately describing observed phenomena,
ΛCDM is based on six parameters and lacks deep-rooted physical principles,
making it an approximation of an unknown underlying theory.

Increasingly precise observations are expected to reveal deviations from ΛCDM.
Indeed, discrepancies such as the value of the Hubble constant (H0) have emerged,
suggesting possible flaws in the model.

These persistent tensions may indicate that new physics is needed to explain these observational shortcomings, potentially signaling the failure of the ΛCDM model.

H0 tension

The most statistically significant tension is the disagreement in the Hubble constant.

The Planck estimate assuming a “vanilla" ΛCDM cosmological model:
$H0 = 67.36 \pm 0.54$ km/s/Mpc
Planck 2018, Astron.Astrophys. 641 (2020) A6

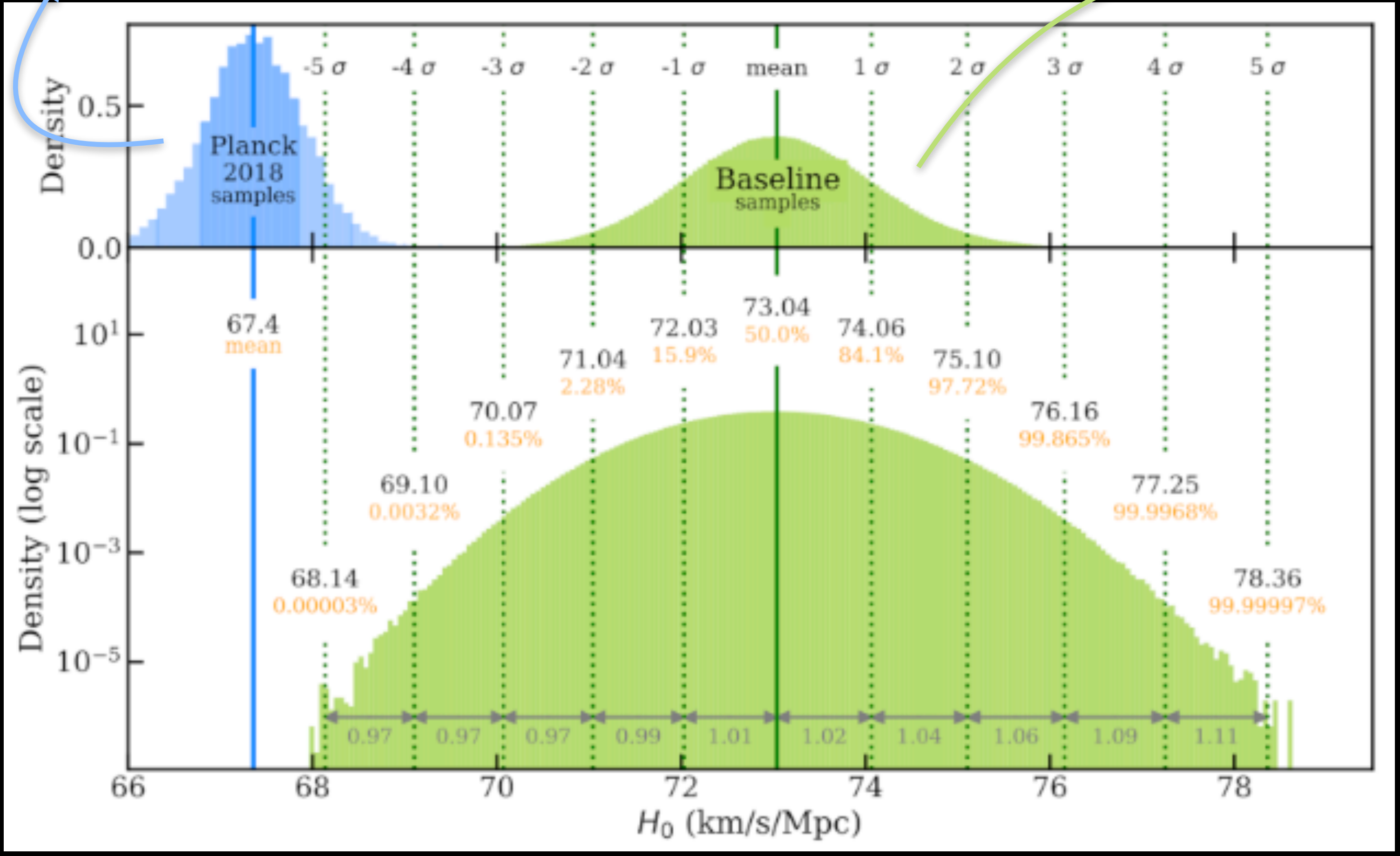

The latest local measurements obtained by the SH0ES collaboration

$H0 = 73.04 \pm 1.04$ km/s/Mpc

Riess et al. arXiv:*2112.04510*

5σ = one in 3.5 million implausible to reconcile the two by chance

The Planck estimate assuming a “vanilla" ΛCDM cosmological model:

H0 = 67.36 ± 0.54 km/s/Mpc

Planck 2018, Astron.Astrophys. 641 (2020) A6

Distance Ladder

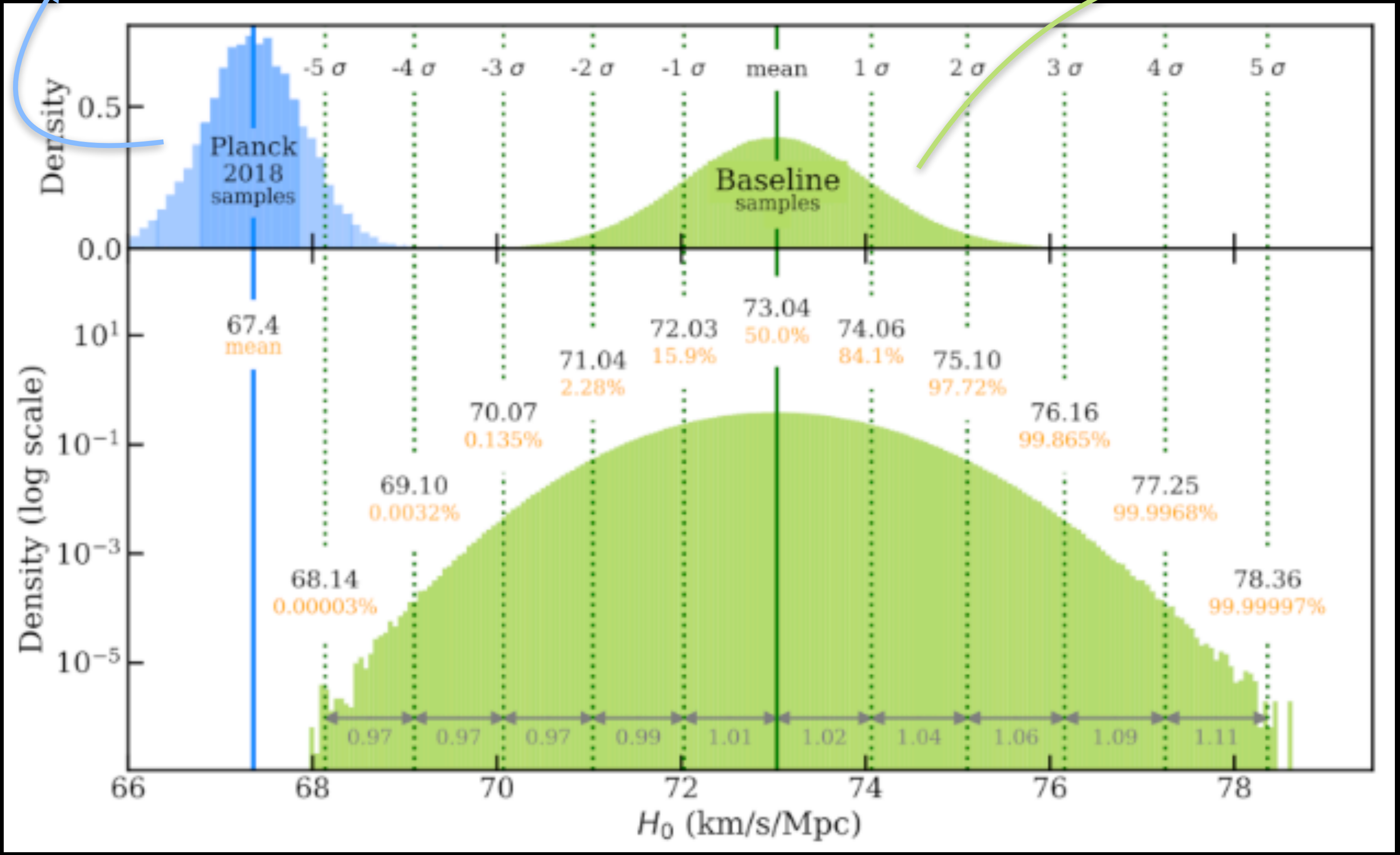

The latest local measurements obtained by the SH0ES collaboration

H0 = 73.04 ± 1.04 km/s/Mpc

Riess et al. arXiv:*2112.04510*

Distance Ladder

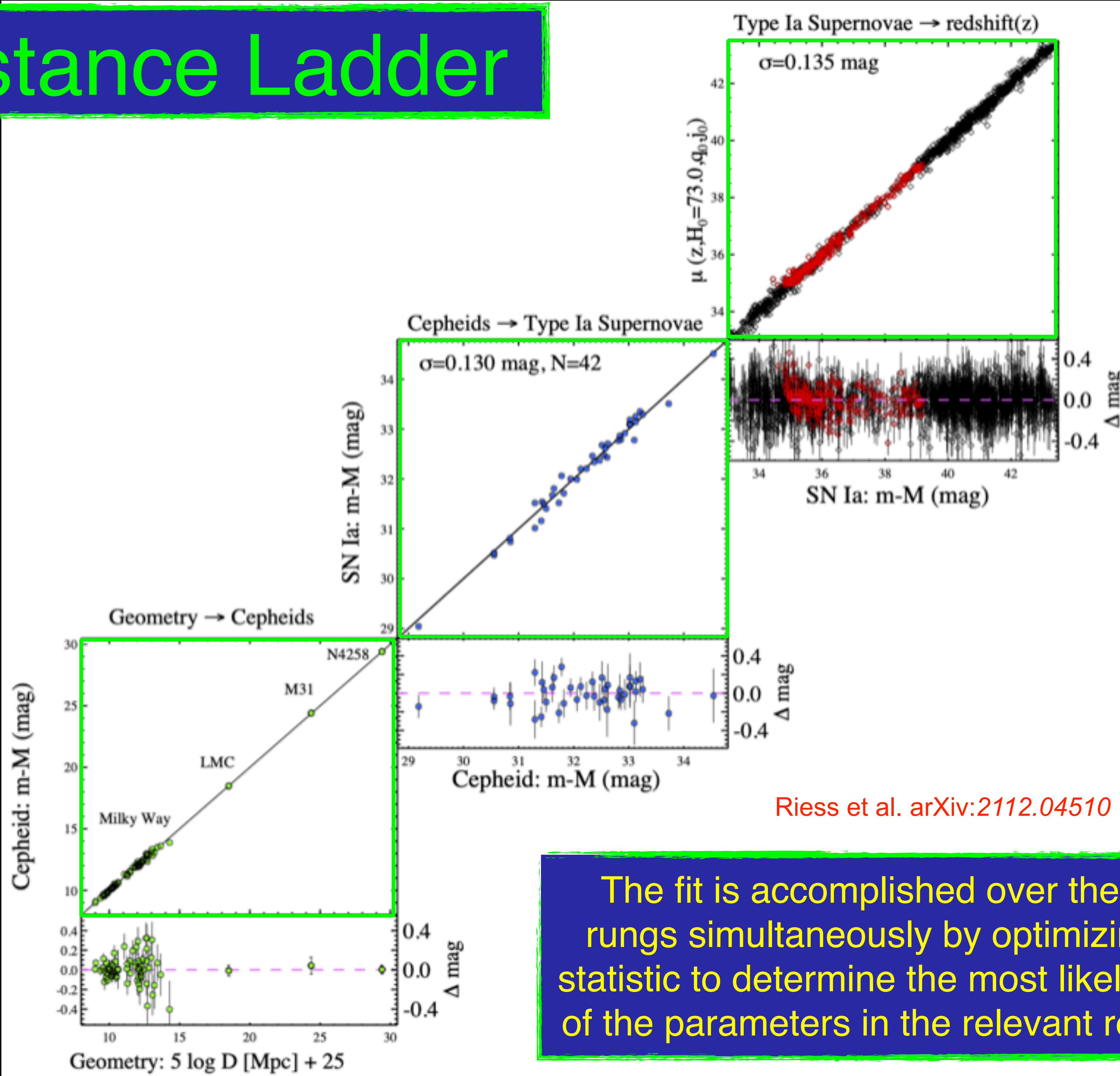

Riess et al. arXiv:*2112.04510*

The fit is accomplished over the three rungs simultaneously by optimizing a χ^2 statistic to determine the most likely values of the parameters in the relevant relations.

Distance Ladder

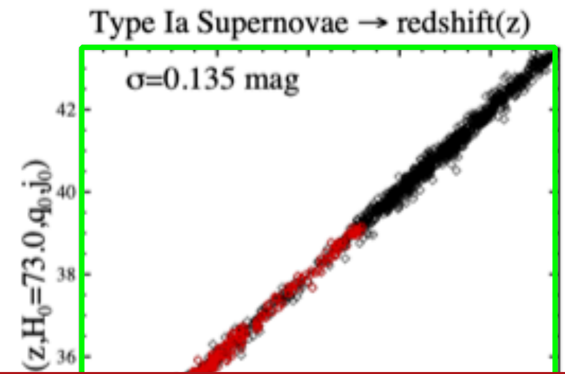

arXiv > astro-ph > arXiv:2404.08038

Search...

Help | Adv

Astrophysics > Cosmology and Nongalactic Astrophysics

[Submitted on 11 Apr 2024]

Small Magellanic Cloud Cepheids Observed with the Hubble Space Telescope Provide a New Anchor for the SH0ES Distance Ladder

Louise Breuval, Adam G. Riess, Stefano Casertano, Wenlong Yuan, Lucas M. Macri, Martino Romaniello, Yukei S. Murakami, Daniel Scolnic, Gagandeep S. Anand, Igor Soszyński

We present photometric measurements of 88 Cepheid variables in the core of the Small Magellanic Cloud (SMC), the first sample obtained with the Hubble Space Telescope (HST) and Wide Field Camera 3, in the same homogeneous photometric system as past measurements of all Cepheids on the SH0ES distance ladder. We limit the sample to the inner core and model the geometry to reduce errors in prior studies due to the non-trivial depth of this Cloud. Without crowding present in ground-based studies, we obtain an unprecedentedly low dispersion of 0.102 mag for a Period-Luminosity relation in the SMC, approaching the width of the Cepheid instability strip. The new geometric distance to 15 late-type detached eclipsing binaries in the SMC offers a rare opportunity to improve the foundation of the distance ladder, increasing the number of calibrating galaxies from three to four. With the SMC as the only anchor, we find $H_0 = 74.1 \pm 2.1$ km s^{-1} Mpc^{-1}. Combining these four geometric distances with our HST photometry of SMC Cepheids, we obtain $H_0 = 73.17 \pm 0.86$ km s^{-1} Mpc^{-1}. By including the SMC in the distance ladder, we also double the range where the metallicity ([Fe/H]) dependence of the Cepheid Period-Luminosity relation can be calibrated, and we find $\gamma = -0.22 \pm 0.05$ mag dex^{-1}. Our local measurement of H_0 based on Cepheids and Type Ia supernovae shows a 5.8σ tension with the value inferred from the CMB assuming a ΛCDM cosmology, reinforcing the possibility of physics beyond ΛCDM.

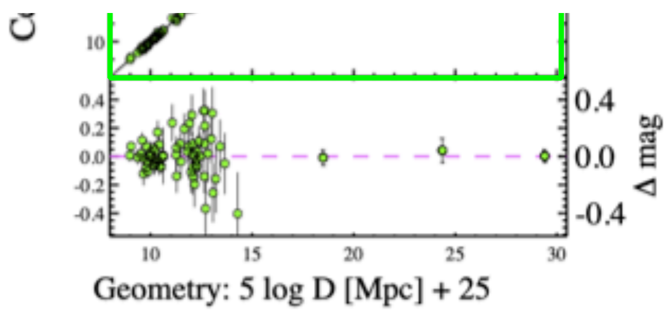

CMB constraints

The Planck estimate assuming a “vanilla"
ΛCDM cosmological model:
H0 = 67.36 ± 0.54 km/s/Mpc

Planck 2018, Astron.Astrophys. 641 (2020) A6

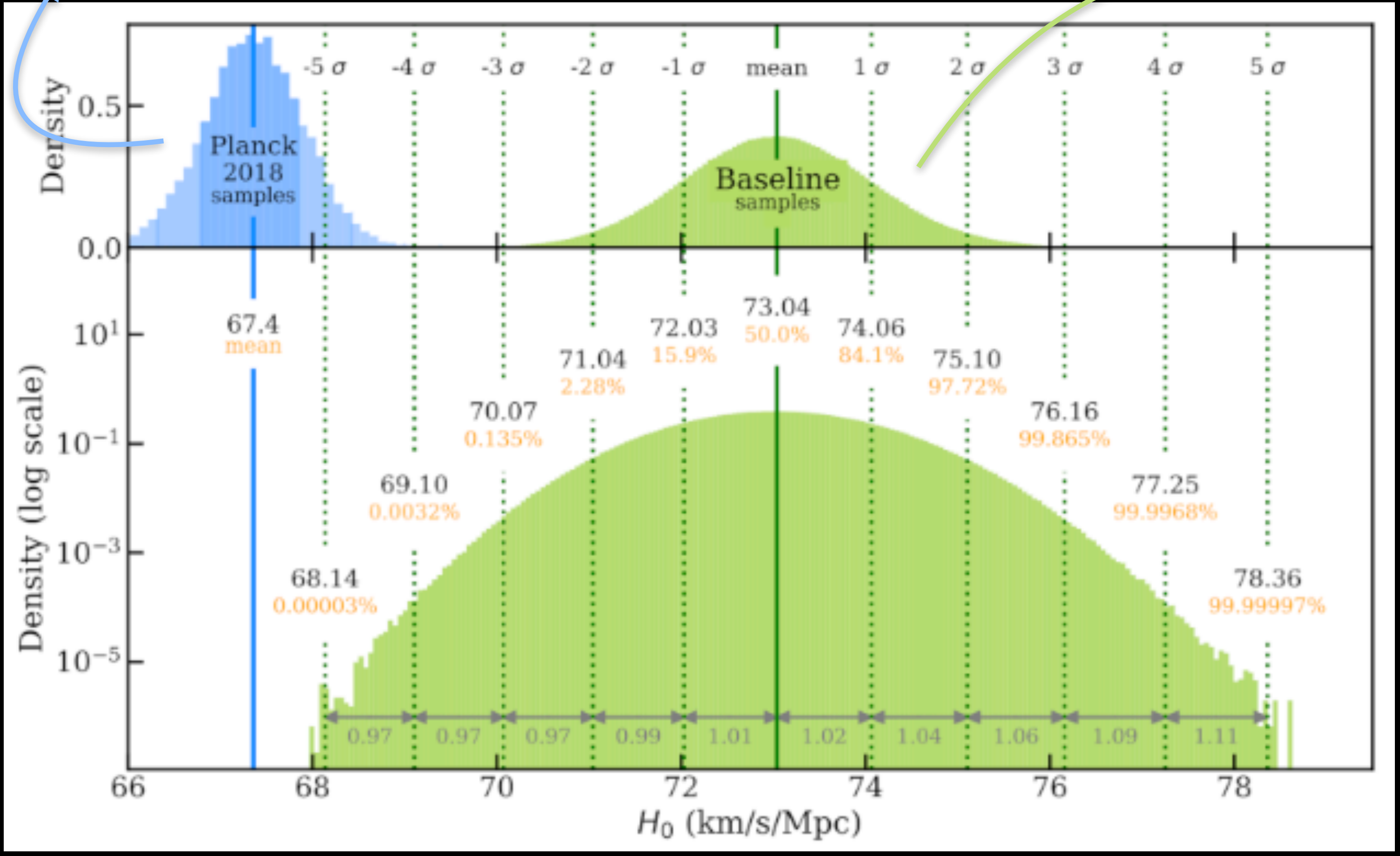

The latest local measurements obtained by the SH0ES collaboration

H0 = 73.04 ± 1.04 km/s/Mpc

Riess et al. arXiv:*2112.04510*

CMB constraints

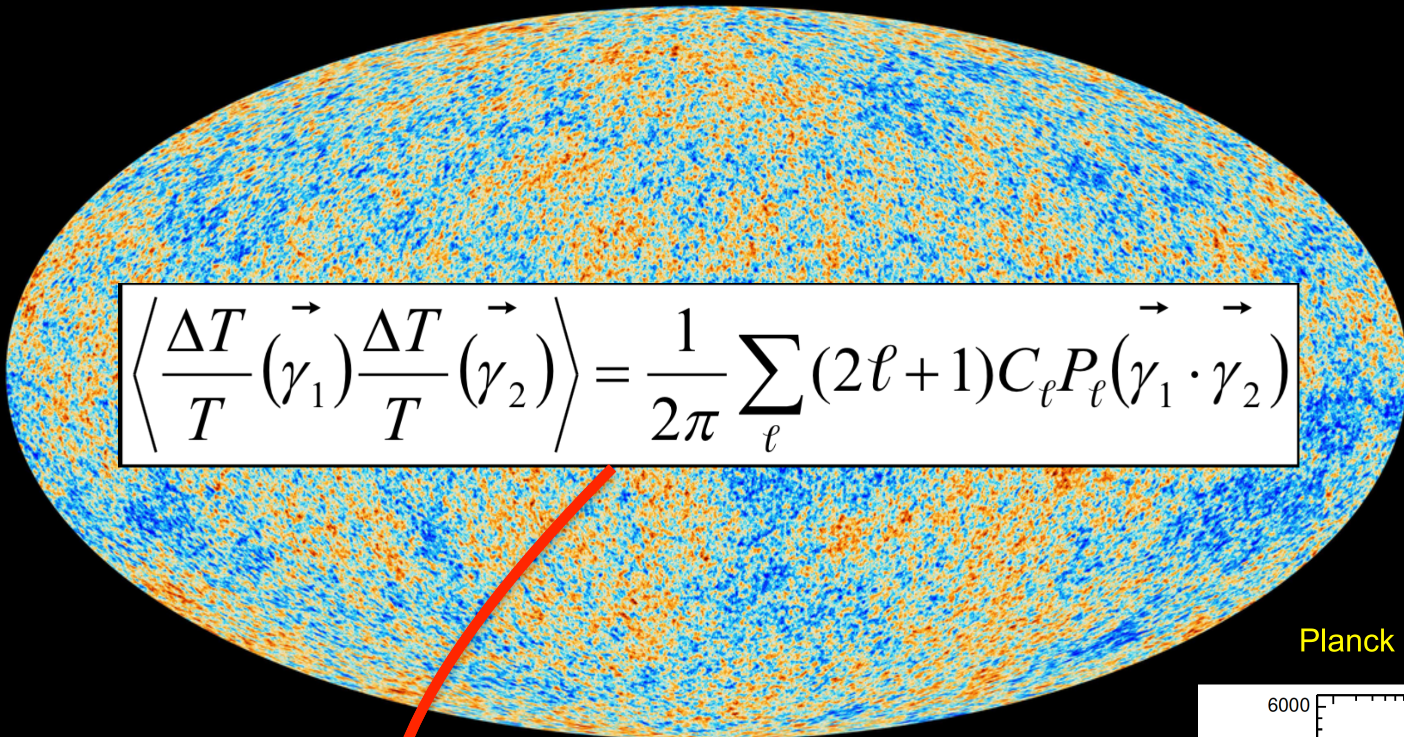

$$\left\langle \frac{\Delta T}{T}(\vec{\gamma}_1)\frac{\Delta T}{T}(\vec{\gamma}_2)\right\rangle = \frac{1}{2\pi}\sum_{\ell}(2\ell+1)C_\ell P_\ell(\vec{\gamma}_1\cdot\vec{\gamma}_2)$$

From the map of the CMB anisotropies we can extract the temperature angular power spectrum.

Planck 2018, Astron.Astrophys. 641 (2020) A6

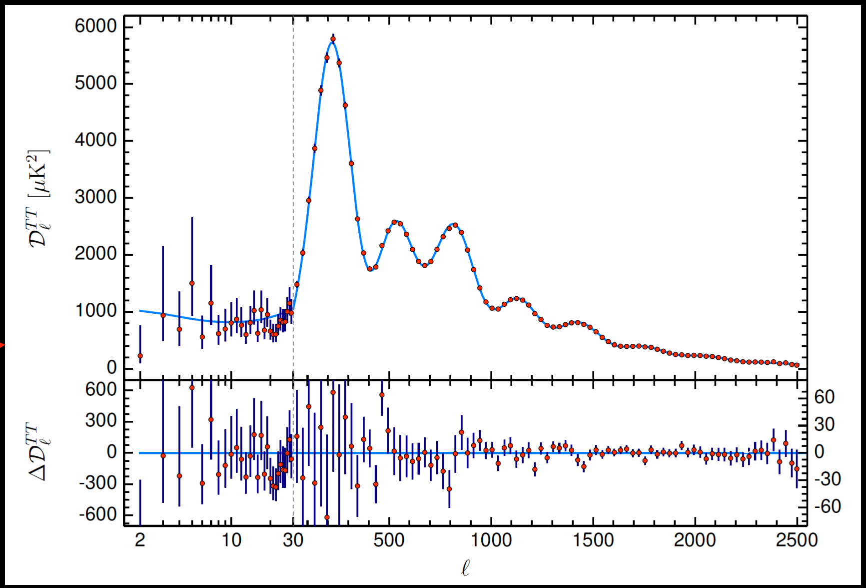

CMB constraints

Parameter	TT+lowE 68% limits	TE+lowE 68% limits	EE+lowE 68% limits	TT,TE,EE+lowE 68% limits	TT,TE,EE+lowE+lensing 68% limits	TT,TE,EE+lowE+lensing+BAO 68% limits
$\Omega_b h^2$	0.02212 ± 0.00022	0.02249 ± 0.00025	0.0240 ± 0.0012	0.02236 ± 0.00015	0.02237 ± 0.00015	0.02242 ± 0.00014
$\Omega_c h^2$	0.1206 ± 0.0021	0.1177 ± 0.0020	0.1158 ± 0.0046	0.1202 ± 0.0014	0.1200 ± 0.0012	0.11933 ± 0.00091
$100\theta_{MC}$	1.04077 ± 0.00047	1.04139 ± 0.00049	1.03999 ± 0.00089	1.04090 ± 0.00031	1.04092 ± 0.00031	1.04101 ± 0.00029
τ	0.0522 ± 0.0080	0.0496 ± 0.0085	0.0527 ± 0.0090	$0.0544^{+0.0070}_{-0.0081}$	0.0544 ± 0.0073	0.0561 ± 0.0071
$\ln(10^{10} A_s)$	3.040 ± 0.016	$3.018^{+0.020}_{-0.018}$	3.052 ± 0.022	3.045 ± 0.016	3.044 ± 0.014	3.047 ± 0.014
n_s	0.9626 ± 0.0057	0.967 ± 0.011	0.980 ± 0.015	0.9649 ± 0.0044	0.9649 ± 0.0042	0.9665 ± 0.0038
H_0 [km s^{-1} Mpc^{-1}] . .	66.88 ± 0.92	68.44 ± 0.91	69.9 ± 2.7	67.27 ± 0.60	67.36 ± 0.54	67.66 ± 0.42
Ω_Λ	0.679 ± 0.013	0.699 ± 0.012	$0.711^{+0.033}_{-0.026}$	0.6834 ± 0.0084	0.6847 ± 0.0073	0.6889 ± 0.0056
Ω_m	0.321 ± 0.013	0.301 ± 0.012	$0.289^{+0.026}_{-0.033}$	0.3166 ± 0.0084	0.3153 ± 0.0073	0.3111 ± 0.0056
$\Omega_m h^2$	0.1434 ± 0.0020	0.1408 ± 0.0019	$0.1404^{+0.0034}_{-0.0039}$	0.1432 ± 0.0013	0.1430 ± 0.0011	0.14240 ± 0.00087
$\Omega_m h^3$	0.09589 ± 0.00046	0.09635 ± 0.00051	$0.0981^{+0.0016}_{-0.0018}$	0.09633 ± 0.00029	0.09633 ± 0.00030	0.09635 ± 0.00030
σ_8	0.8118 ± 0.0089	0.793 ± 0.011	0.796 ± 0.018	0.8120 ± 0.0073	0.8111 ± 0.0060	0.8102 ± 0.0060
$S_8 \equiv \sigma_8(\Omega_m/0.3)^{0.5}$.	0.840 ± 0.024	0.794 ± 0.024	$0.781^{+0.052}_{-0.060}$	0.834 ± 0.016	0.832 ± 0.013	0.825 ± 0.011

Planck 2018, Astron.Astrophys. 641 (2020) A6

2018 Planck results are a wonderful confirmation of the flat standard ΛCDM cosmological model, but are model dependent!

- The cosmological constraints are obtained assuming a cosmological model.
- The results are affected by the degeneracy between the parameters that induce similar effects on the observables.

Are there other H0 estimates?

Latest H0 measurements

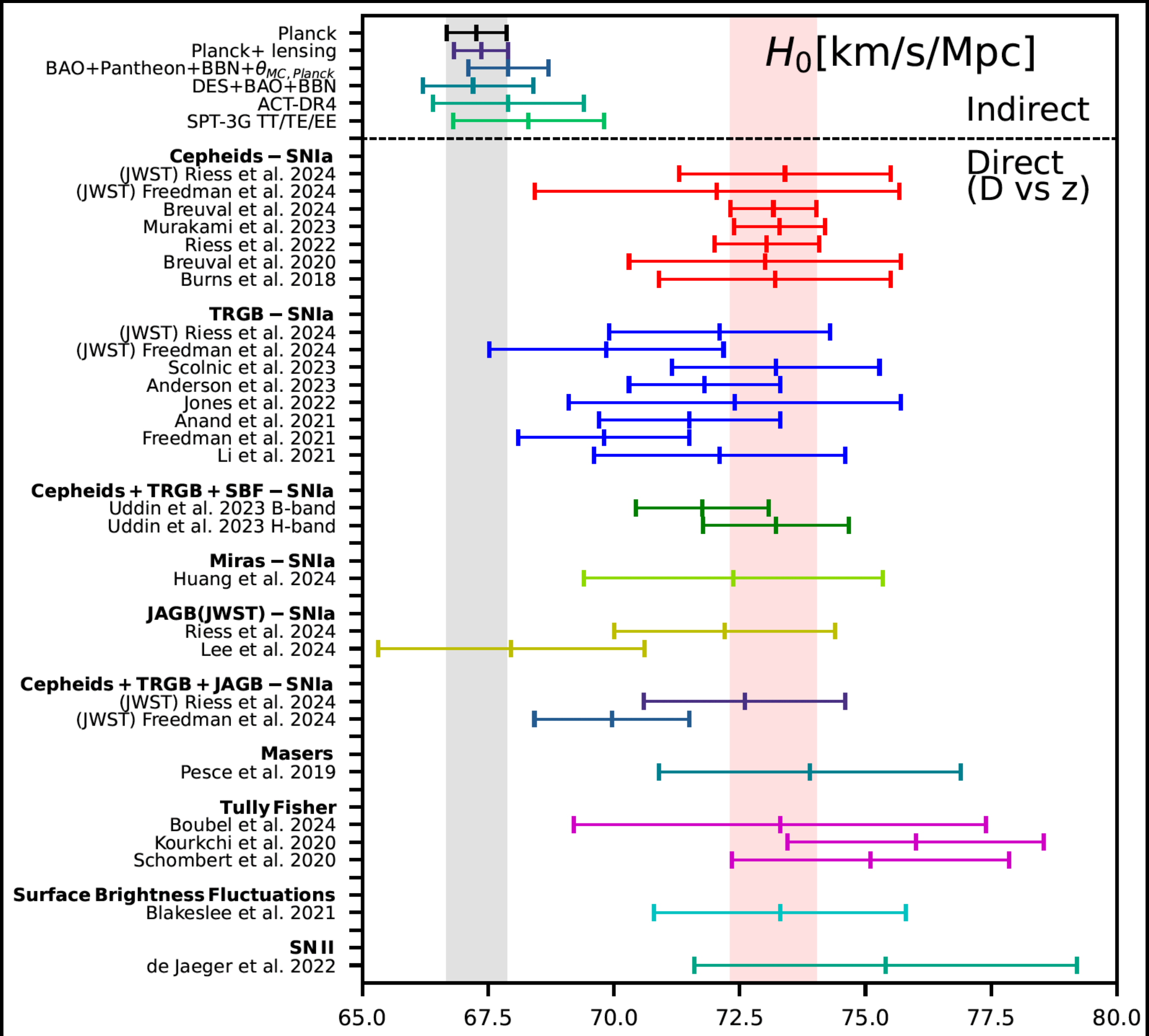

Hubble constant measurements made by different astronomical missions and groups over the years.

The red vertical band corresponds to the H0 value from SH0ES Team and the grey vertical band corresponds to the H0 value as reported by Planck 2018 team within a ΛCDM scenario.

Di Valentino, *MNRAS* 502 (2021) 2, 2065-2073

Latest H0 measurements

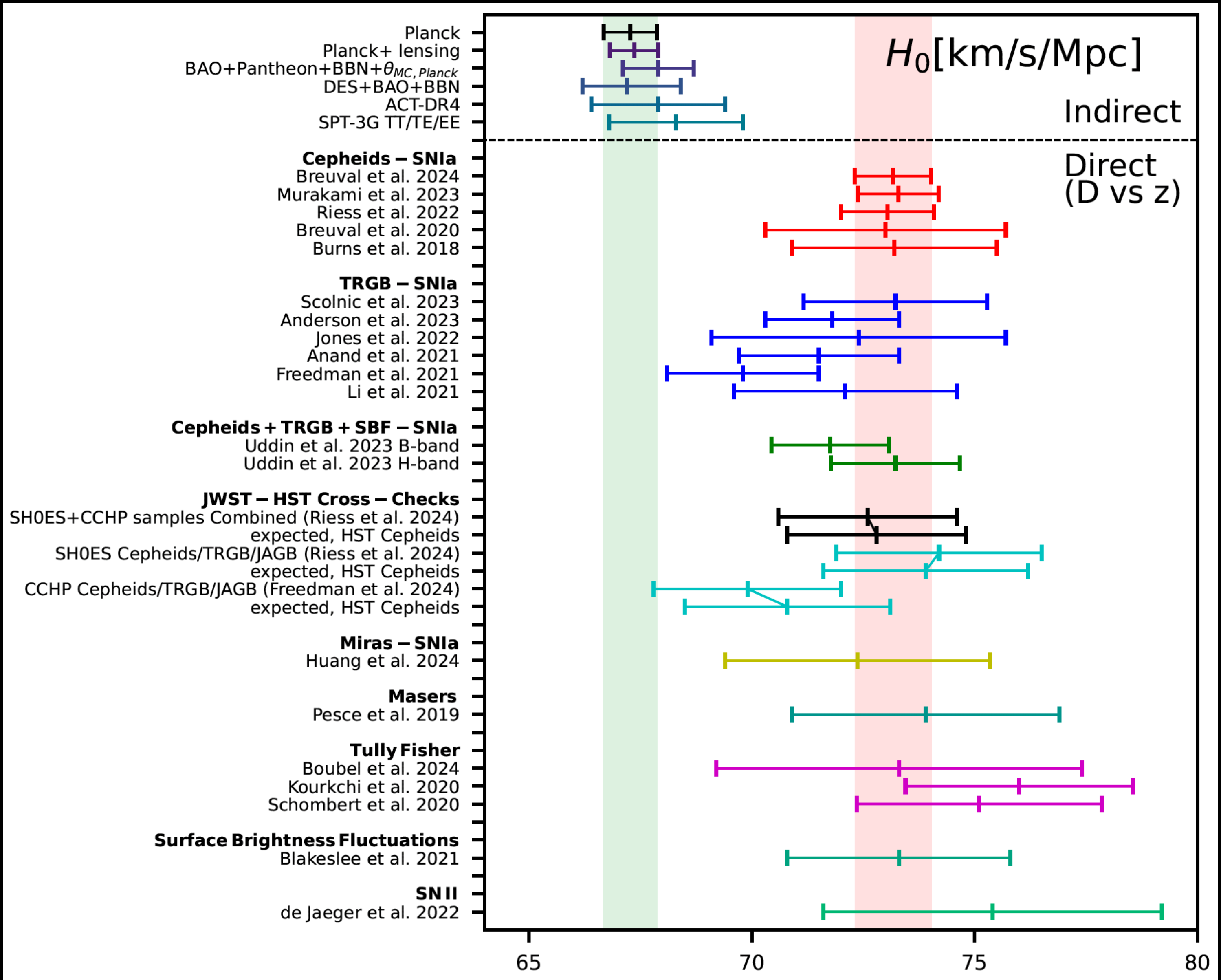

The JWST results serve as "cross-checks": they do not introduce any new objects and represent only a small portion of the full HST sample, which includes 42 SN Ia and 4 anchors, compared to JWST's 10 SNe and 1 anchor.

Therefore, our approach should be to compare the findings from this sub-sample with the corresponding objects observed by HST.

Latest H0 measurements

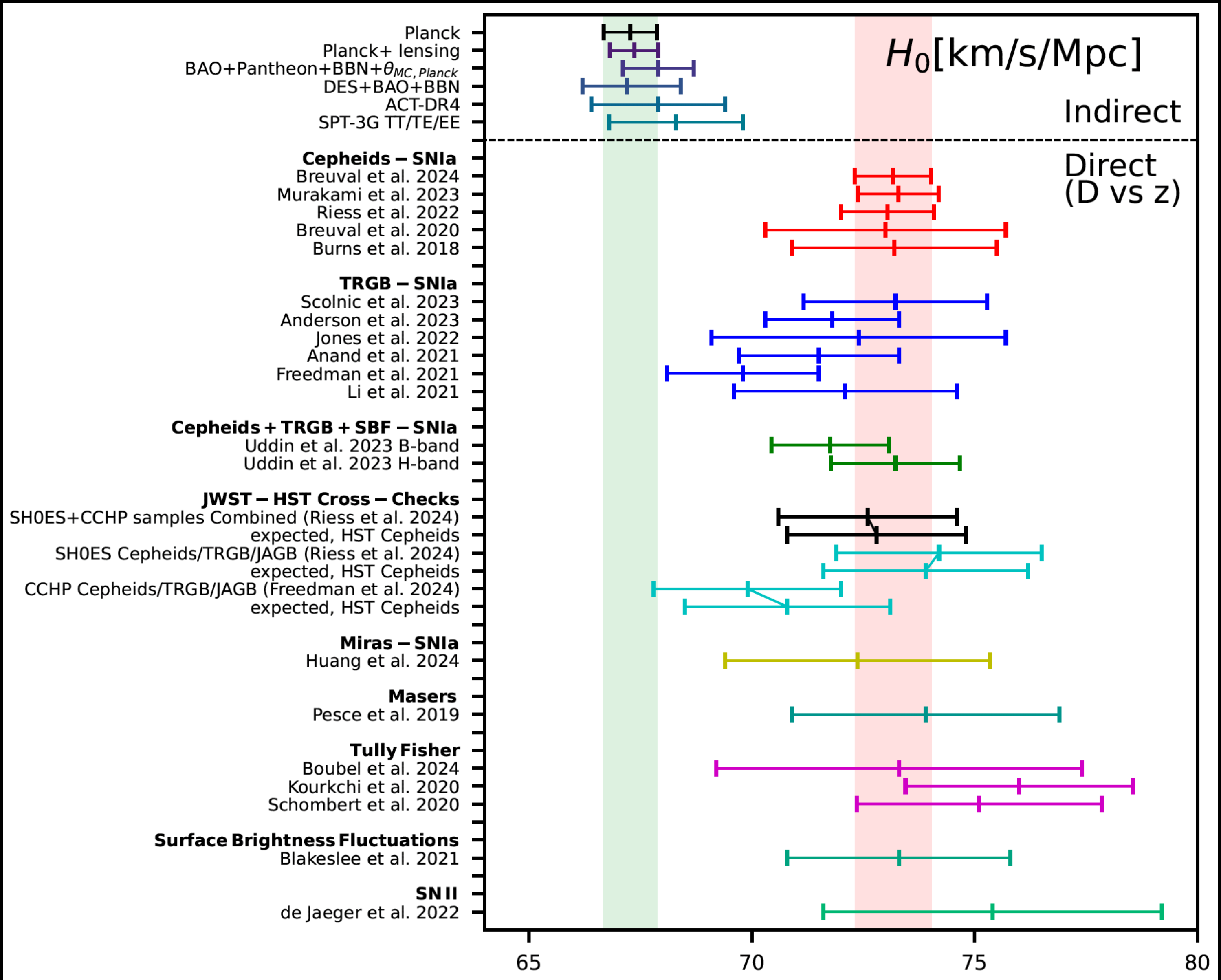

SH0ES+CCHP samples
H0 = 72.6 ± 2.0 km/s/Mpc
expected, HST Cepheids
H0 = 72.8 ± 2.0 km/s/Mpc

SH0ES Ceph/TRGB/JAGB
H0 = 74.2 ± 2.3 km/s/Mpc
expected, HST Cepheids
H0 = 73.9 ± 2.3 km/s/Mpc

CCHP Ceph/TRGB/JAGB
H0 = 69.8 ± 2.1 km/s/Mpc
expected, HST Cepheids
H0 = 70.8 ± 2.3 km/s/Mpc

Riess et al., arXiv: *2408.11770*

It is difficult to attribute the Hubble constant tension
to a single systematic error because such an error would need to consistently explain discrepancies across a wide range of phenomena.

While multiple independent systematic errors could theoretically resolve the tension, they are unlikely to bias the measurements all in the same direction.

Since indirect constraints rely on model assumptions, it is worth exploring modifications to the cosmological model. Investigating these extensions could help resolve discrepancies between different cosmological observations.

Complication:
the sound horizon problem

What about BAO+Pantheon?

BAO+Pantheon measurements constrain the product of H0 and the sound horizon r_s .

In order to have a higher H0 value in agreement with SH0ES, we need r_s near 137 Mpc. However, Planck by assuming ΛCDM, prefers r_s near 147 Mpc. Therefore, a cosmological solution that can increase H0 and at the same time can lower the sound horizon inferred from CMB data is the most promising way to put in agreement all the measurements.

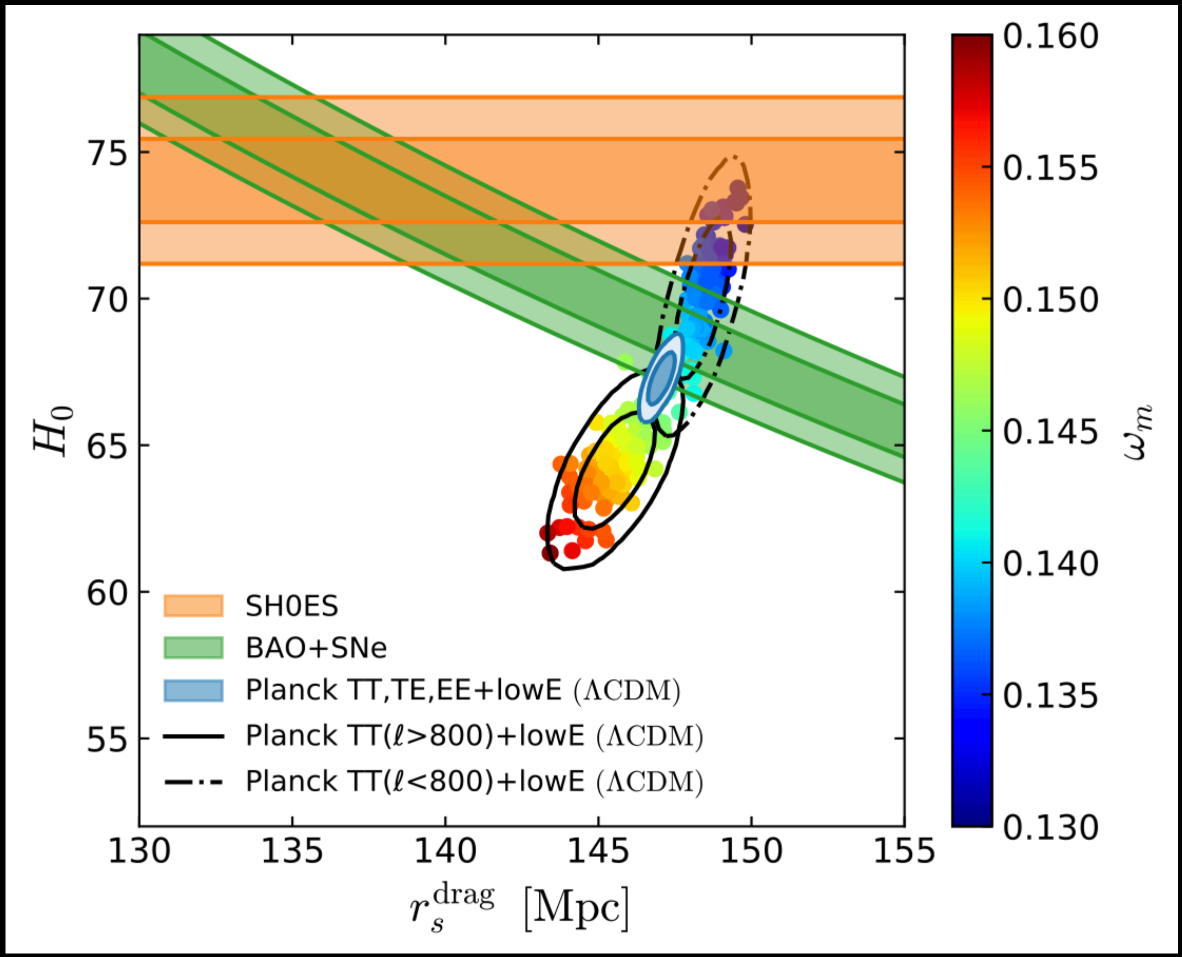

Knox and Millea, *Phys.Rev.D* 101 (2020) 4, 043533

Early vs late time solutions

Here we can see the comparison of the 2σ credibility regions of the CMB constraints and the measurements from late-time observations (SN + BAO + H0LiCOW + SH0ES).

We see that the late time solutions, as wCDM, increase H0 because they decrease the expansion history at intermediate redshift, but leave r_s unaltered.

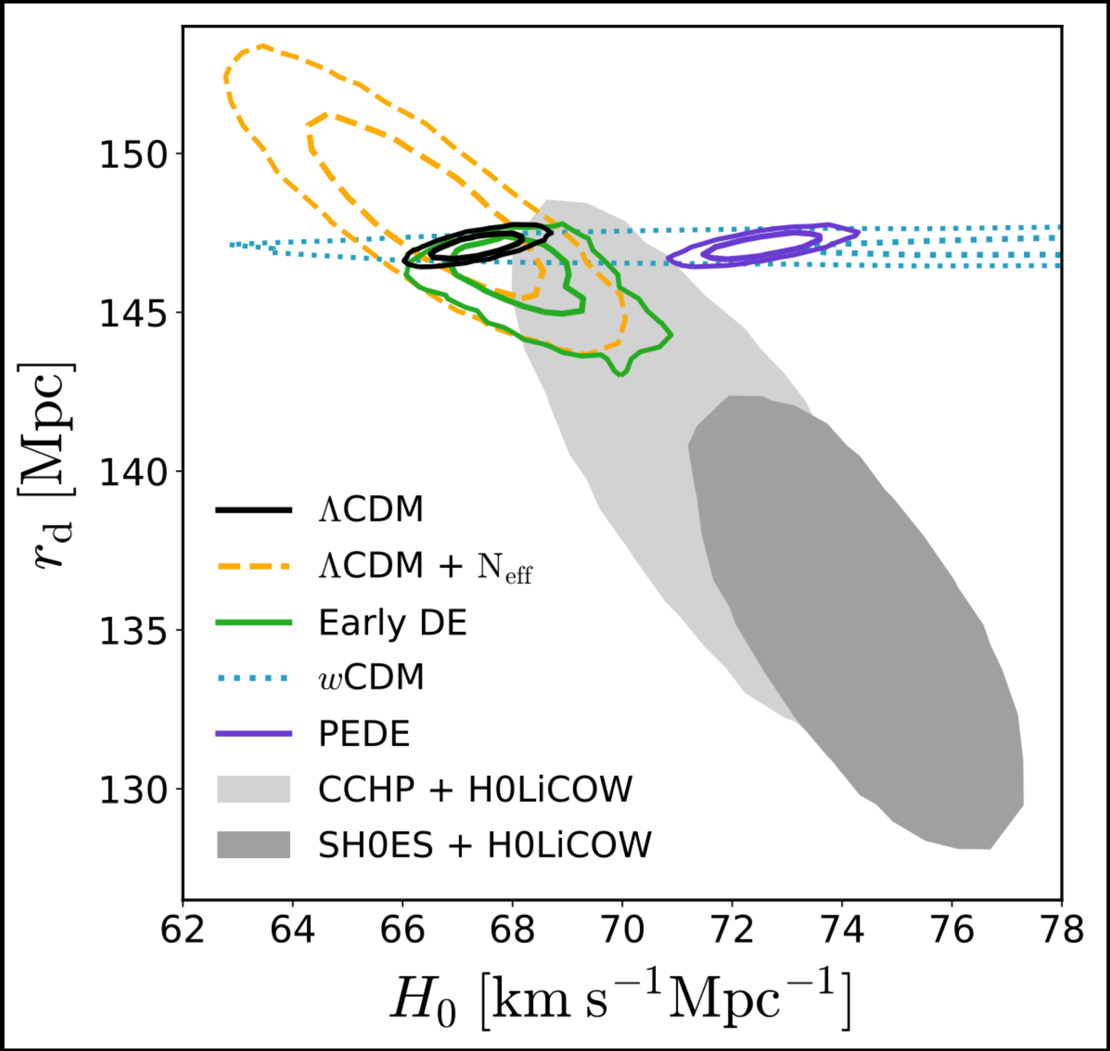

Arendse et al., Astron.Astrophys. 639 (2020) A57

The Dark energy equation of state

Changing the cosmological constant to a form of dark energy with an equation of state w alters the universe's expansion rate:

$$H^2 = \left(\frac{\dot{a}}{a}\right)^2 = H_0^2 \left(\frac{\Omega_r}{a^4} + \frac{\Omega_m}{a^3} + \frac{\Omega_k}{a^2} + \Omega_\Lambda\right)$$

$$H^2 = H_0^2 \Big[\Omega_m (1+z)^3 + \Omega_r (1+z)^4 + \Omega_{\rm de} (1+z)^{3(1+w)} + \Omega_k (1+z)^2\Big]$$

w introduces a geometrical degeneracy with the Hubble constant that is almost unconstrained using the CMB data only, resulting in agreement with SH0ES. We have from Planck only $w = -1.58^{+0.52}_{-0.41}$ with $H0 > 69.9$ km/s/Mpc at 95% c.l.

Planck data suggest a preference for phantom dark energy ($w<-1$), which implies a density increasing over time and could lead to a Big Rip scenario.

Phantom dark energy violates the energy condition $\rho \geq |p|$, allowing matter to move faster than light, leading to negative energy densities and potential vacuum instabilities due to negative kinetic energy.

The state of the Dark energy equation of state

Dataset combination	w	H_0 [km/s/Mpc]
CMB	$-1.57^{+0.16}_{-0.36}$ $(-1.57^{+0.53}_{-0.42})$	> 82.4 (> 69.3)
CMB+BAO	-1.039 ± 0.059 $(-1.04^{+0.11}_{-0.12})$	68.6 ± 1.5 $(68.6^{+3.1}_{-2.8})$
CMB+SN	-0.976 ± 0.029 $(-0.976^{+0.055}_{-0.056})$	66.54 ± 0.81 $(66.5^{+1.6}_{-1.6})$

Escamilla, Giarè, Di Valentino et al., JCAP 05 (2024) 091

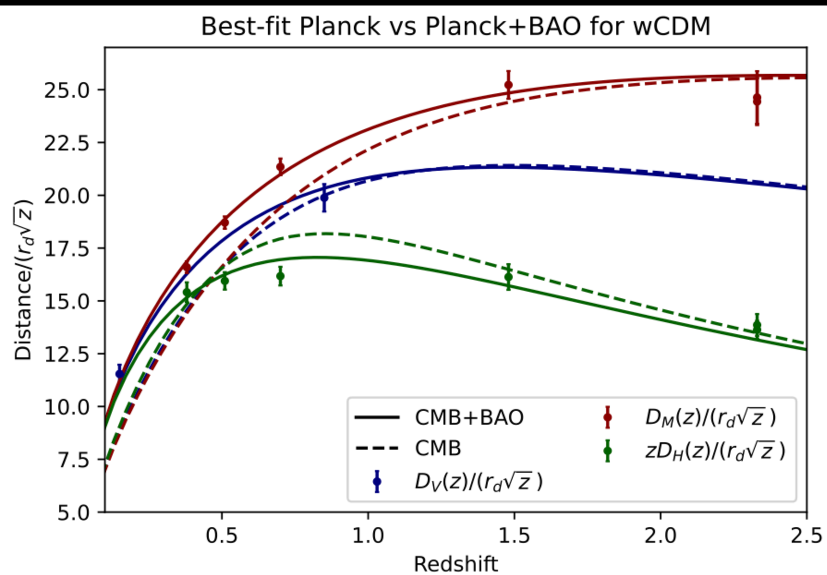

FIG. 5. Best-fit predictions for (rescaled) distance-redshift relations from a wCDM fit to *Planck* CMB data alone (dashed curves) and the CMB+BAO dataset (solid curves). These predictions are presented for the three different types of distances probed by BAO measurements (rescaled as per the y label), each indicated by the colors reported in the legend. The error bars represent $\pm 1\sigma$ uncertainties.

However, if BAO data are included, the wCDM model with w<-1 worsens considerably the fit of the BAO data because the best fit from Planck alone fails in recover the shape of H(z) at low redshifts. Therefore, when the CMB is combined with BAO data, the favoured model is again the ΛCDM one and the H0 tension is restored.

Early vs late time solutions

Here we can see the comparison of the 2σ credibility regions of the CMB constraints and the measurements from late-time observations (SN + BAO + H0LiCOW + SH0ES).

However, the early time solutions, as Neff or Early Dark Energy, move in the right direction both the parameters, but can't solve completely the H0 tension between Planck and SH0ES.

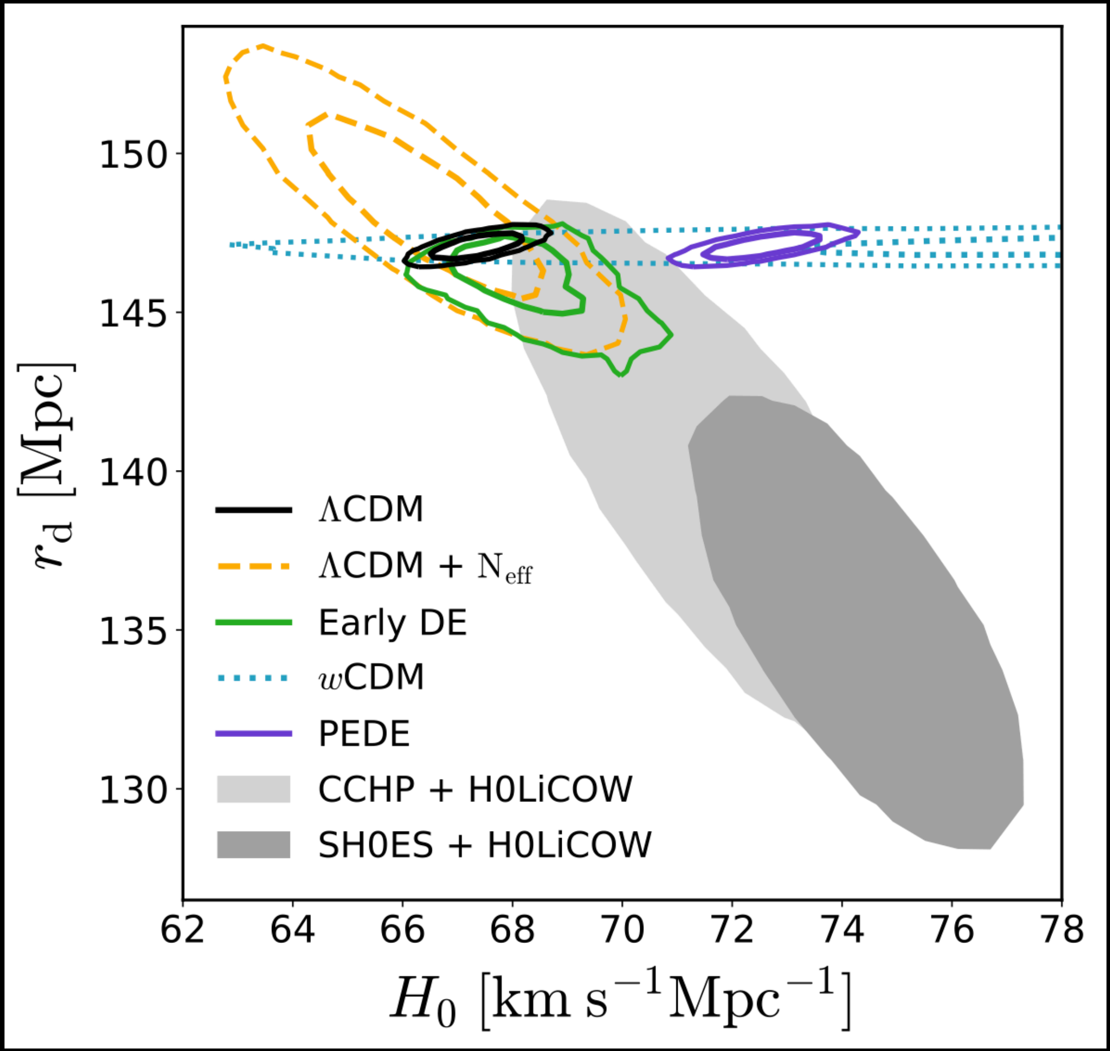

Arendse et al., Astron.Astrophys. 639 (2020) A57

Early Dark Energy

Constraints at 68% cl.

Constraints from *Planck* 2018 data only: TT+TE+EE

Parameter	ΛCDM	EDE ($n=3$)
$\ln(10^{10} A_s)$	$3.044\,(3.055)\ \pm 0.016$	$3.051\,(3.056)\ \pm 0.017$
n_s	$0.9645\,(0.9659)\ \pm 0.0043$	$0.9702\,(0.9769)^{+0.0071}_{-0.0069}$
$100\theta_s$	$1.04185\,(1.04200)\ \pm 0.00029$	$1.04164\,(1.04168)\ \pm 0.00034$
$\Omega_b h^2$	$0.02235\,(0.02244)\ \pm 0.00015$	$0.02250\,(0.02250)\ \pm 0.00020$
$\Omega_c h^2$	$0.1202\,(0.1201)\ \pm 0.0013$	$0.1234\,(0.1268)^{+0.0031}_{-0.0030}$
τ_{reio}	$0.0541\,(0.0587)\ \pm 0.0076$	$0.0549\,(0.0539)\ \pm 0.0078$
$\log_{10}(z_c)$	–	$3.66\,(3.75)^{+0.28}_{-0.24}$
f_{EDE}	–	$< 0.087\,(0.068)$
θ_i	–	$> 0.36\,(2.96)$
H_0 [km/s/Mpc]	$67.29\,(67.44)\ \pm 0.59$	$68.29\,(69.13)^{+1.02}_{-1.00}$
Ω_m	$0.3162\,(0.3147)\ \pm 0.0083$	$0.3145\,(0.3138)\ \pm 0.0086$
σ_8	$0.8114\,(0.8156)\ \pm 0.0073$	$0.8198\,(0.8280)^{+0.0109}_{-0.0107}$
S_8	$0.8331\,(0.8355)\ \pm 0.0159$	$0.8393\,(0.8468)\ \pm 0.0173$
$\log_{10}(f/\mathrm{eV})$	–	$26.57\,(26.36)^{+0.39}_{-0.36}$
$\log_{10}(m/\mathrm{eV})$	–	$-26.94\,(-26.90)^{+0.58}_{-0.53}$

Hill et al. *Phys.Rev.D* 102 (2020) 4, 043507

Planck 2018 results shows no evidence for EDE
and H0 is in agreement with the value obtained assuming ΛCDM.

Sound Horizon from GWSS and 2D BAO

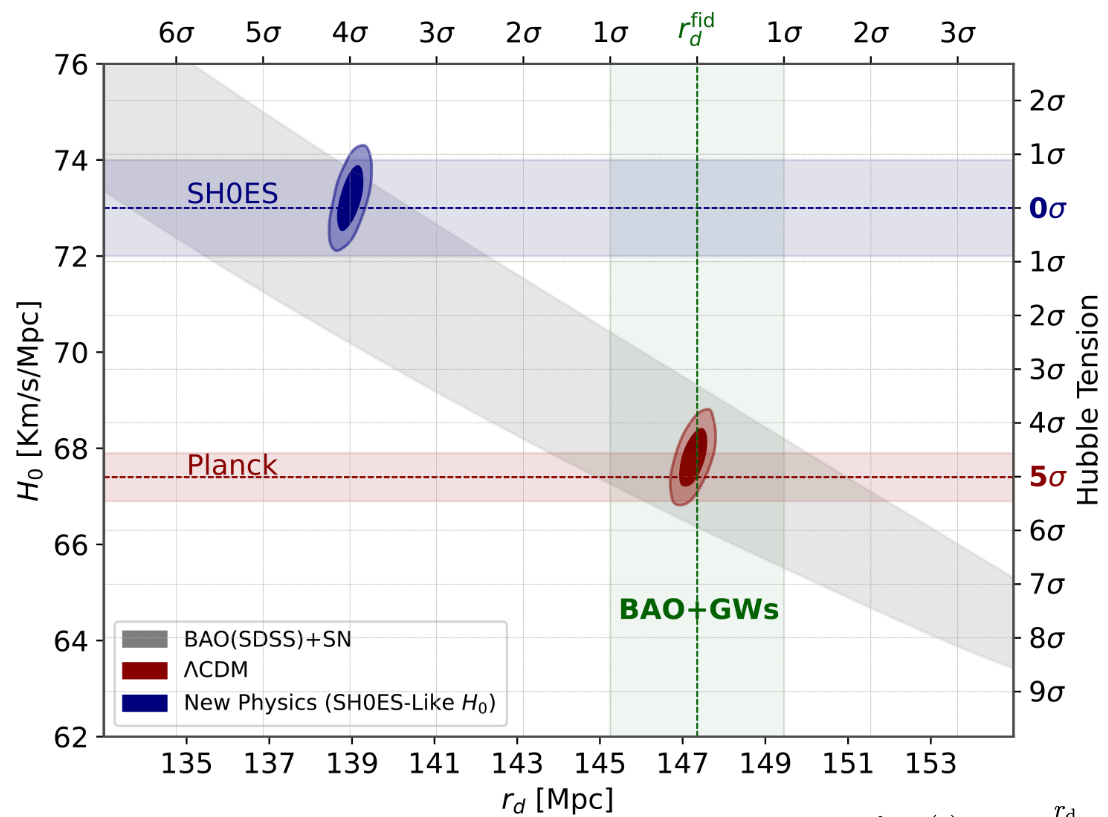

$$\theta_{\rm BAO}(z) = \frac{r_{\rm d}}{(1+z)D_{\rm A}(z)} = \frac{(1+z)\,r_{\rm d}}{D_{\rm L}(z)},$$

Figure 1. Illustrative plot in the $r_{\rm d}$ - H_0 plane of the consistency test proposed to assess the possibility of new physics prior to recombination for solving the Hubble constant tension. The red band represents the present value of H_0 measured by the Planck collaboration within a standard ΛCDM model of cosmology, whereas the 2D contours represent the marginalized 68% and 95% CL constraints obtained from the Planck-2018 data. The grey band represents the 95% CL region of the plane identified by analyzing current BAO measurements from the SDSS collaboration and Type Ia supernovae from the Pantheon+ catalogue. The horizontal blue band represents the value of the Hubble constant measured by the SH0ES collaboration. In order to reconcile all the datasets, a potential model of early-time new physics should shift the ΛCDM red contours along the grey band until the grey band overlaps with the SH0ES result. This scenario is depicted by the 2D blue contours obtained under the assumption that the model of new physics does not increase uncertainties on parameters compared to ΛCDM. The green vertical band represents the model-independent value of the sound horizon we are able to extract from combinations of GW data from LISA and BAO measurements (either from DESI-like or Euclid-like experiments) assuming a fiducial ΛCDM baseline cosmology. As is clear from the top x-axis, this value would be able to confirm or rule out the possibility of new physics at about 4σ.

We forecast a relative precision of $\sigma_{rd}/r_d \sim 1.5\%$ within the redshift range $z \lesssim 1$. These measurements can serve as a consistency test for ΛCDM, potentially clarifying the nature of the Hubble tension and confirming or ruling out new physics prior to recombination with a statistical significance of ~ 4σ.

Giarè, Betts, van de Bruck, and Di Valentino, arXiv:2406.07493

Complication:
the early solutions proposed to alleviate the H_0 tension increase the S_8 tension!

The S8 tension

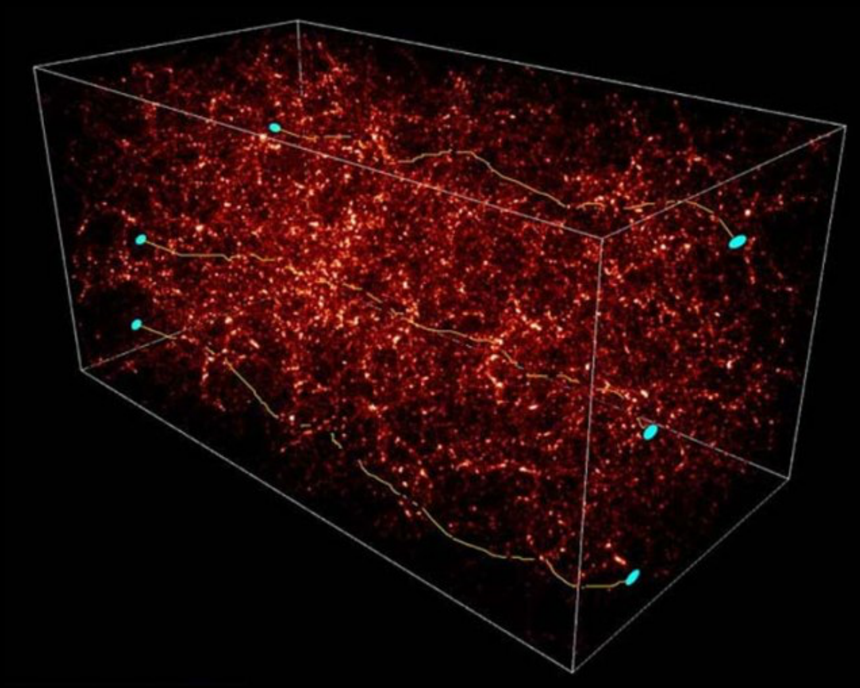

$$S_8 \equiv \sigma_8 \sqrt{\Omega_m / 0.3}$$

A tension on S8 is present between the Planck data in the ΛCDM scenario and the cosmic shear data.

The S8 tension

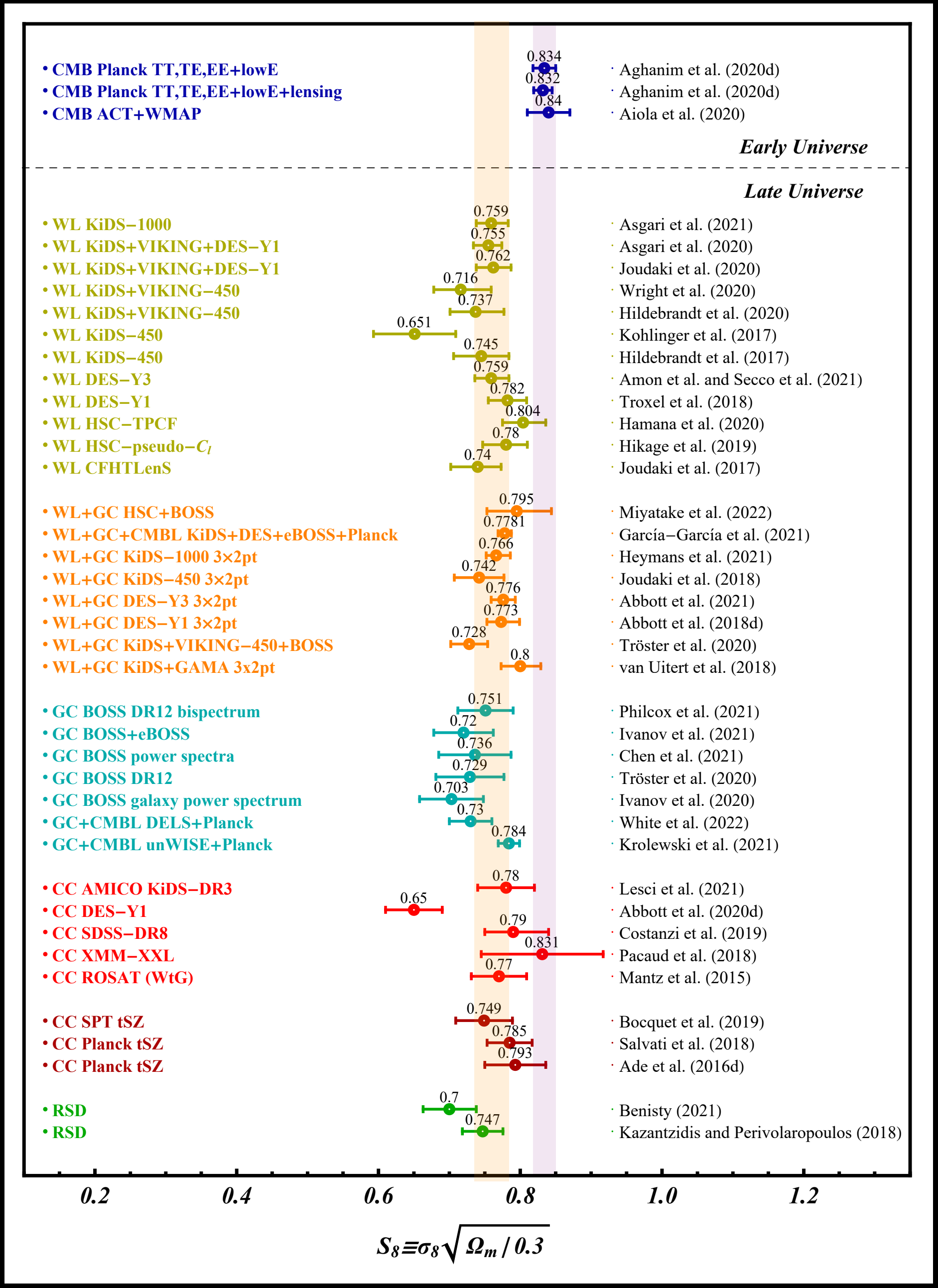

Abdalla et al., *JHEAp* 34 (2022) 49-211

See Di Valentino et al. *Astropart.Phys.* 131 (2021) 102604 and Abdalla et al., arXiv:2203.06142 [astro-ph.CO] for a summary of the possible candidates proposed to solve the S8 tension.

Early solutions to the H0 tension

Actually, a dark energy model that merely changes the value of rd would not completely resolve the tension, since it will affect the inferred value of Ωm and transfer the tension to it.

This is a plot illustrating that achieving a full agreement between CMB, BAO and SH0ES through a reduction of rd requires a higher value of $\Omega_m h^2$.

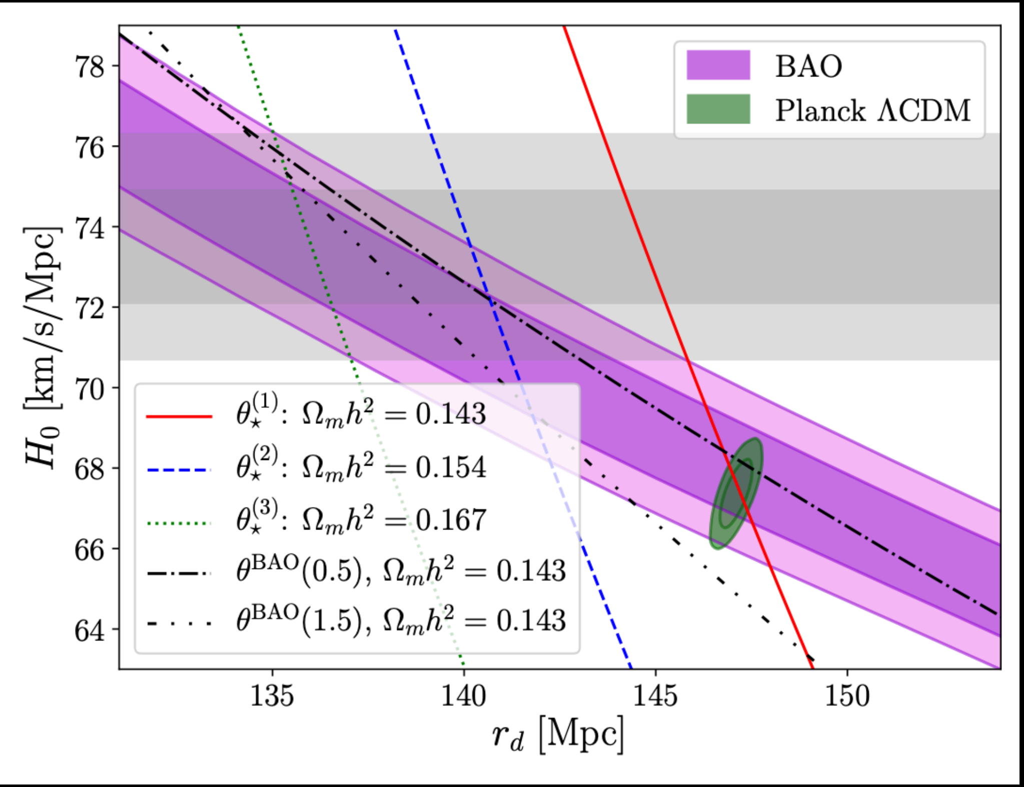

Jedamzik et al., Commun.in Phys. 4 (2021) 123

Early solutions to the H0 tension

Model 2 is defined by the simultaneous fit to BAO and CMB acoustic peaks at $\Omega_m h^2 = 0.155$, while model 3 has $\Omega_m h^2 = 0.167$

The sound horizon problem should be considered not only in the plane H0–rd, but it should be extended to the parameters triplet H0–rd–Ωm.

The figure shows that when attempting to find a full resolution of the Hubble tension, with CMB, BAO and SH0ES in agreement with each other, one exacerbates the tension with DES, KiDS and HSC.

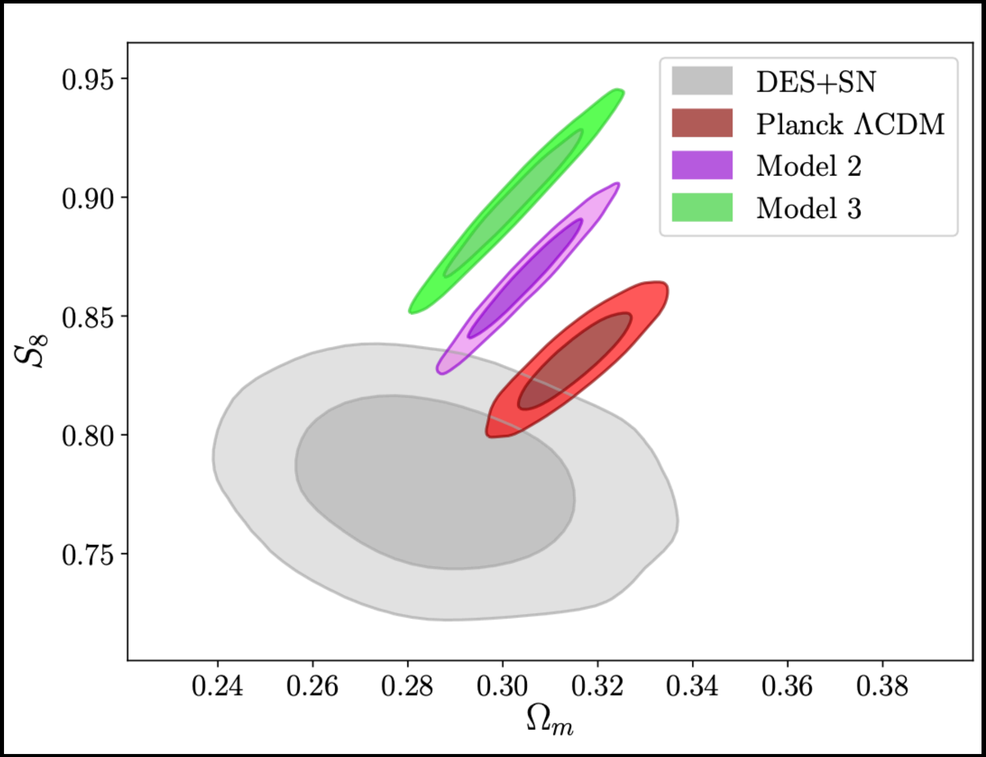

Jedamzik et al., Commun.in Phys. 4 (2021) 123

Successful models?

This is the density of the proposed cosmological models:

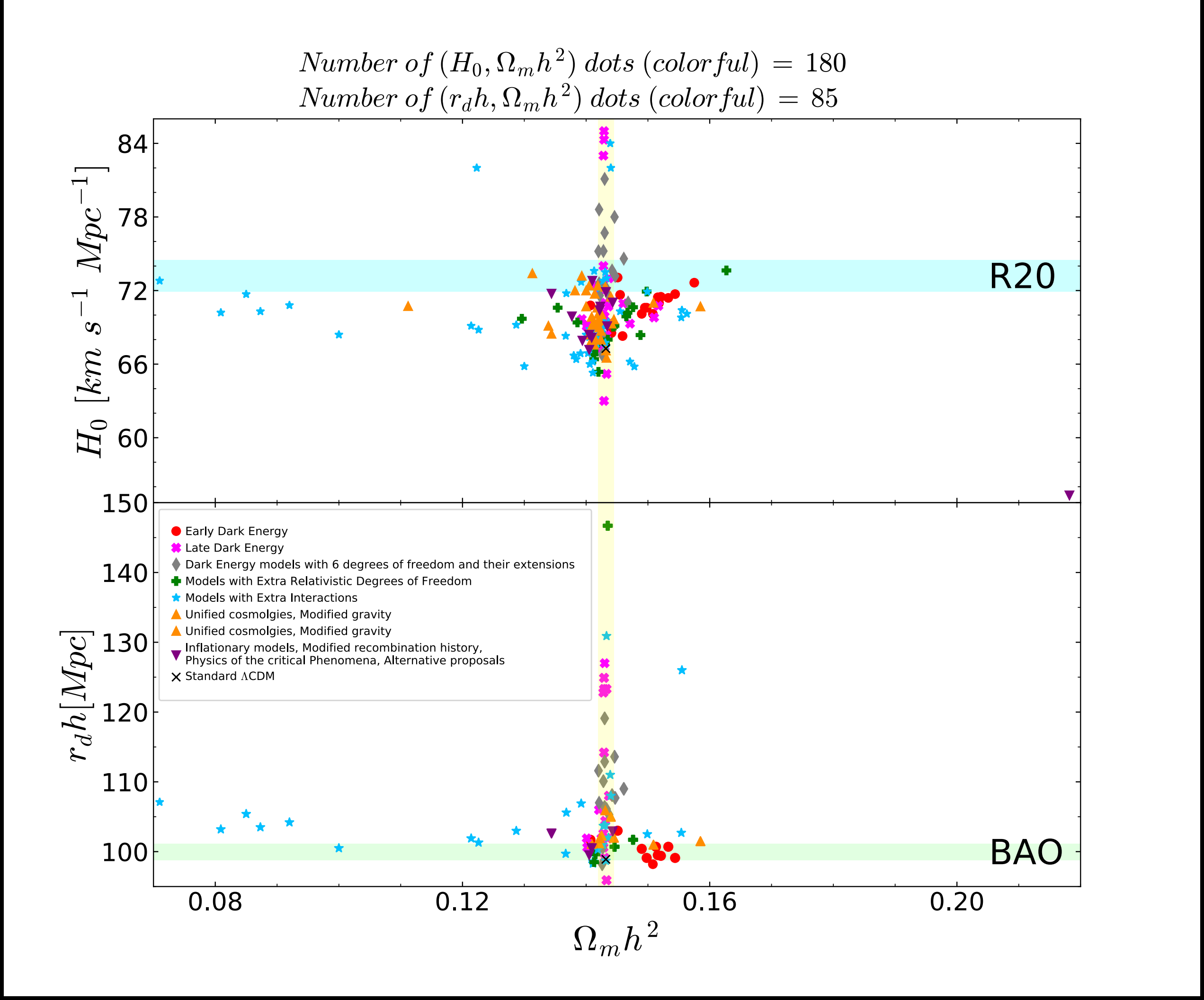

At the moment no specific proposal makes a strong case for being highly likely or far better than all others !!!

Di Valentino et al., Class.Quant.Grav. (2021), arXiv:2103.01183 [astro-ph.CO]

What about the interacting DM-DE models?

The IDE case

In the standard cosmological framework, DM and DE are described as separate fluids not sharing interactions beyond gravitational ones.
At the background level, the conservation equations for the pressureless DM and DE components can be decoupled into two separate equations with an inclusion of an arbitrary function, Q, known as the coupling or interacting function:

$$\begin{aligned} \dot{\rho}_c + 3\mathcal{H}\rho_c &= Q\,, \\ \dot{\rho}_x + 3\mathcal{H}(1+w)\rho_x &= -Q\,, \end{aligned}$$

and we assume the phenomenological form for the interaction rate:

$$Q = \xi \mathcal{H} \rho_x$$

proportional to the dark energy density ρ_x and the conformal Hubble rate $\mathcal{H}$, via a negative dimensionless parameter ξ quantifying the strength of the coupling, to avoid early-time instabilities.

Gavela et al. J. Cosmol. Astropart. Phys. 07 (2009) 034

The IDE case

In this scenario of IDE the tension on H0 between the Planck satellite and SH0ES is completely solved. The coupling could affect the value of the present matter energy density Ω_m. Therefore, if within an interacting model Ω_m is smaller (because for negative ξ the dark matter density will decay into the dark energy one), a larger value of H0 would be required in order to satisfy the peaks structure of CMB observations, which accurately determine the value of $\Omega_m h^2$.

Parameter	*Planck*	*Planck+R19*
$\Omega_b h^2$	0.02239 ± 0.00015	0.02239 ± 0.00015
$\Omega_c h^2$	< 0.105	< 0.0615
n_s	0.9655 ± 0.0043	0.9656 ± 0.0044
$100\theta_s$	$1.0458^{+0.0033}_{-0.0021}$	1.0470 ± 0.0015
τ	0.0541 ± 0.0076	0.0534 ± 0.0080
ξ	$-0.54^{+0.12}_{-0.28}$	$-0.66^{+0.09}_{-0.13}$
H_0 [km s^{-1} Mpc^{-1}]	$72.8^{+3.0}_{-1.5}$	$74.0^{+1.2}_{-1.0}$

TABLE I. Mean values with their 68% C.L. errors on selected cosmological parameters within the $\xi\Lambda$CDM model, considering either the *Planck* 2018 legacy dataset alone, or the same dataset in combination with the *R19* Gaussian prior on H_0 based on the latest local distance measurement from *HST*. The quantity quoted in the case of $\Omega_c h^2$ is the 95% C.L. upper limit.

Di Valentino et al., Phys.Dark Univ. 30 (2020) 100666

The IDE case

Therefore we can safely combine the two datasets together, and we obtain a non-zero dark matter-dark energy coupling ξ at more than FIVE standard deviations.

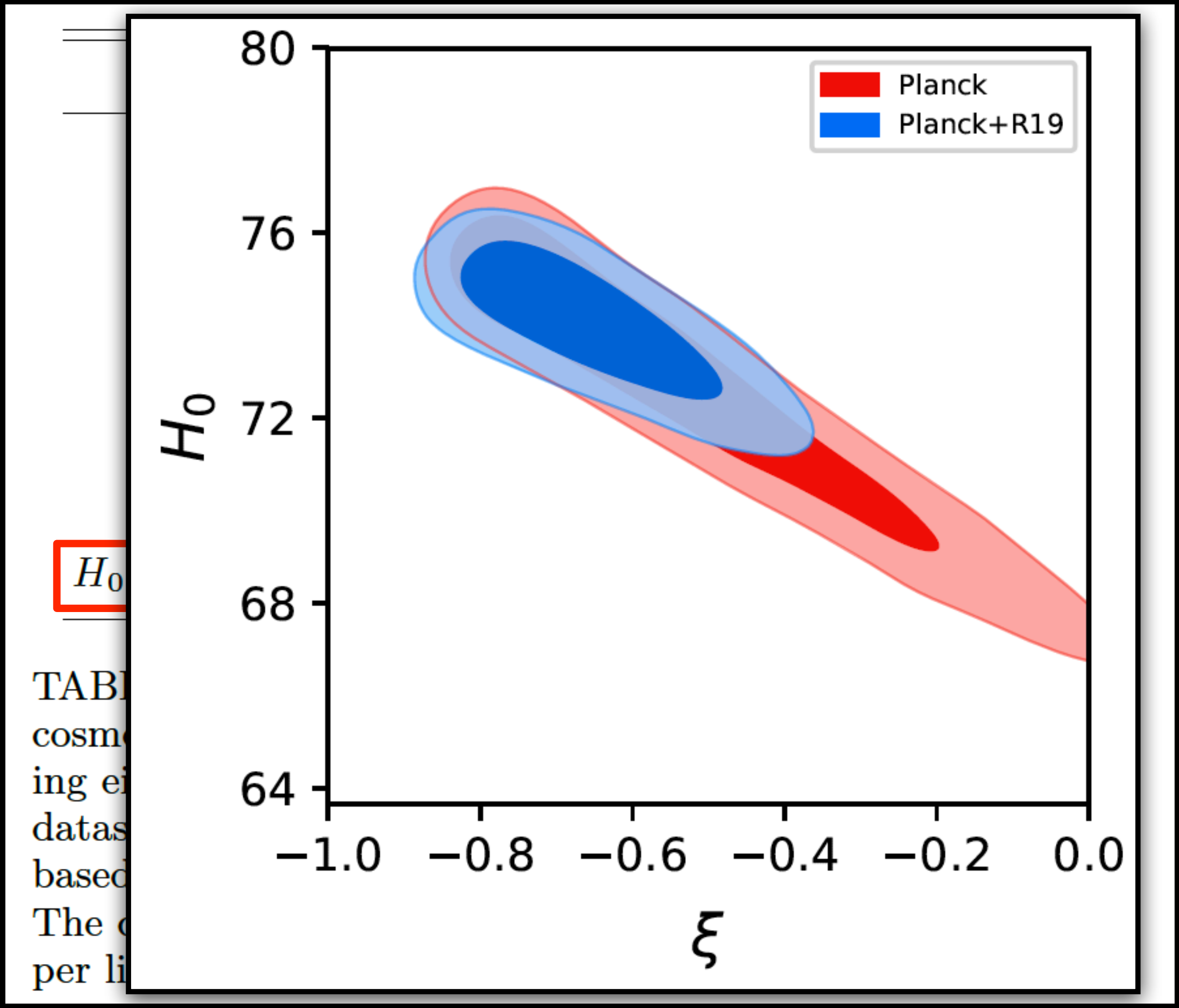

Di Valentino et al., Phys.Dark Univ. 30 (2020) 100666

The IDE case

Moreover, we find a shift of the clustering parameter σ_8 towards a higher value, compensated by a lowering of the matter density Ω_m, both with relaxed error bars.
The reason is that once a coupling is switched on and
Ω_m becomes smaller,
the clustering parameter σ_8 must be larger to have a proper normalization of the (lensing and clustering) power spectra.

This model can therefore significantly reduce the significance of the S8 tension
(See also Lucca, *Phys.Dark Univ.* 34 (2021) 100899)

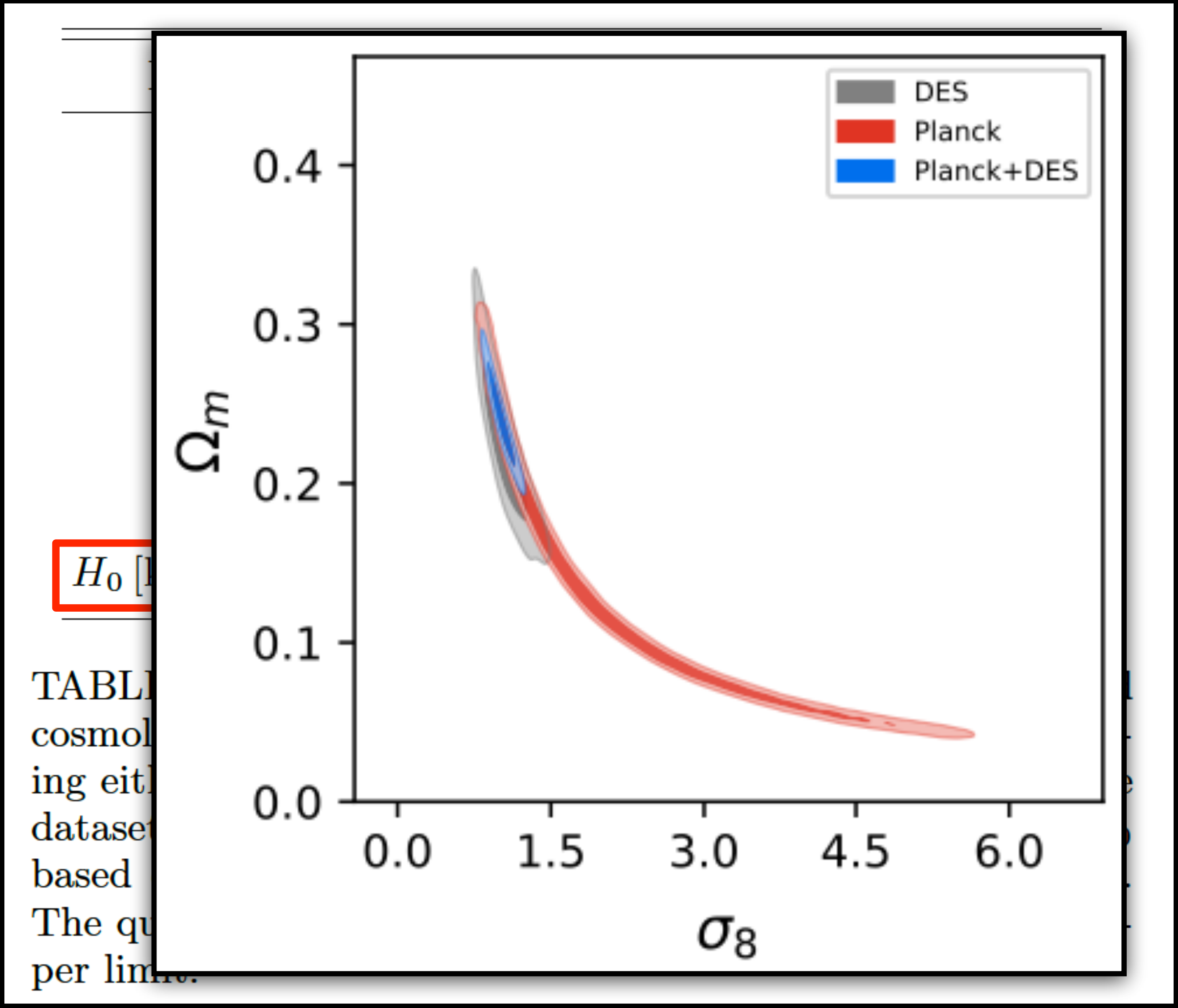

Di Valentino et al., Phys.Dark Univ. 30 (2020) 100666

IDE from ACT

Parameter	Planck	ACT	ACT+WMAP	ACT+Planck
$\Omega_\mathrm{b}h^2$	0.02237 ± 0.00015	0.02153 ± 0.00032	0.02238 ± 0.00020	0.02238 ± 0.00013
$\Omega_\mathrm{c}h^2$	$0.067^{+0.042}_{-0.031}\,(< 0.115)$	$< 0.0754\,(< 0.111)$	$0.070^{+0.046}_{-0.021}\,(< 0.117)$	$0.067^{+0.042}_{-0.030}\,(< 0.115)$
H_0	71.6 ± 2.1	$72.6^{+3.4}_{-2.6}$	$71.3^{+2.6}_{-3.2}$	$71.4^{+2.5}_{-2.8}$
τ_reio	0.0534 ± 0.0079	0.063 ± 0.015	0.061 ± 0.014	0.0533 ± 0.0073
$\log(10^{10}A_\mathrm{s})$	3.042 ± 0.016	3.046 ± 0.030	3.064 ± 0.028	3.047 ± 0.014
n_s	0.9655 ± 0.0045	1.010 ± 0.016	$0.9741^{+0.0066}_{-0.0064}$	0.9699 ± 0.0038
ξ	$-0.40^{+0.23}_{-0.20}$	$-0.46^{+0.20}_{-0.28}$	$-0.38^{+0.35}_{-0.14}$	$-0.40^{+0.27}_{-0.23}$
$\ln \mathcal{B}_{ij}$	-0.17	-0.07	0.06	-0.25

Zhai, Giarè, van de Bruck, Di Valentino, et al, *JCAP* 07 (2023) 032

Let's now consider different combinations of CMB datasets.

IDE from ACT

Parameter	Planck	ACT	ACT+WMAP	ACT+Planck
$\Omega_b h^2$	0.02237 ± 0.00015	0.02153 ± 0.00032	0.02238 ± 0.00020	0.02238 ± 0.00013
$\Omega_c h^2$	$0.067^{+0.}_{-0.}$		.7)	$0.067^{+0.042}_{-0.030}$ (< 0.115)
H_0	71.			$71.4^{+2.5}_{-2.8}$
$\tau_{\rm reio}$	0.053			0.0533 ± 0.0073
$\log(10^{10} A_s)$	3.04			3.047 ± 0.014
n_s	0.965			0.9699 ± 0.0038
ξ	−0.			$-0.40^{+0.27}_{-0.23}$
$\ln \mathcal{B}_{ij}$	-			-0.25

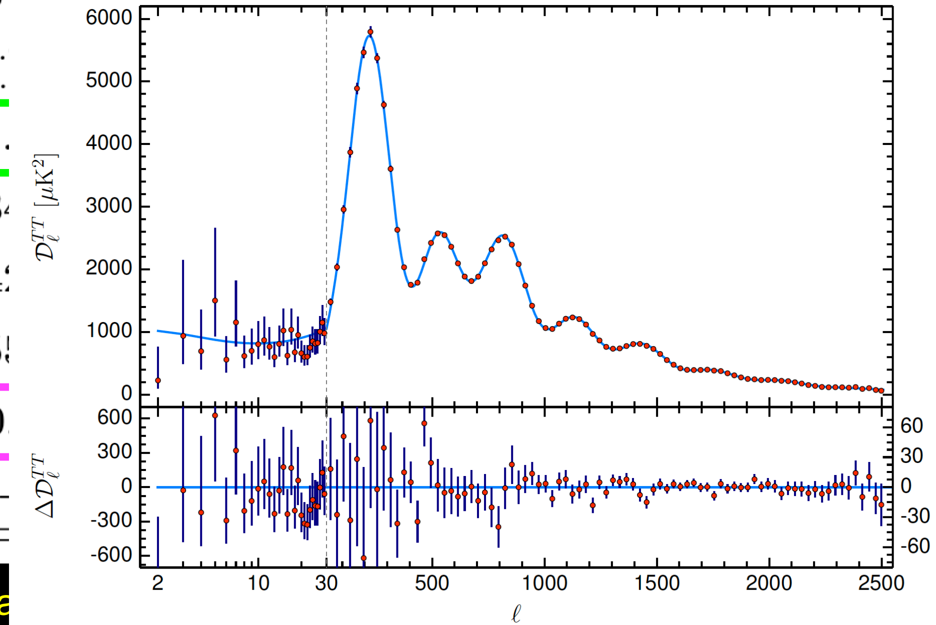

Zha ... 3) 032

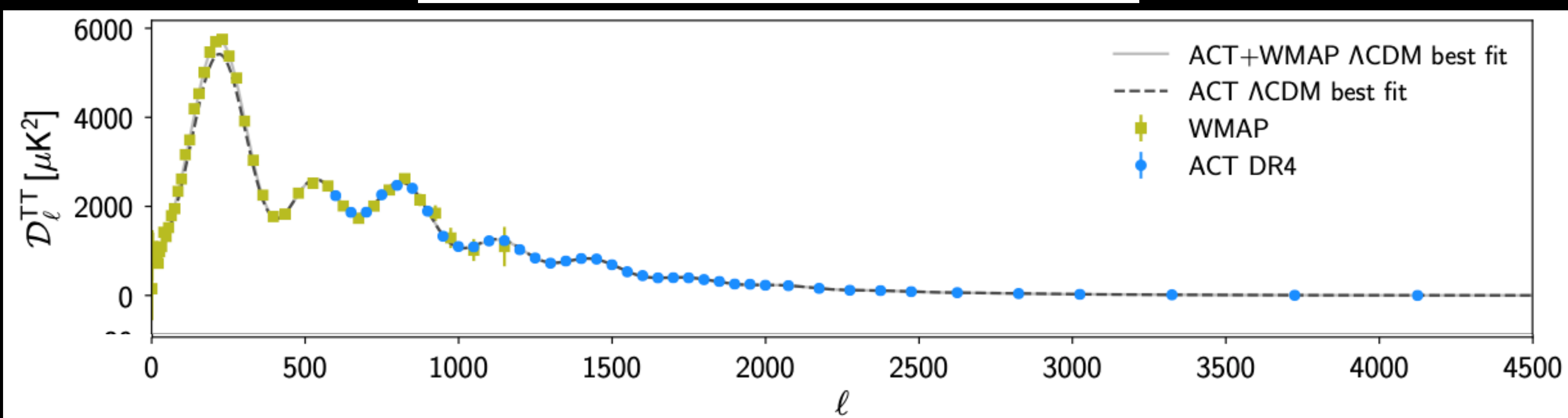

IDE from ACT

Parameter	Planck	ACT	ACT+WMAP	ACT+Planck
$\Omega_{\rm b}h^2$	0.02237 ± 0.00015	0.02153 ± 0.00032	0.02238 ± 0.00020	0.02238 ± 0.00013
$\Omega_{\rm c}h^2$	$0.067^{+0.042}_{-0.031}\,(< 0.115)$	$< 0.0754\,(< 0.111)$	$0.070^{+0.046}_{-0.021}\,(< 0.117)$	$0.067^{+0.042}_{-0.030}\,(< 0.115)$
H_0	71.6 ± 2.1	$72.6^{+3.4}_{-2.6}$	$71.3^{+2.6}_{-3.2}$	$71.4^{+2.5}_{-2.8}$
$\tau_{\rm reio}$	0.0534 ± 0.0079	0.063 ± 0.015	0.061 ± 0.014	0.0533 ± 0.0073
$\log(10^{10}A_{\rm s})$	3.042 ± 0.016	3.046 ± 0.030	3.064 ± 0.028	3.047 ± 0.014
$n_{\rm s}$	0.9655 ± 0.0045	1.010 ± 0.016	$0.9741^{+0.0066}_{-0.0064}$	0.9699 ± 0.0038
ξ	$-0.40^{+0.23}_{-0.20}$	$-0.46^{+0.20}_{-0.28}$	$-0.38^{+0.35}_{-0.14}$	$-0.40^{+0.27}_{-0.23}$
$\ln \mathcal{B}_{ij}$	-0.17	-0.07	0.06	-0.25

Zhai, Giarè, van de Bruck, Di Valentino, et al, *JCAP* 07 (2023) 032

If we consider different combinations of CMB datasets, they provide similar results, favoring IDE with a 95% CL significance in the majority of the cases. Remarkably, such a preference remains consistent when cross-checked through independent probes, while always yielding a value of the expansion rate H0 consistent with the local distance ladder measurements.

IDE from ACT

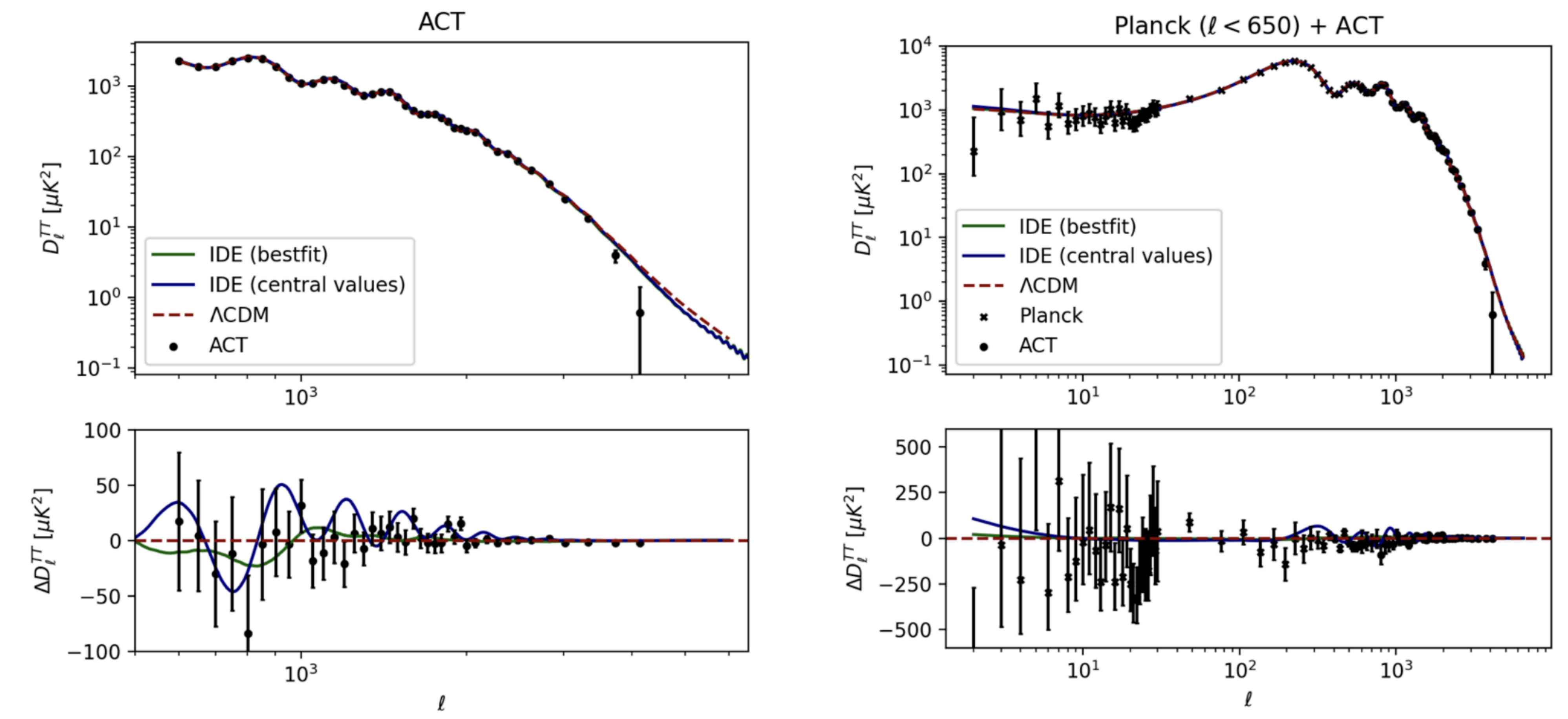

Zhai, Giarè, van de Bruck, Di Valentino, et al, *JCAP* 07 (2023) 032

It is easy to observe that the preference for $\xi < 0$
is primarily driven by the high multipole ACT CMB data that have a reduced amplitude.
These data are also responsible for the improvement of the fit
in the context of IDE models compared to the minimal ΛCDM,
indicating that it is a genuine effect rather than one caused by parameter degeneracies.

fake IDE detection

Parameters	Fiducial model	Planck	Planck+BAO	PICO	PRISM
$\Omega_b h^2$	0.02236	0.02238 ± 0.00015	0.02230 ± 0.00014	0.022364 ± 0.000029	0.022361 ± 0.000019
$\Omega_c h^2$	0.1202	$0.056^{+0.025}_{-0.047}$	$0.101^{+0.019}_{-0.006}$	$0.100^{+0.019}_{-0.008}$	$0.103^{+0.016}_{-0.007}$
$100\theta_{MC}$	1.04090	$1.0451^{+0.0021}_{-0.0032}$	$1.0419^{+0.0005}_{-0.0011}$	$1.04206^{+0.0005}_{-0.0011}$	$1.04191^{+0.00042}_{-0.00094}$
τ	0.0544	$0.0528^{+0.010}_{-0.009}$	0.0517 ± 0.0098	$0.0543^{+0.0016}_{-0.0019}$	$0.0542^{+0.0017}_{-0.0019}$
n_s	0.9649	0.9652 ± 0.0041	0.9624 ± 0.0036	0.9571 ± 0.0014	0.9657 ± 0.0012
$\ln(10^{10}A_s)$	3.045	$3.041^{+0.020}_{-0.018}$	3.042 ± 0.019	$3.0436^{+0.0030}_{-0.0034}$	3.0435 ± 0.0032
ξ	0	$-0.48^{+0.16}_{-0.30}$	> -0.223	> -0.220	> -0.195

Di Valentino & Mena, Mon.Not.Roy.Astron.Soc. 500 (2020) 1, L22-L26, arXiv:2009.12620

For a mock Planck-like experiment, due to the strong correlation present between the standard and the exotic physics parameters, there is a dangerous detection at more than 3σ for a coupling between dark matter and dark energy different from zero, even if the fiducial model has ξ =0:

$-0.85 < \xi < -0.02$ at 99% CL

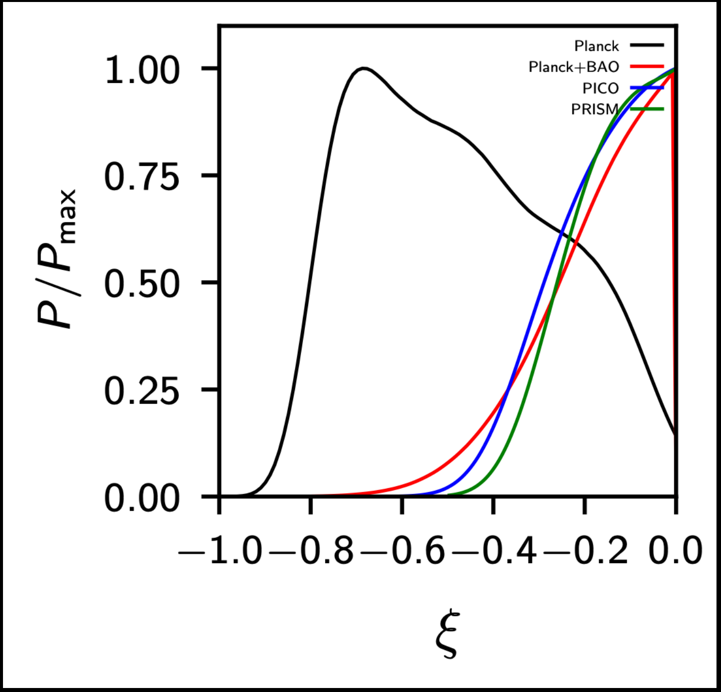

Mock experiments

fake IDE detection

Parameters	Fiducial model	Planck	Planck+BAO	PICO	PRISM
$\Omega_b h^2$	0.02236	0.02238 ± 0.00015	0.02230 ± 0.00014	0.022364 ± 0.000029	0.022361 ± 0.000019
$\Omega_c h^2$	0.1202	$0.056^{+0.025}_{-0.047}$	$0.101^{+0.019}_{-0.006}$	$0.100^{+0.019}_{-0.008}$	$0.103^{+0.016}_{-0.007}$
$100\theta_{MC}$	1.04090	$1.0451^{+0.0021}_{-0.0032}$	$1.0419^{+0.0005}_{-0.0011}$	$1.04206^{+0.0005}_{-0.0011}$	$1.04191^{+0.00042}_{-0.00094}$
τ	0.0544	$0.0528^{+0.010}_{-0.009}$	0.0517 ± 0.0098	$0.0543^{+0.0016}_{-0.0019}$	$0.0542^{+0.0017}_{-0.0019}$
n_s	0.9649	0.9652 ± 0.0041	0.9624 ± 0.0036	0.9571 ± 0.0014	0.9657 ± 0.0012
$\ln(10^{10} A_s)$	3.045	$3.041^{+0.020}_{-0.018}$	3.042 ± 0.019	$3.0436^{+0.0030}_{-0.0034}$	3.0435 ± 0.0032
ξ	0	$-0.48^{+0.16}_{-0.30}$	> -0.223	> -0.220	> -0.195

Di Valentino & Mena, Mon.Not.Roy.Astron.Soc. 500 (2020) 1, L22-L26, arXiv:2009.12620

The inclusion of mock BAO data, a mock dataset built using the same fiducial cosmological model than that of the CMB, helps in breaking the degeneracy, providing a lower limit for the coupling ξ in perfect agreement with zero.

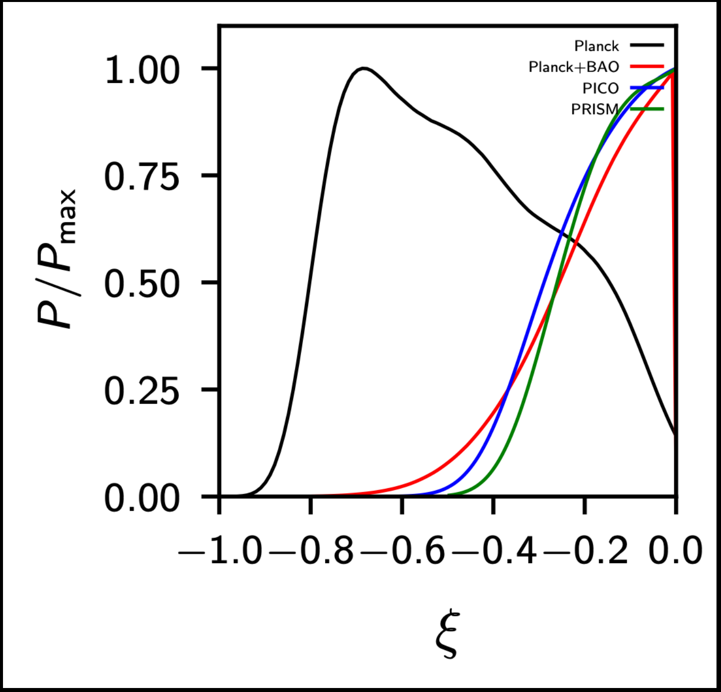

Mock experiments

The IDE case

Constraints at 68% cl.

Parameter	*CMB+BAO*	*CMB+FS*	*CMB+BAO+FS*
ω_c	$0.094^{+0.022}_{-0.010}$	$0.101^{+0.015}_{-0.009}$	$0.115^{+0.005}_{-0.001}$
ξ	$-0.22^{+0.18}_{-0.09}[> -0.48]$	> -0.35	> -0.12
H_0 [km/s/Mpc]	$69.55^{+0.98}_{-1.60}$	$69.04^{+0.84}_{-1.10}$	$68.02^{+0.49}_{-0.60}$
Ω_m	$0.243^{+0.054}_{-0.030}$	$0.261^{+0.038}_{-0.025}$	$0.299^{+0.015}_{-0.007}$

Nunes, Vagnozzi, Kumar, Di Valentino, and Mena, *Phys.Rev.D* 105 (2022) 12, 123506

The addition of low-redshift measurements, as BAO data, still hints to the presence of a coupling, albeit at a lower statistical significance. Also for this data sets the Hubble constant value is larger than that obtained in the case of a pure ΛCDM scenario, enough to bring the H0 tension at 2.1σ with SH0ES.

Baryon Acoustic Oscillations

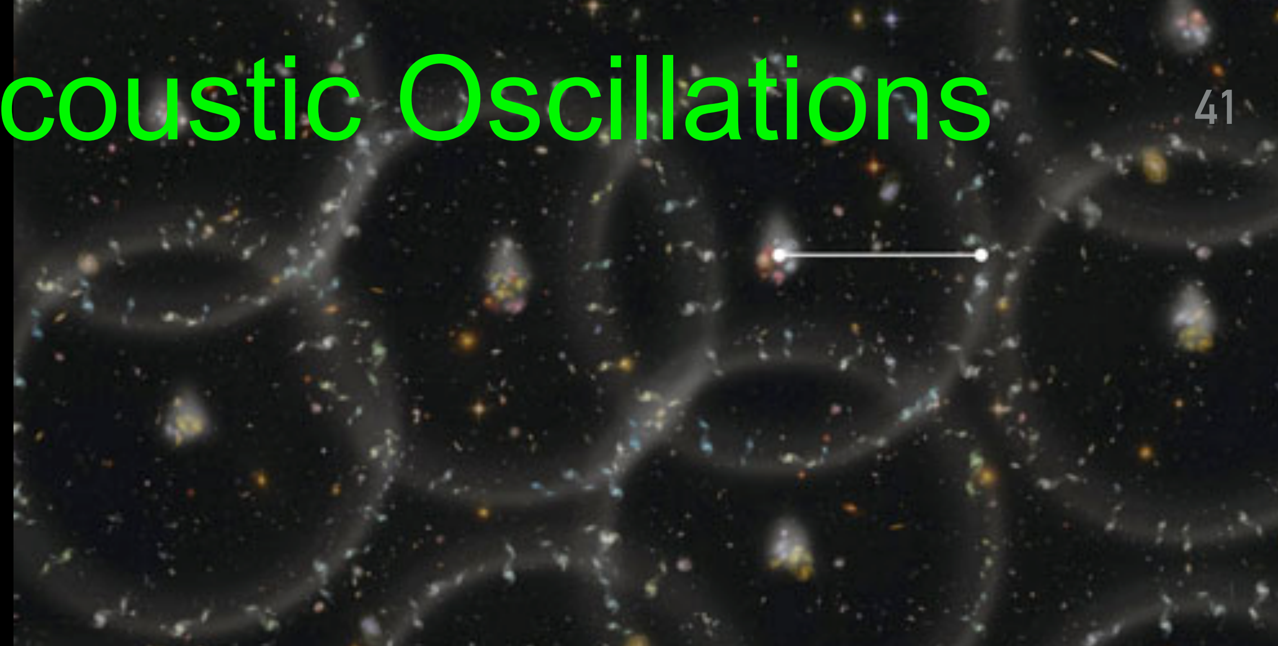

BAO is formed in the early universe, when baryons are strongly coupled to photons, and the gravitational collapse due to the CDM is counterbalanced by the radiation pressure. Sound waves that propagate in the early universe imprint a characteristic scale on the CMB. Since the scale of these oscillations can be measured at recombination, BAO is considered a "standard ruler". These fluctuations have evolved and we can observe BAO at low redshifts in the distribution of galaxies.

Since the data reduction process leading to these measurements involves making certain assumptions about the fiducial cosmology, this makes BAO measurements dependent on the cosmological model being used.

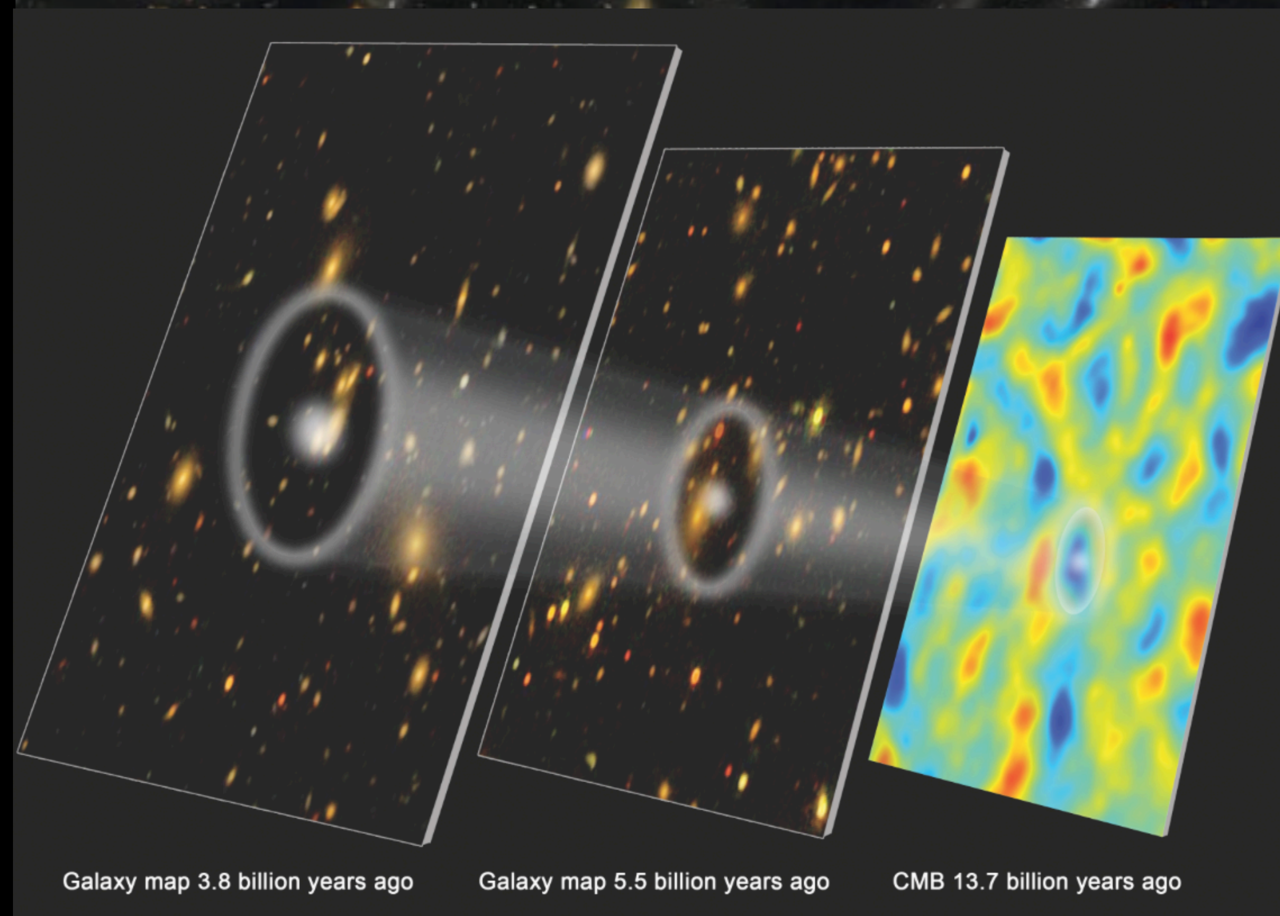

Baryon Acoustic Oscillations

In other words, the tension between Planck+BAO and SH0ES could be due to a statistical fluctuation in this case.

Actually, BAO data are extracted under the assumption of ΛCDM, and the modified scenario of interacting dark energy could affect the result.

In fact, the full procedure which leads to the BAO datasets carried out by the different collaborations might be not necessarily valid in extended DE models with important perturbations in the non-linear scales.

BAO datasets (both the pre- and post- reconstruction measurements) might need to be revised in a non-trivial manner when applied to constrain more exotic dark energy cosmologies.

Baryon Acoustic Oscillations

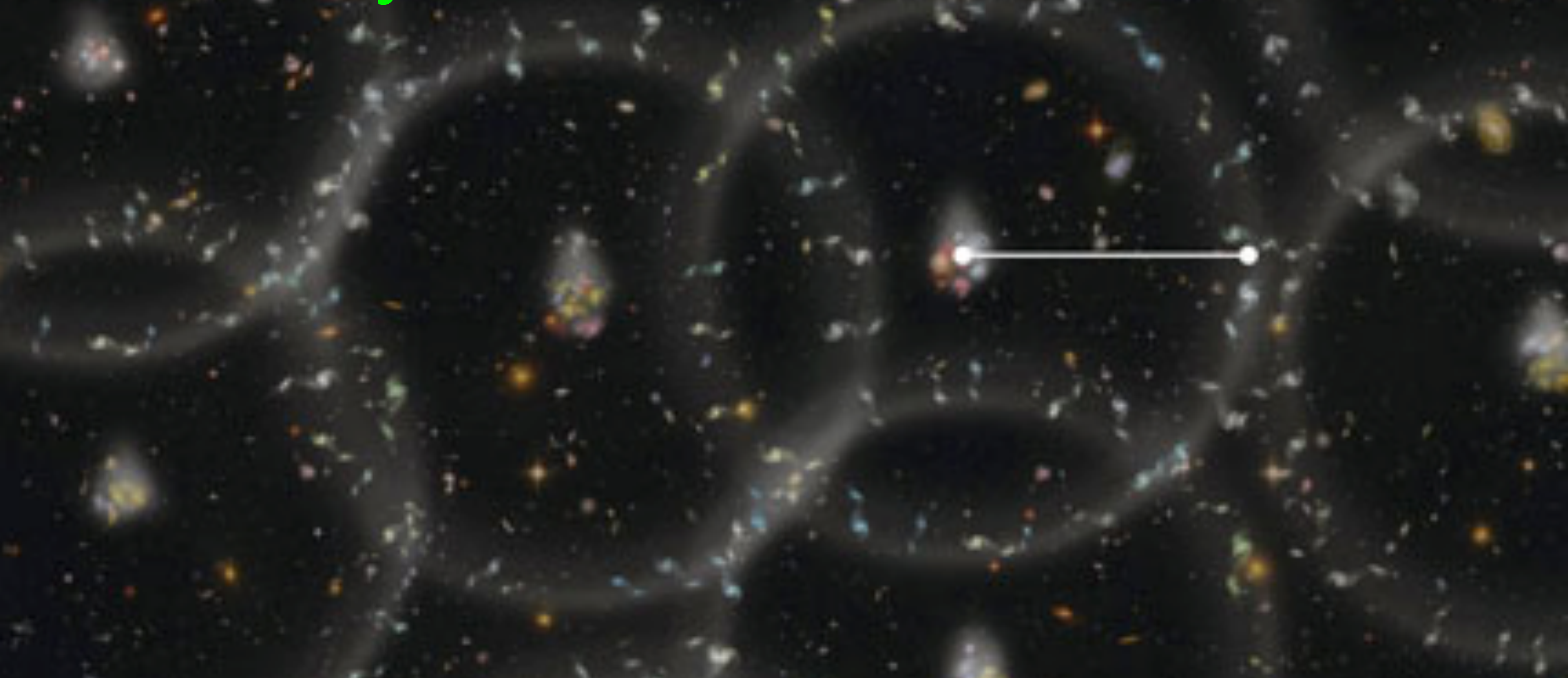

The problem is that for 3D BAO data one needs to reconstruct the comoving distance and this is done assuming a fiducial model.

We can try to see what happens using 2D BAO measurements, that are less model dependent because they are obtained working on spherical shells with redshift thickness Δz and only considering their angular distribution.

The IDE case

Parameter	Planck	+ lensing	Planck + BAO	+ lensing	Planck + BAOtr	+ lensing	Planck + BAOtr + H_0	+ lensing
H_0 [Km/s/Mpc]	67.32 ± 0.62	67.32 ± 0.53	67.65 ± 0.44	67.60 ± 0.43	69.01 ± 0.51	68.85 ± 0.55	69.88 ± 0.48	69.65 ± 0.44
S_8	0.832 ± 0.016	0.834 ± 0.013	0.825 ± 0.012	0.827 ± 0.011	0.794 ± 0.013	0.802 ± 0.012	0.774 ± 0.013	$0.7871^{+0.0095}_{-0.011}$
r_s [Mpc]	147.06 ± 0.30	147.04 ± 0.27	$147.21^{+0.23}_{-0.26}$	147.13 ± 0.23	147.75 ± 0.26	147.64 ± 0.26	148.06 ± 0.25	147.91 ± 0.24

A comparison between the 3D BAO data,
model dependent and obtained assuming ΛCDM,
and the 2D BAO measurements, less model dependent,
shows almost the same results for the ΛCDM scenario.

Bernui, Di Valentino, Giarè, Kumar, and Nunes, *Phys.Rev.D* 107 (2023) 10, 103531

The IDE case

Parameter		Planck	+ lensing	Planck + BAO	+ lensing	Planck + BAOtr	+ lensing	Planck + BAOtr + H_0	+ lensing
ξ	68% CL	$-0.43^{+0.28}_{-0.21}$	$-0.40^{+0.23}_{-0.20}$	> -0.207	> -0.210	$-0.683^{+0.088}_{-0.11}$	$-0.683^{+0.087}_{-0.12}$	-0.58 ± 0.11	-0.53 ± 0.11
	95% CL	(> -0.775)	$(-0.40^{+0.40}_{-0.32})$	(> -0.389)	(> -0.411)	$(-0.68^{+0.21}_{-0.19})$	$(-0.68^{+0.23}_{-0.20})$	$(-0.58^{+0.22}_{-0.21})$	$(-0.53^{+0.19}_{-0.20})$
	99% CL	$[> -0.819]$	$[> -0.743]$	$[> -0.486]$	$[> -0.527]$	$[-0.68^{+0.29}_{-0.23}]$	$[-0.68^{+0.37}_{-0.27}]$	$[-0.58^{+0.31}_{-0.29}]$	$[-0.53^{+0.39}_{-0.25}]$
H_0 [Km/s/Mpc]		$71.7^{+2.3}_{-2.7}$	71.6 ± 2.1	$68.93^{+0.79}_{-1.2}$	$69.08^{+0.74}_{-1.3}$	$75.2^{+1.2}_{-0.75}$	$75.3^{+1.3}_{-0.75}$	73.99 ± 0.88	$73.45^{+0.71}_{-0.59}$
S_8		$1.109^{+0.063}_{-0.28}$	$1.053^{+0.079}_{-0.21}$	$0.891^{+0.025}_{-0.062}$	$0.893^{+0.021}_{-0.065}$	$1.49^{+0.24}_{-0.29}$	1.49 ± 0.26	$1.23^{+0.11}_{-0.22}$	$1.15^{+0.10}_{-0.14}$
r_s [Mpc]		147.08 ± 0.30	147.12 ± 0.27	147.03 ± 0.25	147.05 ± 0.25	147.32 ± 0.27	147.35 ± 0.29	$147.31^{+0.25}_{-0.29}$	$147.32^{+0.26}_{-0.29}$
$\ln B_{ij}$		0.85	−0.17	1.60	0.60	−9.22	−11.68	−14.04	−15.21

A comparison between the 3D BAO data,
model dependent and obtained assuming ΛCDM,
and the 2D BAO measurements, less model dependent,
shows completely different results for the IDE model.
There is a strong evidence for the coupling at more than 99% CL,
solving at the same time the H0 tension with SH0ES.

Bernui, Di Valentino, Giarè, Kumar, and Nunes, *Phys.Rev.D* 107 (2023) 10, 103531

The IDE case

Parameter		Planck	ck + BAOtr + H_0	+ lensing
ξ	68% CL	$-0.43^{+0.}_{-0.}$	-0.58 ± 0.11	-0.53 ± 0.11
	95% CL	$(> -0.77$	$(-0.58^{+0.22}_{-0.21})$	$(-0.53^{+0.19}_{-0.20})$
	99% CL	$[> -0.81$	$[-0.58^{+0.31}_{-0.29}]$	$[-0.53^{+0.39}_{-0.25}]$
H_0 [Km/s/Mpc]		$71.7^{+2.}_{-2.}$	73.99 ± 0.88	$73.45^{+0.71}_{-0.59}$
S_8		$1.109^{+0.0}_{-0.2}$	$1.23^{+0.11}_{-0.22}$	$1.15^{+0.10}_{-0.14}$
r_s [Mpc]		147.08 ± 0	$147.31^{+0.25}_{-0.29}$	$147.32^{+0.26}_{-0.29}$
$\ln B_{ij}$		0.85	-14.04	-15.21

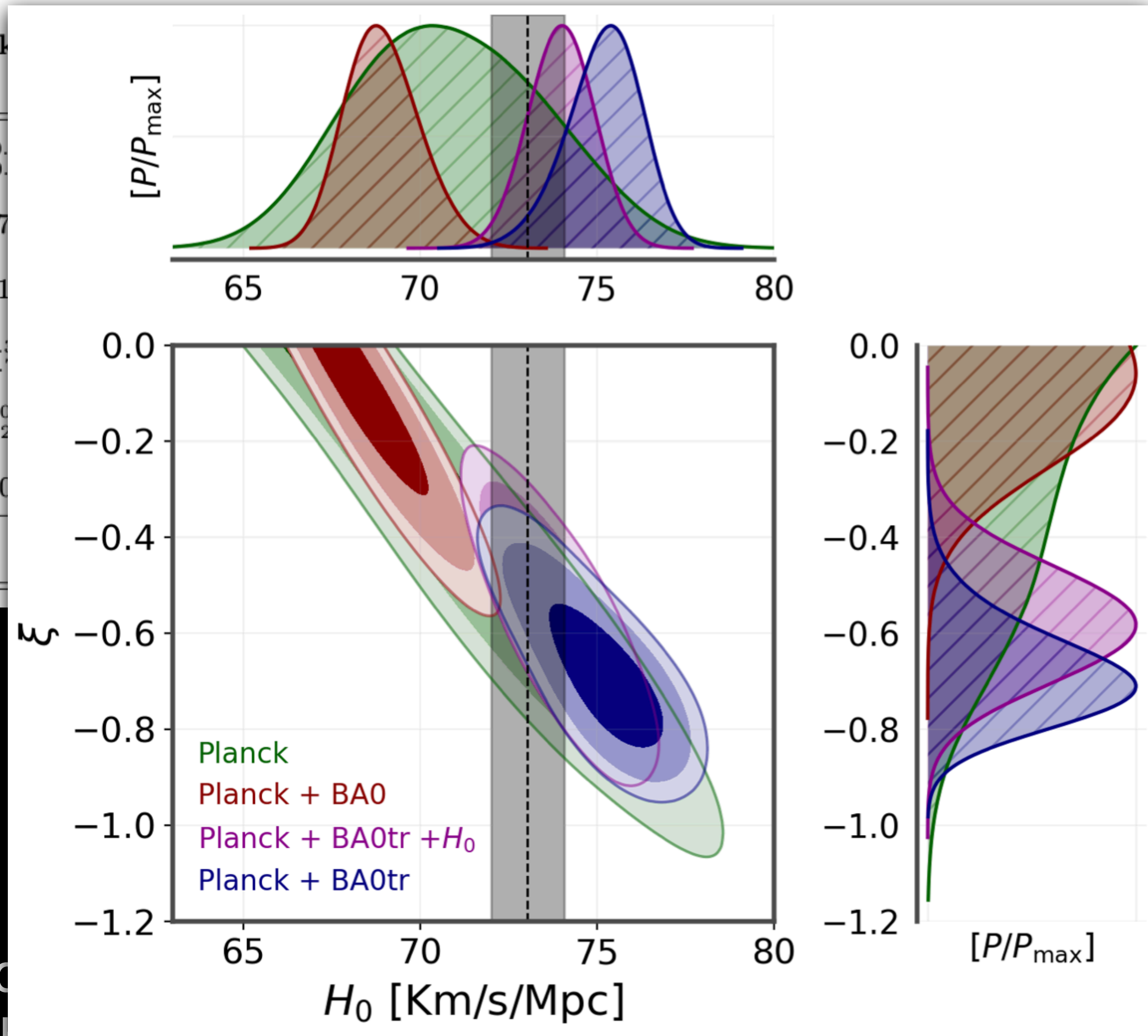

M,

anc ndent,

sl odel.

There is a strong evidence for the coupling at more than 99% CL, solving at the same time the H0 tension with SH0ES.

Bernui, Di Valentino, Giarè, Kumar, and Nunes, *Phys.Rev.D* 107 (2023) 10, 103531

The IDE case

Table II. Constraints at 68% CL on the parameters of the ΛCDM model.

Parameter	CMB	CMB+BAO-3D	CMB+BAO-2D (ON)	CMB+BAO-2D (M&M)
$10^2 \times \Omega_b h^2$	2.236 ± 0.015	2.245 ± 0.013	2.263 ± 0.014	2.246 ± 0.014
$\Omega_c h^2$	0.1202 ± 0.0014	0.11911 ± 0.00096	0.1165 ± 0.0011	0.11877 ± 0.00097
H_0	67.32 ± 0.62	67.84 ± 0.43	69.01 ± 0.51	67.96 ± 0.44
$\tau_{\rm reio}$	0.0536 ± 0.0081	0.0590 ± 0.0070	0.0606 ± 0.0081	0.0567 ± 0.0080
$\log(10^{10} A_s)$	3.043 ± 0.016	3.053 ± 0.015	3.049 ± 0.017	3.047 ± 0.016
n_s	0.9646 ± 0.0045	0.9677 ± 0.0037	0.9742 ± 0.0038	0.9688 ± 0.0037

A comparison between the 3D BAO data
and the 2D BAO measurements Menote & Marra arXiv:2112.10000,
from the same BOSS DR12 and eBOSS DR16,
gives exactly the same results for the ΛCDM scenario.

Giarè, Di Valentino, et al. in preparation

The IDE case

Table I. Constraints at 68% (95%) CL on the parameters of the IDE model.

Parameter	CMB	CMB+BAO-3D	CMB+BAO-2D (ON)	CMB+BAO-2D (M&M)
$10^2 \times \Omega_b h^2$	2.239 ± 0.015	2.236 ± 0.013	2.248 ± 0.014	2.237 ± 0.014
$\Omega_c h^2$	$0.067^{+0.042}_{-0.031}$ (< 0.115)	$0.101^{+0.016}_{-0.012}$	$0.022^{+0.014}_{-0.019}$	$0.089^{+0.019}_{-0.016}$
H_0	71.6 ± 2.1	$68.92^{+0.96}_{-1.2}$	$75.2^{+1.1}_{-0.96}$	69.9 ± 1.1
τ_{reio}	0.0534 ± 0.0079	0.0544 ± 0.0079	0.0556 ± 0.0082	0.0537 ± 0.0078
$\log(10^{10} A_s)$	3.042 ± 0.016	3.045 ± 0.016	3.044 ± 0.017	3.044 ± 0.016
n_s	0.9655 ± 0.0045	0.9650 ± 0.0037	0.9695 ± 0.0040	0.9657 ± 0.0039
ξ	$-0.40^{+0.23}_{-0.20}$ (> -0.775)	$> -0.207 (> -0.389)$	$-0.683^{+0.088}_{-0.11}$	$-0.26^{+0.18}_{-0.12}$ (> -0.505)

A comparison between the 3D BAO data and the 2D BAO measurements Menote & Marra arXiv:2112.10000, from the same BOSS DR12 and eBOSS DR16, gives different H0 values for the IDE scenario.

Giarè, Di Valentino, et al. in preparation

Baryon Acoustic Oscillations

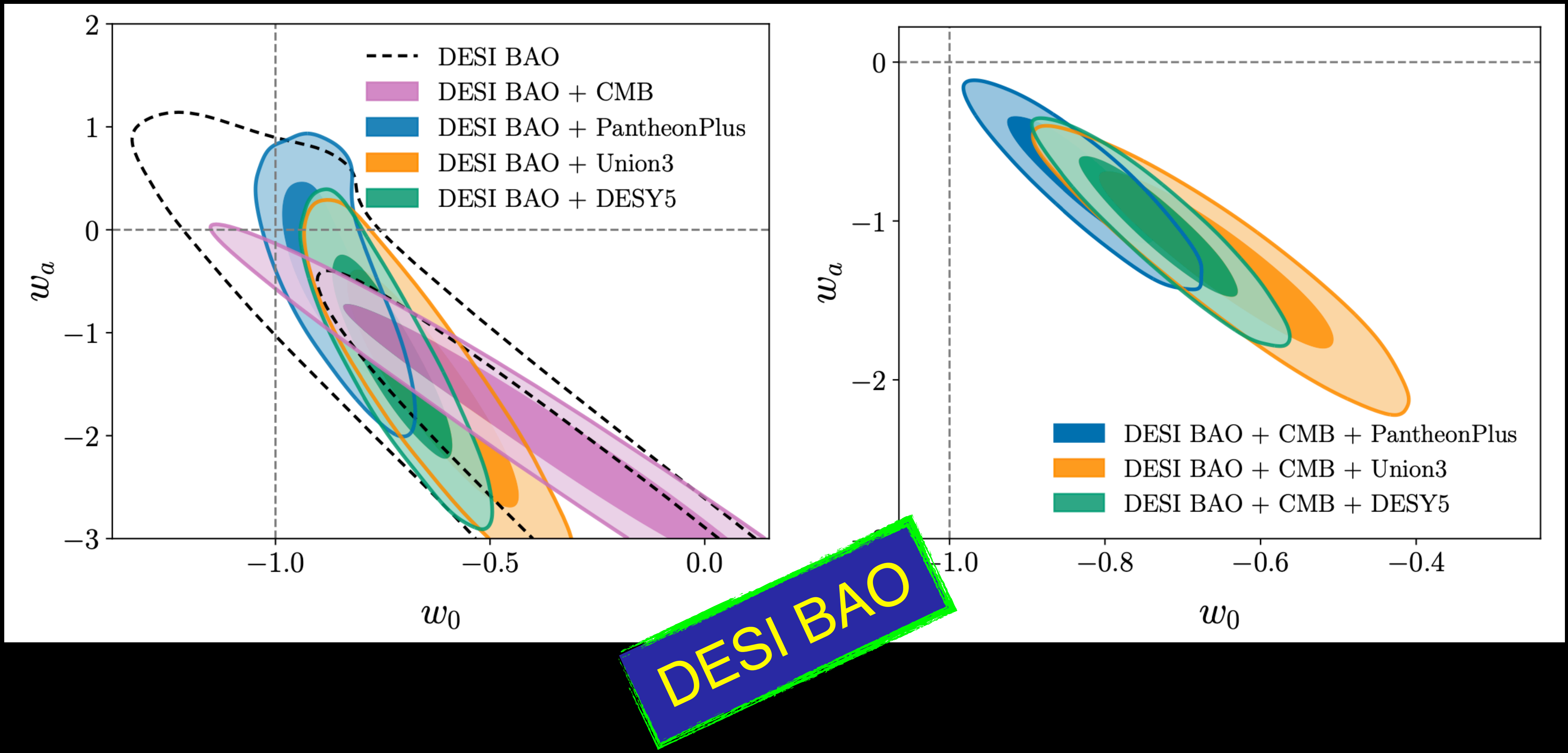

DESI collaboration, Adame et al., arXiv:2404.03002

Baryon Acoustic Oscillations

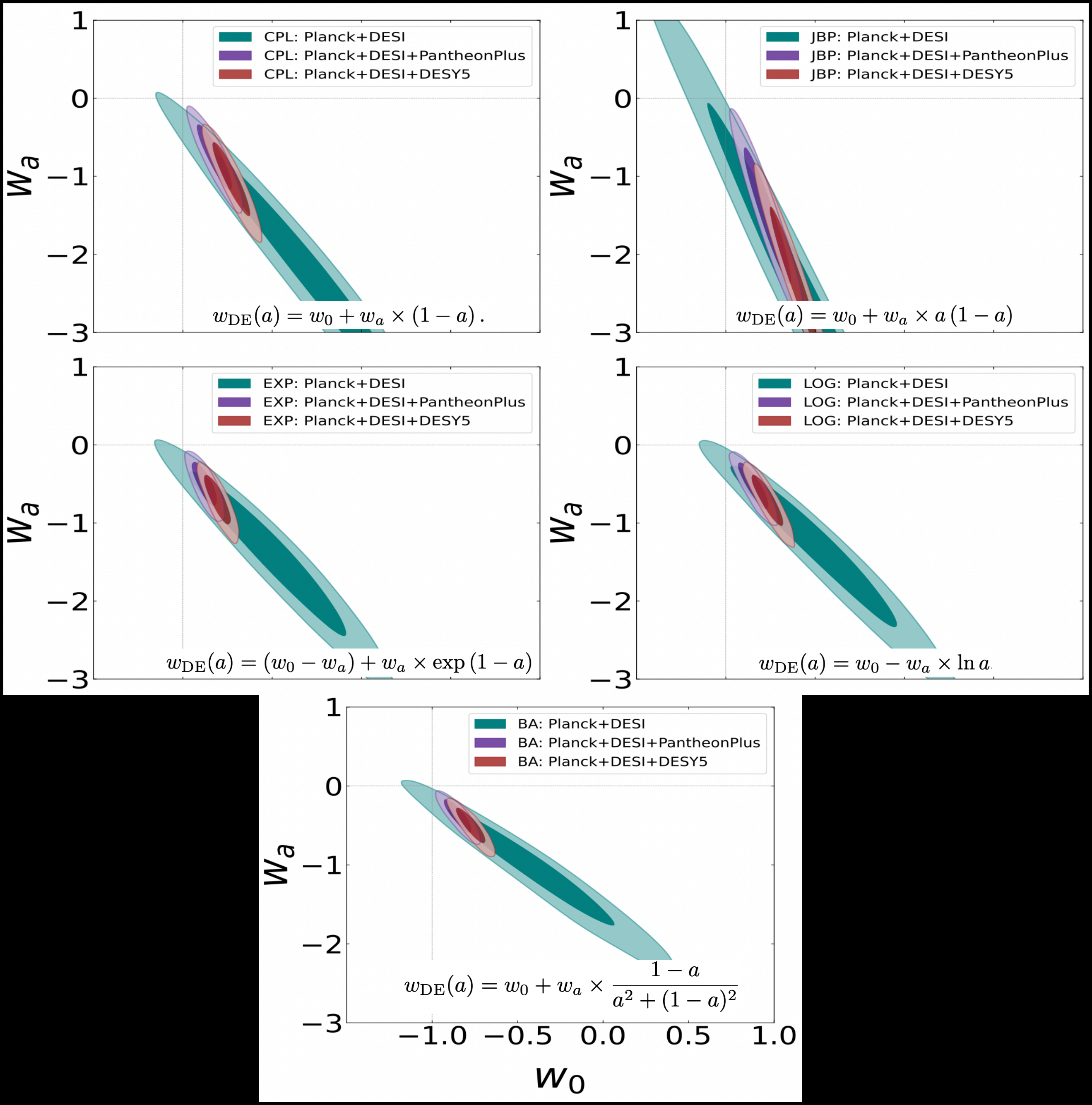

Giarè, Najafi, Pan, Di Valentino & Firouzjaee, arXiv:2404.03002

Constraints at 68% cl.

The IDE case

Parameter	Planck-2018+DESI	Planck-2018+DESI+SN
$\Omega_b h^2$	$0.02243 \pm 0.00014\,(0.02243^{+0.00028}_{-0.00026})$	$0.02254 \pm 0.00013\,(0.02254^{+0.00026}_{-0.00027})$
$\Omega_c h^2$	$0.079^{+0.025}_{-0.016}\,(0.079^{+0.037}_{-0.042})$	$0.0962^{+0.0085}_{-0.0074}\,(0.096^{+0.015}_{-0.015})$
$100\theta_s$	$1.04198 \pm 0.00029\,(1.04198^{+0.00056}_{-0.00056})$	$1.04211 \pm 0.00028\,(1.04211^{+0.00055}_{-0.00057})$
τ_{reio}	$0.0555 \pm 0.0074\,(0.055^{+0.015}_{-0.014})$	$0.0592^{+0.0069}_{-0.0079}\,(0.059^{+0.016}_{-0.014})$
n_s	$0.9672 \pm 0.0037\,(0.9672^{+0.0073}_{-0.0072})$	$0.9696 \pm 0.0038\,(0.9696^{+0.0075}_{-0.0073})$
$\log(10^{10} A_s)$	$3.045 \pm 0.014\,(3.045^{+0.029}_{-0.028})$	$3.051 \pm 0.015\,(3.051^{+0.031}_{-0.028})$
ξ	$-0.32^{+0.18}_{-0.14}\,(-0.32^{+0.30}_{-0.29})$	$-0.186 \pm 0.068\,(-0.19^{+0.13}_{-0.14})$
H_0 [km/s/Mpc]	$70.8^{+1.4}_{-1.7}\,(70.8^{+2.8}_{-2.7})$	$69.87 \pm 0.60\,(69.9^{+1.2}_{-1.2})$
Ω_m	$0.206^{+0.056}_{-0.044}\,(0.206^{+0.090}_{-0.096})$	$0.245 \pm 0.020\,(0.245^{+0.037}_{-0.039})$
σ_8	$1.23^{+0.14}_{-0.36}\,(1.23^{+0.74}_{-0.52})$	$0.974^{+0.059}_{-0.088}\,(0.97^{+0.15}_{-0.14})$
r_{drag} [Mpc]	$147.28 \pm 0.23\,(147.28^{+0.45}_{-0.45})$	$147.42 \pm 0.23\,(147.42^{+0.44}_{-0.46})$
$\Delta\chi^2$	-1.02	-2.27
$\ln \mathcal{B}_{ij}$	-0.10	-0.32

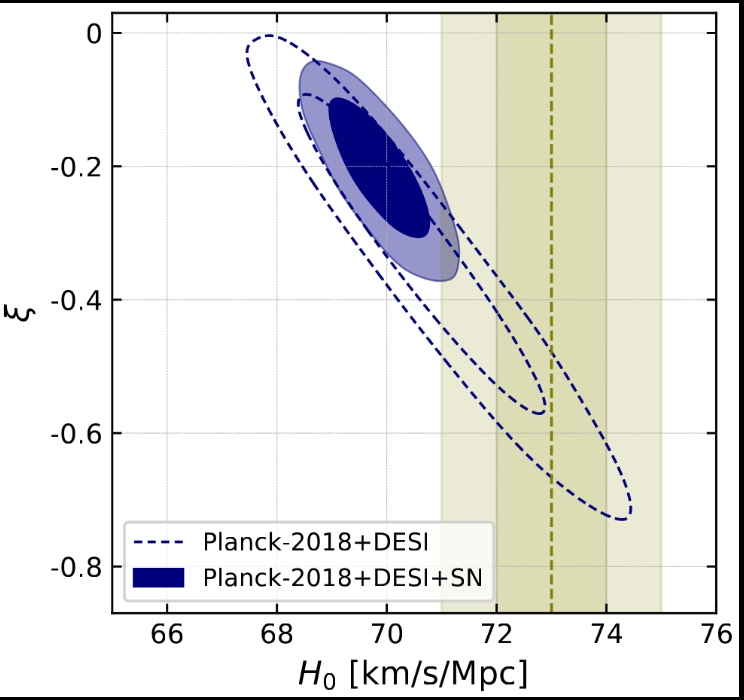

Giarè, Sabogal, Nunes, Di Valentino, arXiv:2404.15232

By combining Planck-2018 and DESI data,
we observe a preference for interactions exceeding the 95% CL, yielding a present-day expansion rate $H0 = 70.8^{+1.4}_{-1.7}$ km/s/Mpc, in agreement with SH0ES at less than 1.3σ.
This preference remains robust when including Type-Ia Supernovae sourced from the Pantheon-plus catalog using the SH0ES Cepheid host distances as calibrators.

Constraints at 68% cl.

The IDE case

Parameter	Planck-2018+DESI	Planck-2018+DESI+SN
$\Omega_\mathrm{b} h^2$	$0.02243 \pm 0.00014\,(0.02243^{+0.00028}_{-0.00026})$	$0.02254 \pm 0.00013\,(0.02254^{+0.00026}_{-0.00027})$
$\Omega_\mathrm{c} h^2$	$0.079^{+0.025}_{-0.016}\,(0.079^{+0.037}_{-0.042})$	$0.0962^{+0.0085}_{-0.0074}\,(0.096^{+0.015}_{-0.015})$
$100\theta_\mathrm{s}$	$1.04198 \pm 0.00029\,(1.04198^{+0.00056}_{-0.00056})$	$1.04211 \pm 0.00028\,(1.04211^{+0.00055}_{-0.00057})$
τ_reio	$0.0555 \pm 0.0074\,(0.055^{+0.015}_{-0.014})$	$0.0592^{+0.0069}_{-0.0079}\,(0.059^{+0.016}_{-0.014})$
n_s	$0.9672 \pm 0.0037\,(0.9672^{+0.0073}_{-0.0072})$	$0.9696 \pm 0.0038\,(0.9696^{+0.0075}_{-0.0073})$
$\log(10^{10} A_\mathrm{s})$	$3.045 \pm 0.014\,(3.045^{+0.029}_{-0.028})$	$3.051 \pm 0.015\,(3.051^{+0.031}_{-0.028})$
ξ	$-0.32^{+0.18}_{-0.14}\,(-0.32^{+0.30}_{-0.29})$	$-0.186 \pm 0.068\,(-0.19^{+0.13}_{-0.14})$
H_0 [km/s/Mpc]	$70.8^{+1.4}_{-1.7}\,(70.8^{+2.8}_{-2.7})$	$69.87 \pm 0.60\,(69.9^{+1.2}_{-1.2})$
Ω_m	$0.206^{+0.056}_{-0.044}\,(0.206^{+0.090}_{-0.096})$	$0.245 \pm 0.020\,(0.245^{+0.037}_{-0.039})$
σ_8	$1.23^{+0.14}_{-0.36}\,(1.23^{+0.74}_{-0.52})$	$0.974^{+0.059}_{-0.088}\,(0.97^{+0.15}_{-0.14})$
r_drag [Mpc]	$147.28 \pm 0.23\,(147.28^{+0.45}_{-0.45})$	$147.42 \pm 0.23\,(147.42^{+0.44}_{-0.46})$
$\Delta\chi^2$	-1.02	-2.27
$\ln \mathcal{B}_{ij}$	-0.10	-0.32

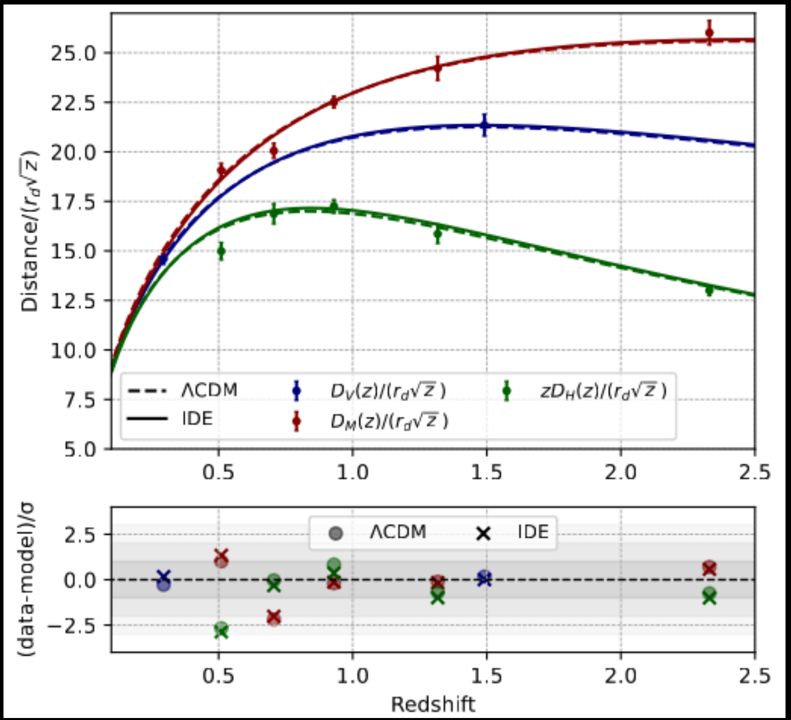

Giarè, Sabogal, Nunes, Di Valentino, arXiv:2404.15232

Overall, high and low redshift data can be equally or better explained within the IDE framework compared to ΛCDM, while also yielding higher values of H0 in better agreement with the local distance ladder estimate.

What if the problem is on the CMB side?

A_L internal anomaly

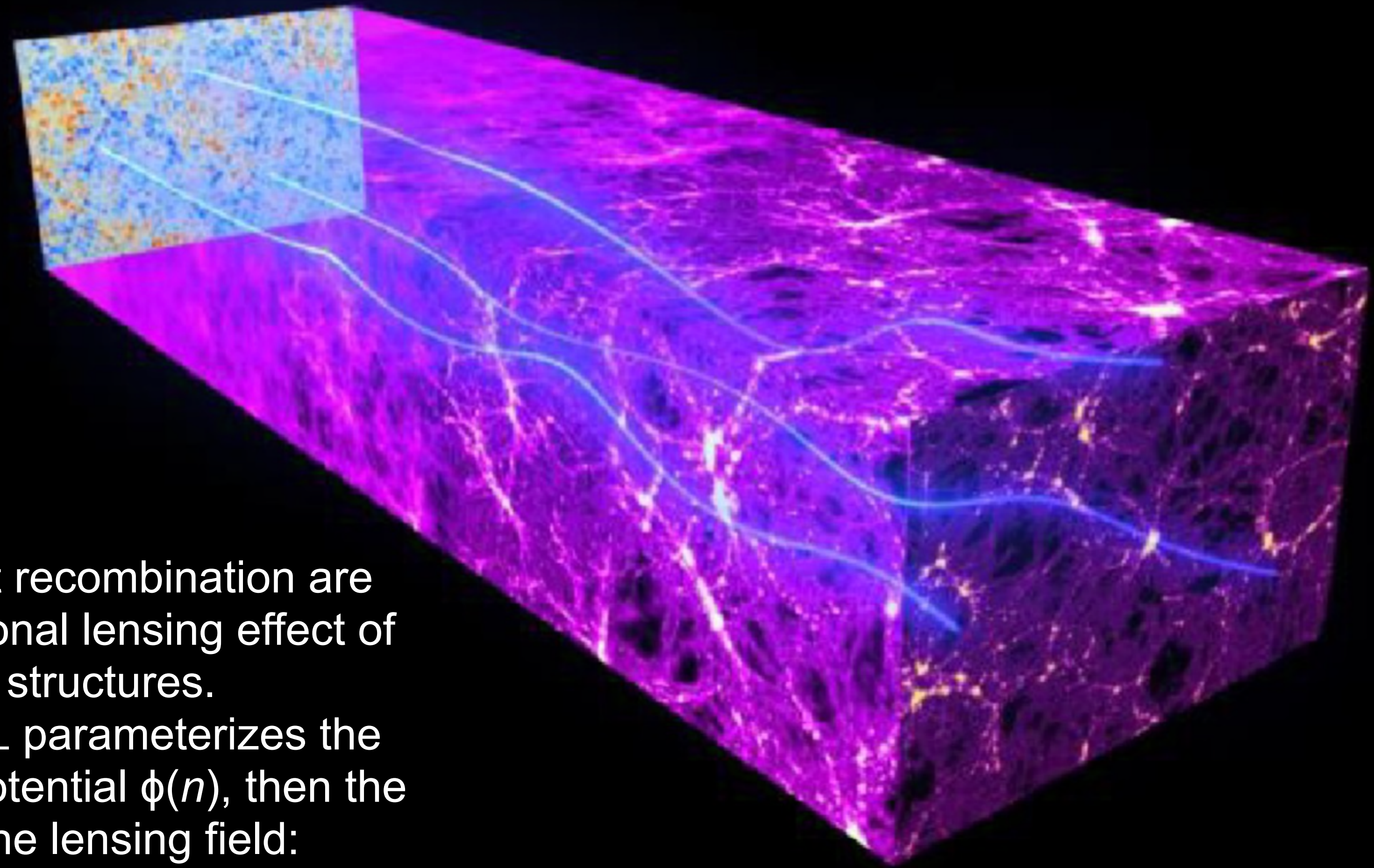

CMB photons emitted at recombination are deflected by the gravitational lensing effect of massive cosmic structures.
The lensing amplitude A_L parameterizes the rescaling of the lensing potential ϕ(*n*), then the power spectrum of the lensing field:

$$C_\ell^{\phi\phi} \to A_\mathrm{L} C_\ell^{\phi\phi}$$

The gravitational lensing deflects the photon path by a quantity defined by the gradient of the lensing potential ϕ(*n*), integrated along the line of sight *n*, remapping the temperature field.

A_L internal anomaly

Its effect on the power spectrum is the smoothing of the acoustic peaks, increasing AL.

Interesting consistency checks is if the amplitude of the smoothing effect in the CMB power spectra matches the theoretical expectation AL = 1 and whether the amplitude of the smoothing is consistent with that measured by the lensing reconstruction.

If AL =1 then the theory is correct, otherwise we have a new physics or systematics.

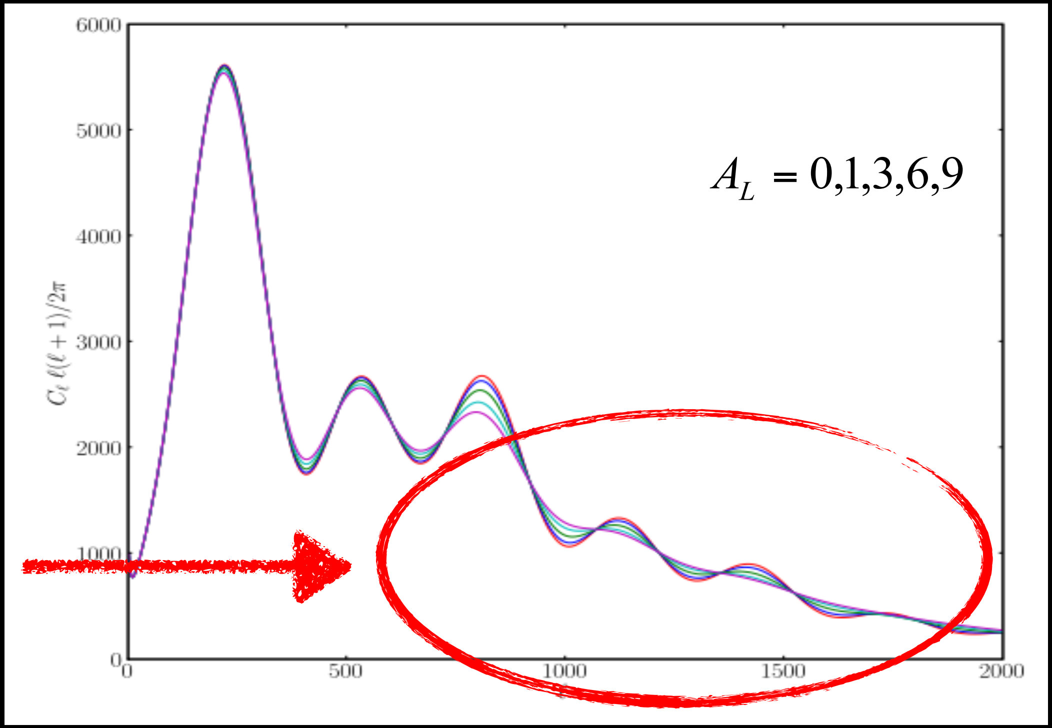

Calabrese et al., Phys. Rev. D, 77, 123531

A_L : a failed consistency check

The Planck lensing-reconstruction power spectrum is consistent with the amplitude expected for ΛCDM models that fit the CMB spectra, so the Planck lensing measurement is compatible with AL = 1.

However, the distributions of AL inferred from the CMB power spectra alone indicate a preference for AL > 1.

The joint combined likelihood shifts the value preferred by the TT data downwards towards AL = 1, but the error also shrinks, increasing the significance of AL > 1 to 2.8σ.

The preference for high AL is not just a volume effect in the full parameter space, with the best fit improved by $\Delta\chi^2$~9 when adding AL for TT+lowE and 10 for TTTEEE+lowE.

Planck 2018, Astron.Astrophys. 641 (2020) A6

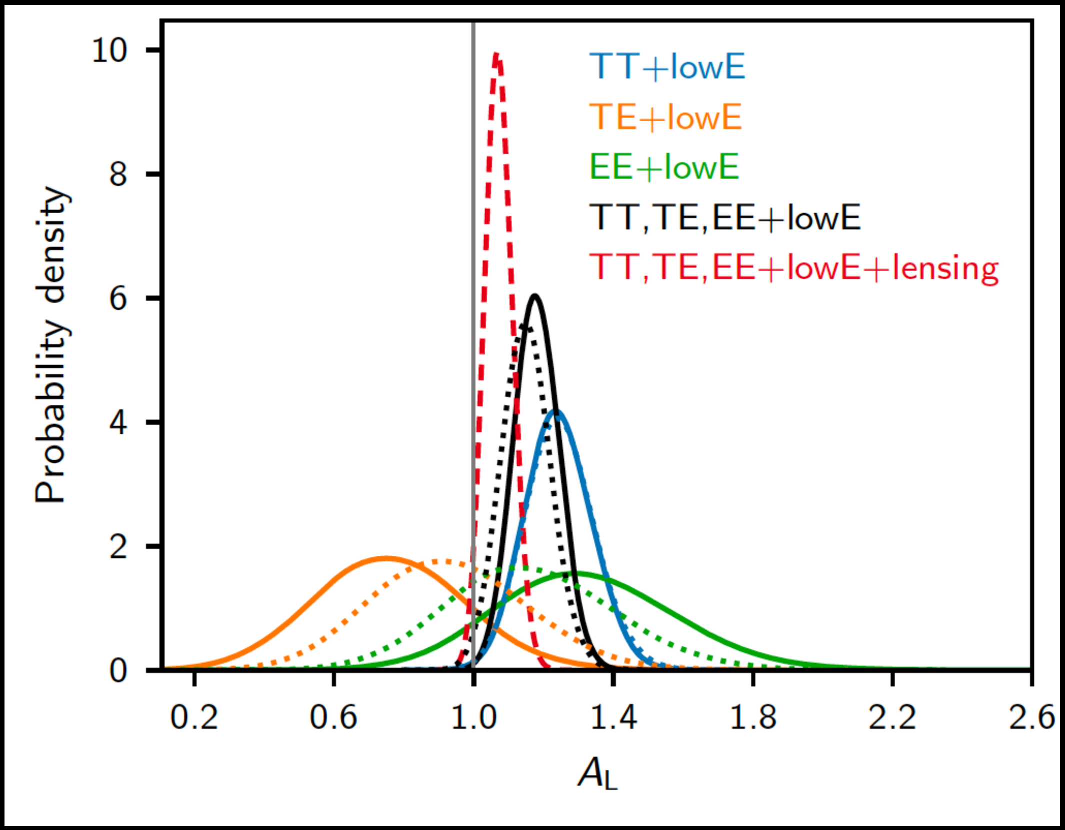

$$A_L = 1.243 \pm 0.096 \quad (68\,\%,\ \textit{Planck}\ \mathrm{TT+lowE}),$$
$$A_L = 1.180 \pm 0.065 \quad (68\,\%,\ \textit{Planck}\ \mathrm{TT,TE,EE+lowE}),$$

A_L can explain the S8 tension

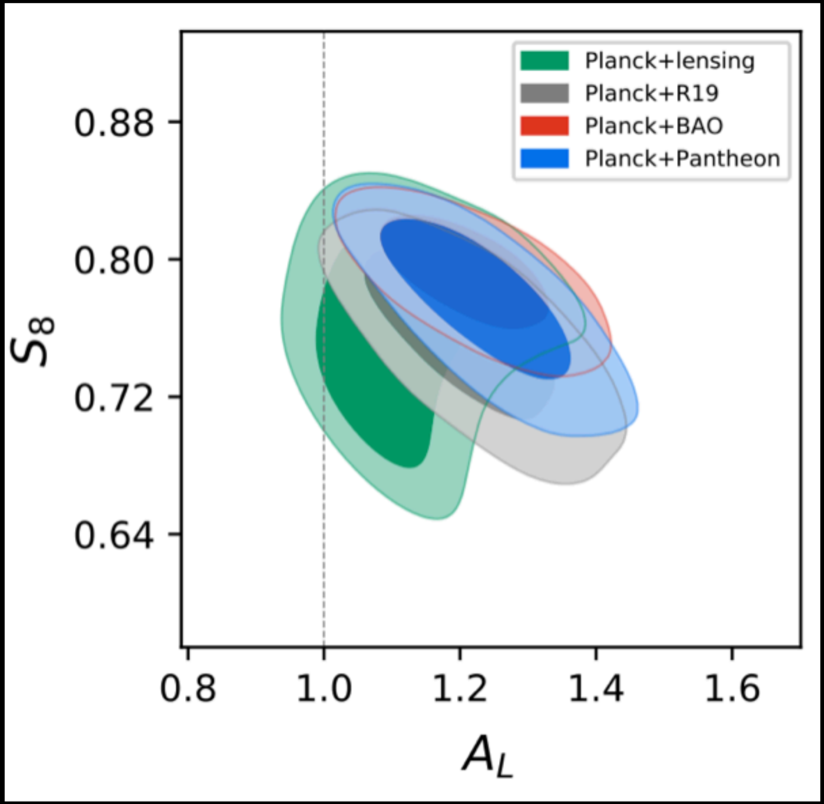

Di Valentino, Melchiorri and Silk, JCAP 2001 (2020) no.01, 013

A_L that is larger than the expected value at about 3 standard deviations even when combining the Planck data with BAO and supernovae type Ia external datasets.

Alternative CMB are not in significant tension

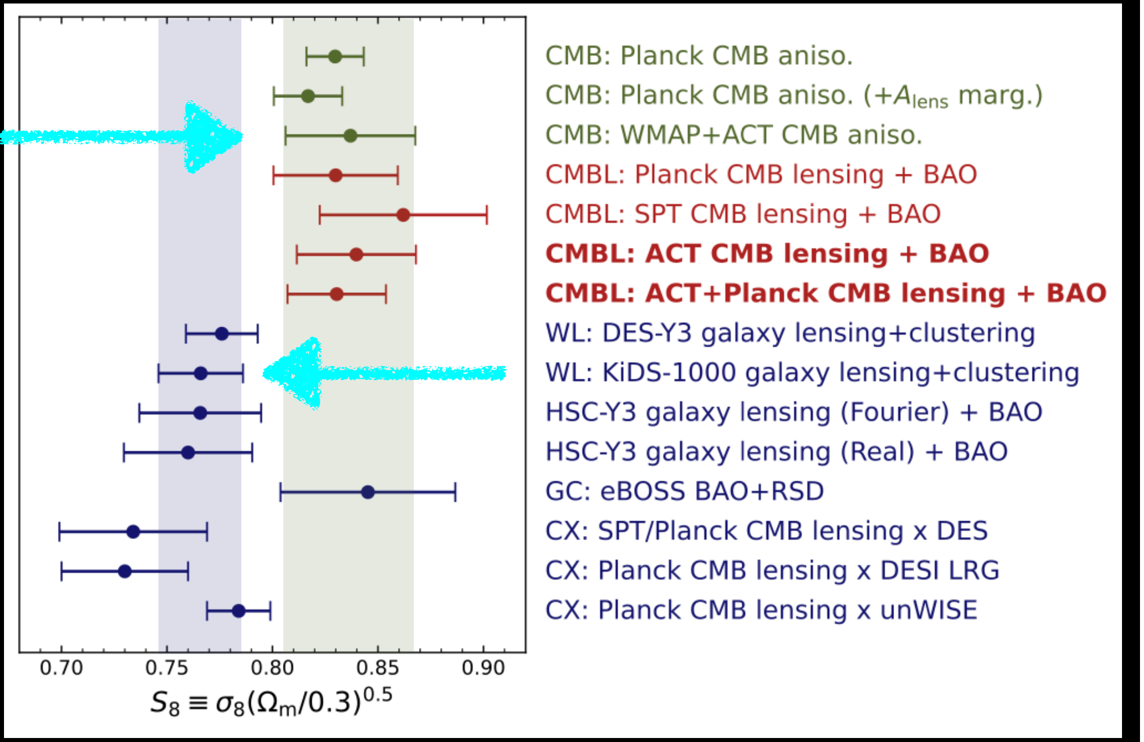

ACT collaboration, arXiv:2304.05203

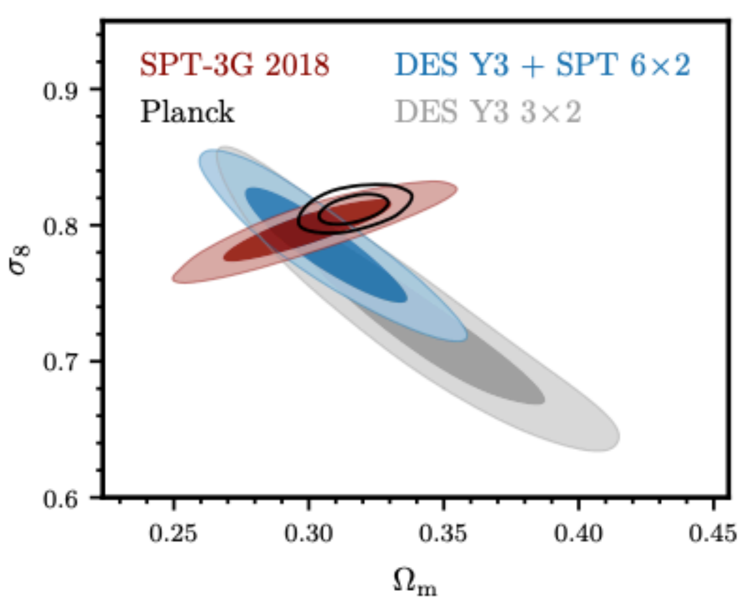

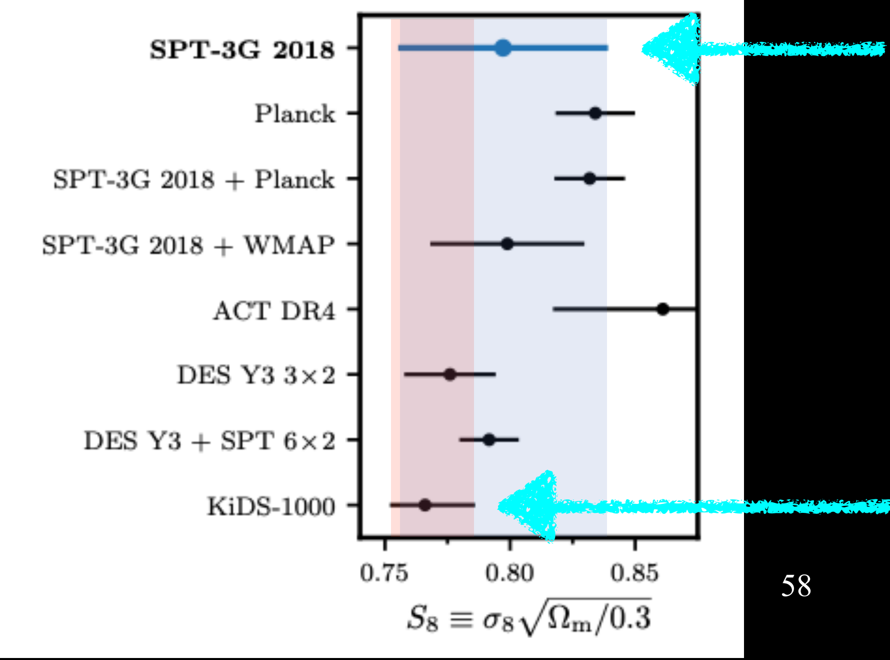

SPT-3G collaboration, arXiv:2212.05642

But…
assuming General Relativity,
is there a physical explanation
for A_L?

Astronomy & Astrophysics manuscript no. ms
September 24, 2019

Planck 2018 results. VI. Cosmological parameters

Planck Collaboration: N. Aghanim[54], Y. Akrami[15,57,59], M. Ashdown[65,5], J. Aumont[95], C. Baccigalupi[78], M. Ballardini[21,41], A. J. Banday[95,8], R. B. Barreiro[61], N. Bartolo[29,62], S. Basak[85], R. Battye[64], K. Benabed[55,90], J.-P. Bernard[95,8], M. Bersanelli[32,45], P. Bielewicz[75,78], J. J. Bock[63,10], J. R. Bond[7], J. Borrill[12,93], F. R. Bouchet[55,90], F. Bou
J.-F. Cardoso[55,90], J. Carron[23], A. Challinor[58,65,11], H. C. Chi
F. Cuttaia[41], P. de Bernardis[31], G. de Zotti[42], J. Delabroui
A. Ducout[66], X. Dupac[35], S. Dusini[62], G. Efstathiou[65
J. Fergusson[11], R. Fernandez-Cobos[61], F. Finelli[41,47], F. For
S. Galli[55,90†], K. Ganga[2], R. T. Génova-Santos[60,16], M.
A. Gruppuso[41,47], J. E. Gudmundsson[94,25], J. Hamann[86],
Z. Huang[83], A. H. Jaffe[53], W. C. Jones[25], A. Karakci[59],
N. Krachmalnicoff[78], M. Kunz[14,54,3], H. Kurki-Suonio[24,40],
M. Le Jeune[2], P. Lemos[58,65], J. Lesgourgues[56], F. Levri
M. López-Caniego[35], P. M. Lubin[28], Y.-Z. Ma[77,80,74], J.
A. Marcos-Caballero[61], M. Maris[43], P. G. Martin[7], M. Mar
P. R. Meinhold[28], A. Melchiorri[31,50], A. Mennella[32,45]
D. Molinari[30,41,48], L. Montier[95,8], G. Morgante[41], A. Mo
B. Partridge[39], G. Patanchon[2], H. V. Peiris[22], F. Perrot
J. P. Rachen[18], M. Reinecke[72], M. Remazeilles[64], A.
B. Ruiz-Granados[60,16], L. Salvati[54], M. Sandri[41], M. Savelai
R. Sunyaev[72,91], A.-S. Suur-Uski[24,40], J. A. Tauber[36], D.
L. Valenziano[41], J. Valiviita[24,40], B. Van Tent[69], L. Vibert[54
S. D. M. W
(*Affiliation*

We present cosmological parameter results from the final f
isotropies, combining information from the temperature an
improved measurements of large-scale polarization allow th
cant gains in the precision of other correlated parameters. Im
many parameters, with residual modelling uncertainties estim
spatially-flat 6-parameter ΛCDM cosmology having a power
from polarization, temperature, and lensing, separately and i
baryon density $\Omega_b h^2 = 0.0224 \pm 0.0001$, scalar spectral inde
68 % confidence regions on measured parameters and 95 %
$100\theta_* = 1.0411 \pm 0.0003$. These results are only weakly depe
in many commonly considered extensions. Assuming the ba
Hubble constant $H_0 = (67.4 \pm 0.5)\,\mathrm{km\,s^{-1}Mpc^{-1}}$; matter densi
We find no compelling evidence for extensions to the base-ΛCDM model. Combining with baryon acoustic oscillation (BAO) measurements (and
considering single-parameter extensions) we constrain the ef
the Standard Model prediction $N_{\rm eff} = 3.046$, and find that th
to prefer higher lensing amplitudes than predicted in base ΛC
from the ΛCDM model; however, this is not supported by t
BAO data. The joint constraint with BAO measurements on s
with Type Ia supernovae (SNe), the dark-energy equation of
constant. We find no evidence for deviations from a purely
Keck Array data, we place a limit on the tensor-to-scalar ra
deuterium abundances for the base-ΛCDM cosmology are i
agreement with BAO, SNe, and some galaxy lensing obser
including galaxy clustering (which prefers lower fluctuation
measurements of the Hubble constant (which prefer a highe
favoured by the *Planck* data.

Key words. Cosmology: observations – Cosmology: theory – Cosmic background radiation – cosmological parameters

$$\Omega_K = -0.044^{+0.018}_{-0.015} \quad (68\,\%,\ \textit{Planck}\ \text{TT,TE,EE+lowE}), \qquad (46b)$$

a detection of curvature at about 3.4σ

an apparent detection of curvature at well over $2\,\sigma$. The 99 % probability region for the TT,TE,EE+lowE result is $-0.095 < \Omega_K < -0.007$, with only about 1/10000 samples at $\Omega_K \geq 0$. This is not entirely a volume effect, since the best-fit χ^2 changes by $\Delta\chi^2_{\rm eff} = -11$ compared to base ΛCDM when adding the one additional curvature parameter. The reasons for the pull towards

*Corresponding author: G. Efstathiou, gpe@ast.cam.ac.uk
†Corresponding author: S. Galli, gallis@iap.fr
‡Corresponding author: A. Lewis, antony@cosmologist.info

*Corresponding author: G. Efstathio
†Corresponding author: S. Galli, gal
‡Corresponding author: A. Lewis, antony@cosmologist.info

Curvature of the universe

Curvature of the universe

Planck can provide an unbiased and reliable estimate of the universe's curvature, although there is a "geometrical degeneracy" with Ωm, because the gravitational lensing, which depends on matter density, helps in breaking it.
Simulations show that Planck can constrain curvature with a 2% uncertainty without significant bias towards closed models.
Planck suggests a closed universe ($\Omega_k < 0$) with 99.985% probability, providing a better fit than a flat model.
The best-fit $\Delta\chi^2$ improves by -11 when adding the curvature parameter to the base ΛCDM model.
This improvement is attributed not only to volume effects but also to the agreement of closed models with the observed low CMB anisotropy quadrupole, which may result from a large-scale cut-off in primordial density fluctuations.

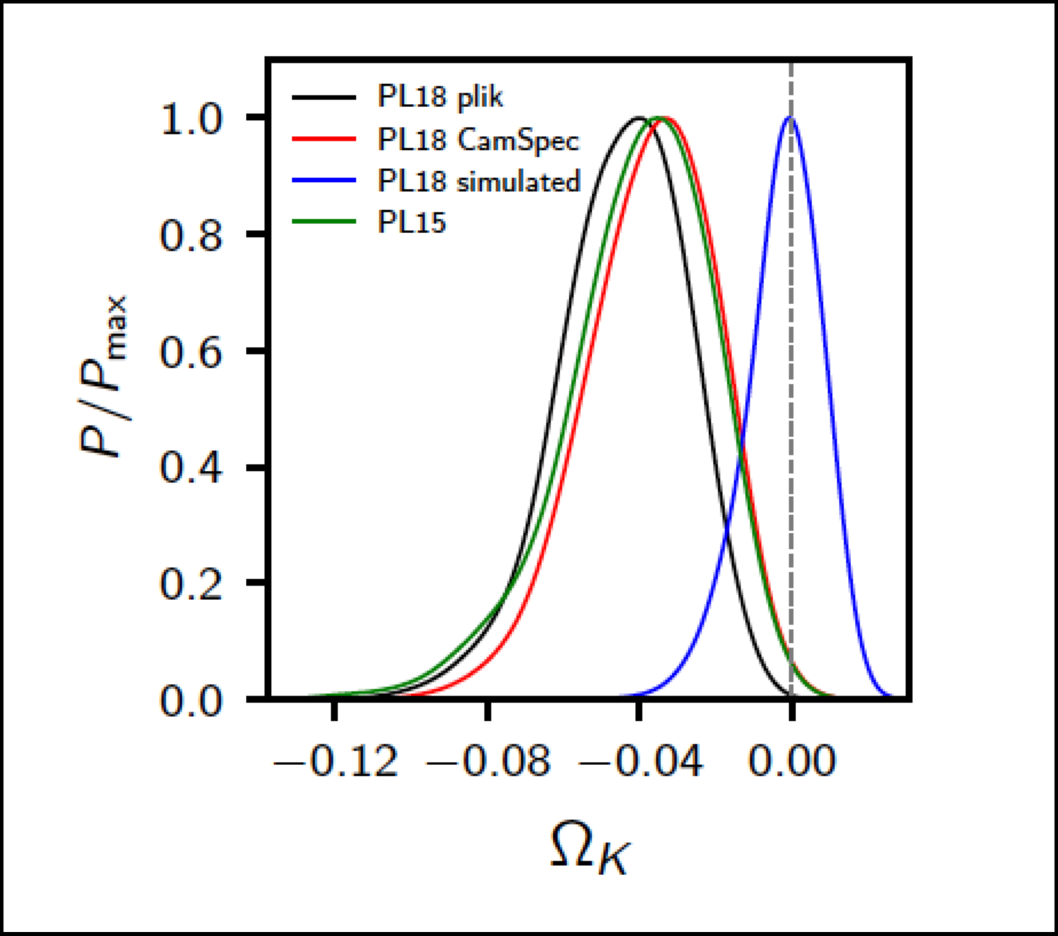

Di Valentino, Melchiorri and Silk, *Nature Astron.* 4 (2019) 2, 196-203

Low CMB anisotropy quadrupole

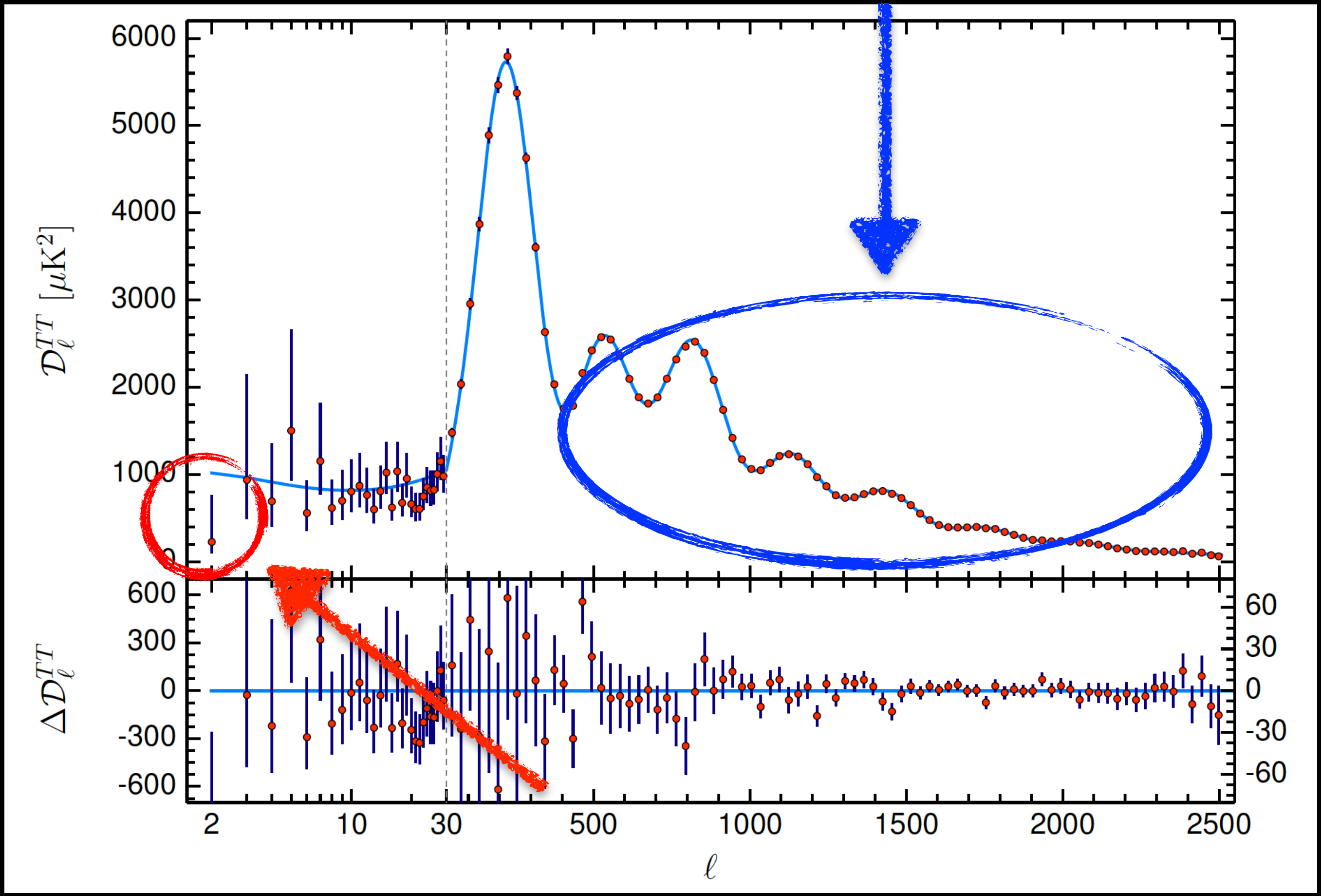

Planck 2018, Astron.Astrophys. 641 (2020) A6

A model with $\Omega_K < 0$ is slightly preferred with respect to a flat model with $A_L > 1$, because closed models better fit not only the damping tail, but also the low-multipole data, especially the quadrupole.

What about Planck PR4 (NPIPE) with CamSpec?

arXiv > astro-ph > arXiv:2205.10869

Search...

Help | Advar

Astrophysics > Cosmology and Nongalactic Astrophysics

[Submitted on 22 May 2022 (v1), last revised 11 Nov 2022 (this version, v2)]

CMB power spectra and cosmological parameters from Planck PR4 with CamSpec

Erik Rosenberg, Steven Gratton, George Efstathiou

We present angular power spectra and cosmological parameter constraints derived from the Planck PR4 (NPIPE) maps of the Cosmic Microwave Background. NPIPE, released by the Planck Collaboration in 2020, is a new processing pipeline for producing calibrated frequency maps from Planck data. We have created new versions of the CamSpec likelihood using these maps and applied them to constrain LCDM and single-parameter extensions. We find excellent consistency between NPIPE and the Planck 2018 maps at the parameter level, showing that the Planck cosmology is robust to substantial changes in the mapmaking. The lower noise of NPIPE leads to ~10% tighter constraints, and we see both smaller error bars and a shift toward the LCDM values for beyond-LCDM parameters including Omega_K and A_Lens.

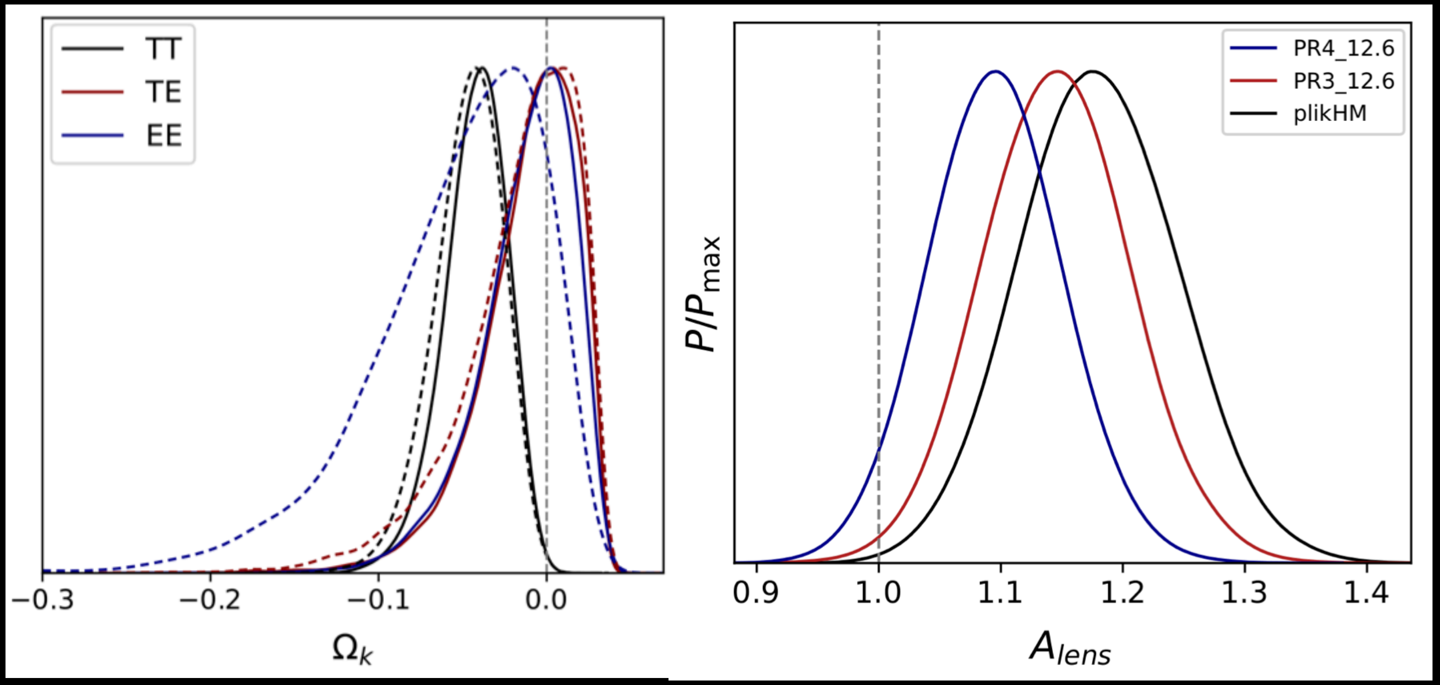

Planck PR4 (NPIPE) with CamSpec

PR4_12.6	A_L	Ω_K	$N_{\rm eff}$	m_ν
TTTEEE	1.095 ± 0.056	$-0.025^{+0.013}_{-0.010}$	3.00 ± 0.21	< 0.161
TT	1.198 ± 0.084	$-0.042^{+0.022}_{-0.016}$	$2.98^{+0.28}_{-0.35}$	< 0.278
TE	0.96 ± 0.15	$-0.010^{+0.035}_{-0.015}$	$3.11^{+0.38}_{-0.42}$	< 0.400
EE	0.995 ± 0.15	$-0.012^{+0.034}_{-0.017}$	4.6 ± 1.3	< 2.37

PR3_12.6	A_L	Ω_K	$N_{\rm eff}$	m_ν
TTTEEE	1.146 ± 0.061	$-0.035^{+0.016}_{-0.012}$	$2.94^{+0.20}_{-0.23}$	< 0.143
TT	1.215 ± 0.089	$-0.047^{+0.024}_{-0.017}$	$2.89^{+0.28}_{-0.32}$	< 0.248
TE	0.96 ± 0.17	$-0.015^{+0.043}_{-0.015}$	$2.96^{+0.42}_{-0.49}$	< 0.504
EE	1.15 ± 0.20	$-0.053^{+0.063}_{-0.029}$	$2.46^{+0.94}_{-1.7}$	-

…but this new likelihood is not really solving the problem of AL/ΩK, that is mainly coming from the TT power spectrum.
And the constraints coming from TT are not changing in the 2 releases…

Rosenberg et al., arXiv:2205.10869

Planck PR4 (NPIPE) with CamSpec

PR4_12.6	A_L	Ω_K	$N_{\rm eff}$	m_ν
				61
				78
				00
				37
				43
				48
				04

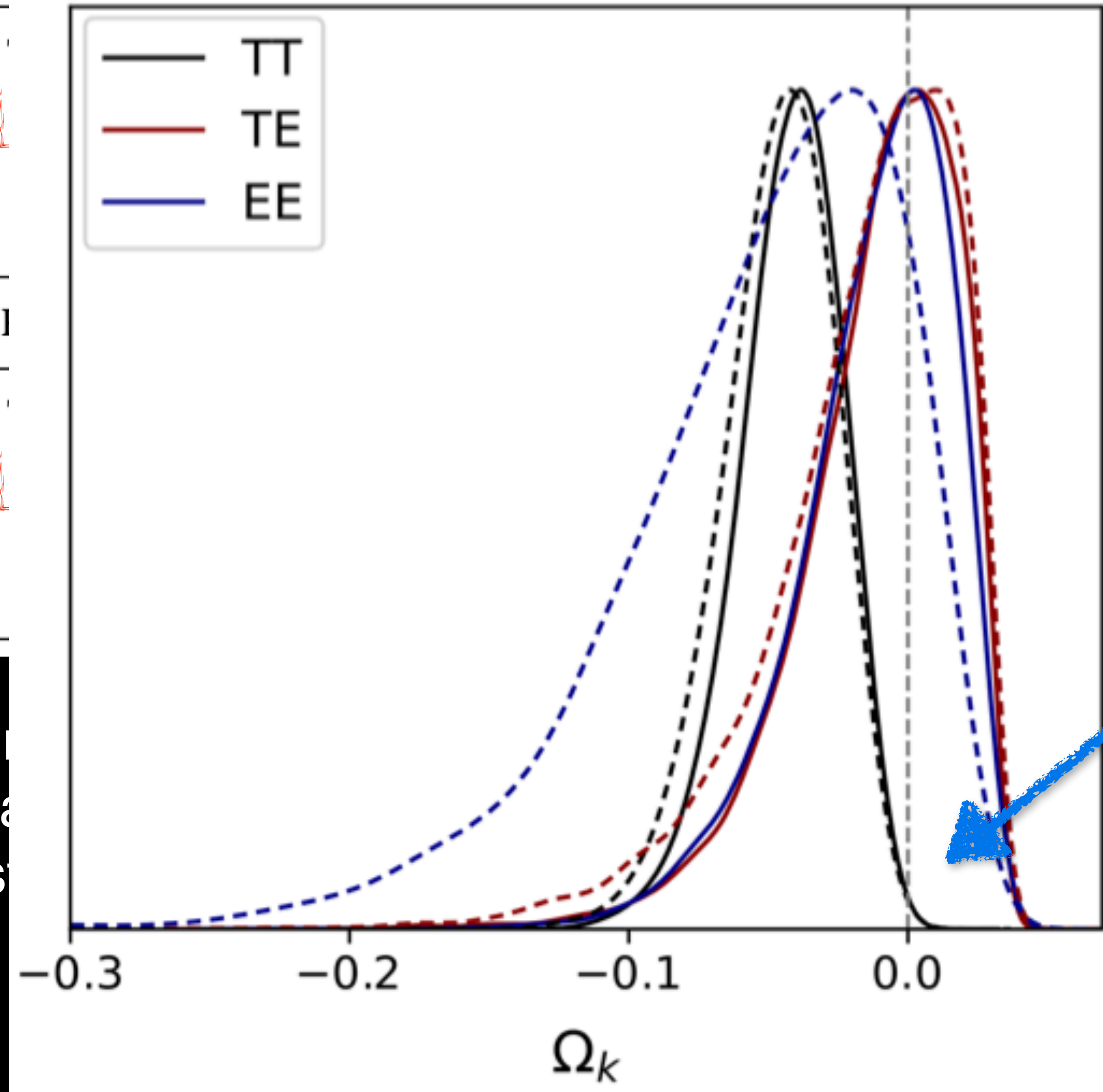

…but this … m of AL/ΩK,
tha … um.
And the cons … e 2 releases…

Rosenberg et al., arXiv:2205.10869

Planck PR4 (NPIPE) with CamSpec

PR4_12.6	A_L	Ω_K	$N_{\rm eff}$	m_ν
TTTEEE	1.095 ± 0.056	$-0.025^{+0.013}_{-0.010}$	3.00 ± 0.21	< 0.161
TT	1.198 ± 0.084	$-0.042^{+0.022}_{-0.016}$	$2.98^{+0.28}_{-0.35}$	< 0.278
TE	0.96 ± 0.15	$-0.010^{+0.035}_{-0.015}$	$3.11^{+0.38}_{-0.42}$	< 0.400
EE	0.995 ± 0.15	$-0.012^{+0.034}_{-0.017}$	4.6 ± 1.3	< 2.37
PR3_12.6	**A_L**	**Ω_K**	**$N_{\rm eff}$**	**m_ν**
TTTEEE	1.146 ± 0.061	$-0.035^{+0.016}_{-0.012}$	$2.94^{+0.20}_{-0.23}$	< 0.143
TT	1.215 ± 0.089	$-0.047^{+0.024}_{-0.017}$	$2.89^{+0.28}_{-0.32}$	< 0.248
TE	0.96 ± 0.17	$-0.015^{+0.043}_{-0.015}$	$2.96^{+0.42}_{-0.49}$	< 0.504
EE	1.15 ± 0.20	$-0.053^{+0.063}_{-0.029}$	$2.46^{+0.94}_{-1.7}$	-

…but this new likelihood is not really solving the problem of AL/ΩK, that is mainly coming from the TT power spectrum. And the constraints coming from TT are not changing in the 2 releases…

The constraints derived from the EE power spectrum are instead those pulling all the parameters towards ΛCDM and thus alleviating the tensions.

Rosenberg et al., arXiv:2205.10869

Planck PR4 (NPIPE) with CamSpec

PR	m_ν
TT	< 0.161
	< 0.278
	< 0.400
	< 2.37

PR	m_ν
TT	< 0.143
	< 0.248
	< 0.504
	-

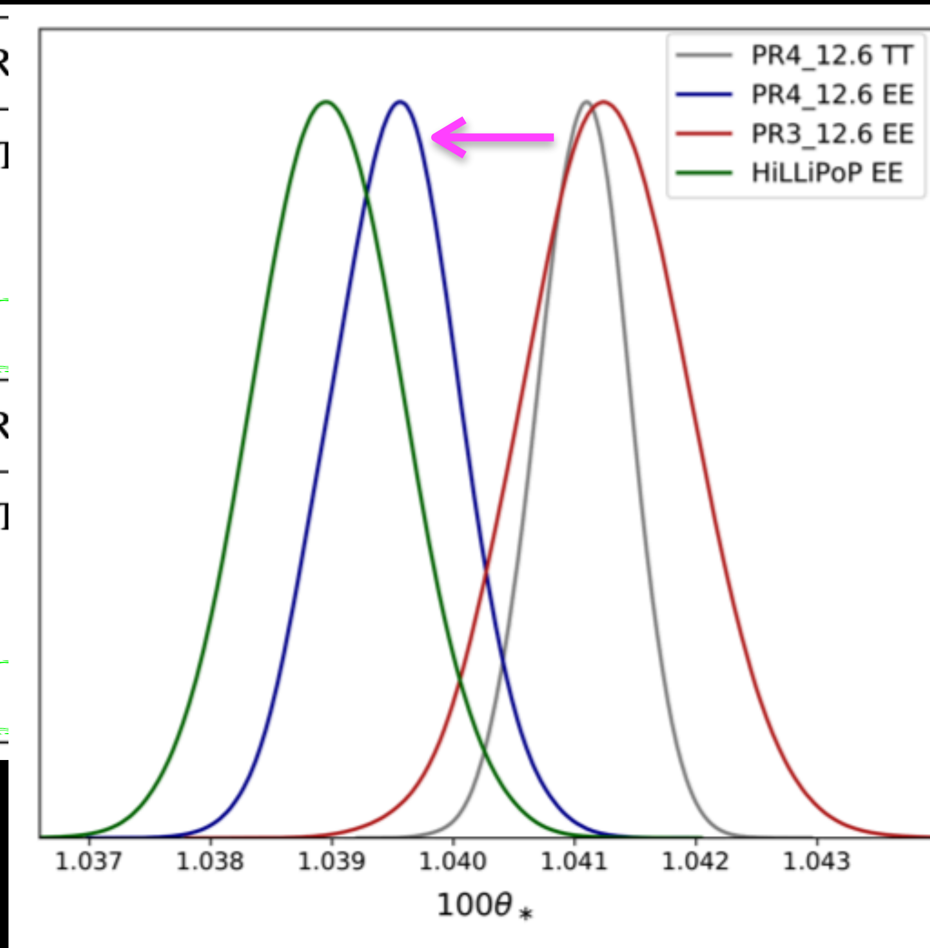

However, this change in EE is producing a significant shift of the acoustic scale parameter θ, and an internal tension at 2.8σ between TT and EE, that becomes more than 3.2-3.3σ when AL/ΩK vary.

Rosenberg et al., arXiv:2205.10869

Planck PR4 (NPIPE) with CamSpec

	ℓ range	N_D	$\hat{\chi}^2$	$(\hat{\chi}^2 - 1)/\sqrt{2/N_D}$
TT 143x143	30 – 2000	1971	1.021	0.67
TT 143x217	500 – 2500	2001	0.985	-0.47
TT 217x217	500 – 2500	2001	1.002	0.05
TT All	30 – 2500	5973	1.074	4.07
TE	30 – 2000	1971	1.055	1.73
EE	30 – 2000	1971	1.026	0.82
TEEE	20 – 2000	3942	1.046	2.02
TTTEEE	30 – 2500	9915	1.063	4.46

Table 1. χ^2 of the different components of the PR4_12.6 likelihood with respect to the TTTEEE best-fit model. N_D is the size of the data vector. $\hat{\chi}^2 = \chi^2/N_D$ is the reduced χ^2. The last column gives the number of standard deviations of $\hat{\chi}^2$ from unity.

..but more significantly, the reduced χ2 values show a more than 4σ tension of the data with the best-fit obtained by TTTEEE assuming a ΛCDM model.

Should we really prioritize
enhancing the agreement with the ΛCDM model over preventing
an internal inconsistency and a worse fit of the data?

Rosenberg et al., arXiv:2205.10869

A_L for different data releases

Table 1. Posterior A_L Constraints from Analyses of Planck Temperature and Polarization Data since 2018 Release

Reference	Data Version	Likelihood	Data Combination	A_L	'Nσ' Preference for $A_L > 1$
Planck Collaboration VI (2020)	PR3/2018	plik	TTTEEE+lowl/lowE	1.180 ± 0.065	2.8σ
	PR3/2018	plik	TT+lowl/lowE	1.243 ± 0.096	2.5σ
Rosenberg et al. (2022)	PR3/2018	CamSpec	TTTEEE+lowl/lowE	1.146 ± 0.061	2.4σ
	PR3/2018	CamSpec	TT+lowl/lowE	1.215 ± 0.089	2.4σ
	PR4/NPIPE	CamSpec	TTTEEE+lowl/lowE	1.095 ± 0.056	1.7σ
	PR4/NPIPE	CamSpec	TT+lowl/lowE	1.198 ± 0.084	2.4σ
Tristram et al. (2023)	PR4/NPIPE	HiLLiPoP	TTTEEE+lowl/LoLLiPoP[a]	1.036 ± 0.051	0.7σ
	PR4/NPIPE	HiLLiPoP	TT+lowl/LoLLiPoP	1.068 ± 0.081	0.8σ

Addison et al, arXiv:2310.03127

$S_8 = 0.834 \pm 0.016$

$H0 = 67.36 \pm 0.54$ km/s/Mpc

Planck 2018, Aghanim et al., arXiv:1807.06209 [astro-ph.CO]

$S_8 = 0.819 \pm 0.014$

$H0 = 67.64 \pm 0.52$ km/s/Mpc

Tristram et al., arXiv:2309.10034 [astro-ph.CO]

The role of the optical depth: can the anomalies such as lensing and curvature recast a wrong calibration of τ?

The optical depth

During the cosmic reionization, CMB photons undergo Thomson scattering off free electrons at scales smaller than the horizon size.

As a result, they deviate from their original trajectories, reaching us from a direction different from the one set during recombination.

Similarly to recombination, this introduces a novel 'last scattering' surface at later times and produces distinctive imprints in the angular power spectra of temperature and polarization anisotropies.

A well-known effect of reionization is an enhancement of the spectrum of CMB polarization at large angular scales alongside a suppression of temperature anisotropies occurring at smaller scales ($A_s e^{-2\tau}$).

The distinctive polarization bump produced by reionization on large scales dominates the signal in the EE spectrum whose amplitude strongly depends on the total integrated optical depth to reionization:

$$\tau = \sigma_T \int_0^{z_{rec}} dz\, \bar{n}_e(z)\, \frac{dr}{dz},$$

where σ_T is the Thomson scattering cross-section, $\bar{n}_e(z)$ is the free electron proper number density at redshift z, and dr/dz is the line-of-sight proper distance per unit redshift.

For this reason, precise observations of E-mode polarization on large scales are crucial.

Giarè, Di Valentino, Melchiorri, Phys.Rev.D 109 (2024) 10, 103519

The optical depth

Thanks to large-scale polarization measurements released by the Planck satellite, we have achieved an unprecedented level of accuracy, constraining the optical depth at reionization down to $\tau = 0.054 \pm 0.008$ at 68% CL, from the WMAP9 value of $\tau = 0.089 \pm 0.014$. Measuring τ to such a level of precision holds implications that extend beyond reionization models. For example, the constraints on the Hubble parameter H_0 and the scalar spectral index n_s both improve by approximately 22% when incorporating Planck large-scale polarization data in the analysis. However, as often happens when dealing with high-precision measurements at low multipoles, there are certain aspects that remain less than entirely clear:

- The detected signal in the EE spectrum is extremely small, on scales where cosmic variance sets itself a natural limit on the maximum precision achievable, and even minor undetected systematic errors could have a substantial impact on the results.

- Small, undetected foreground effects could play a role in determining polarization measurements.

- Measurements of temperature and polarization anisotropies at large angular scales exhibit a series of anomalies. For example, the TE spectrum at low multipoles shows an excess variance compared to simulations, for reasons that are not understood, and is commonly disregarded for cosmological data analyses.

Giarè, Di Valentino, Melchiorri, Phys.Rev.D 109 (2024) 10, 103519

The optical depth

$$C_\ell^{EE} \propto \tau^2/\ell^4$$

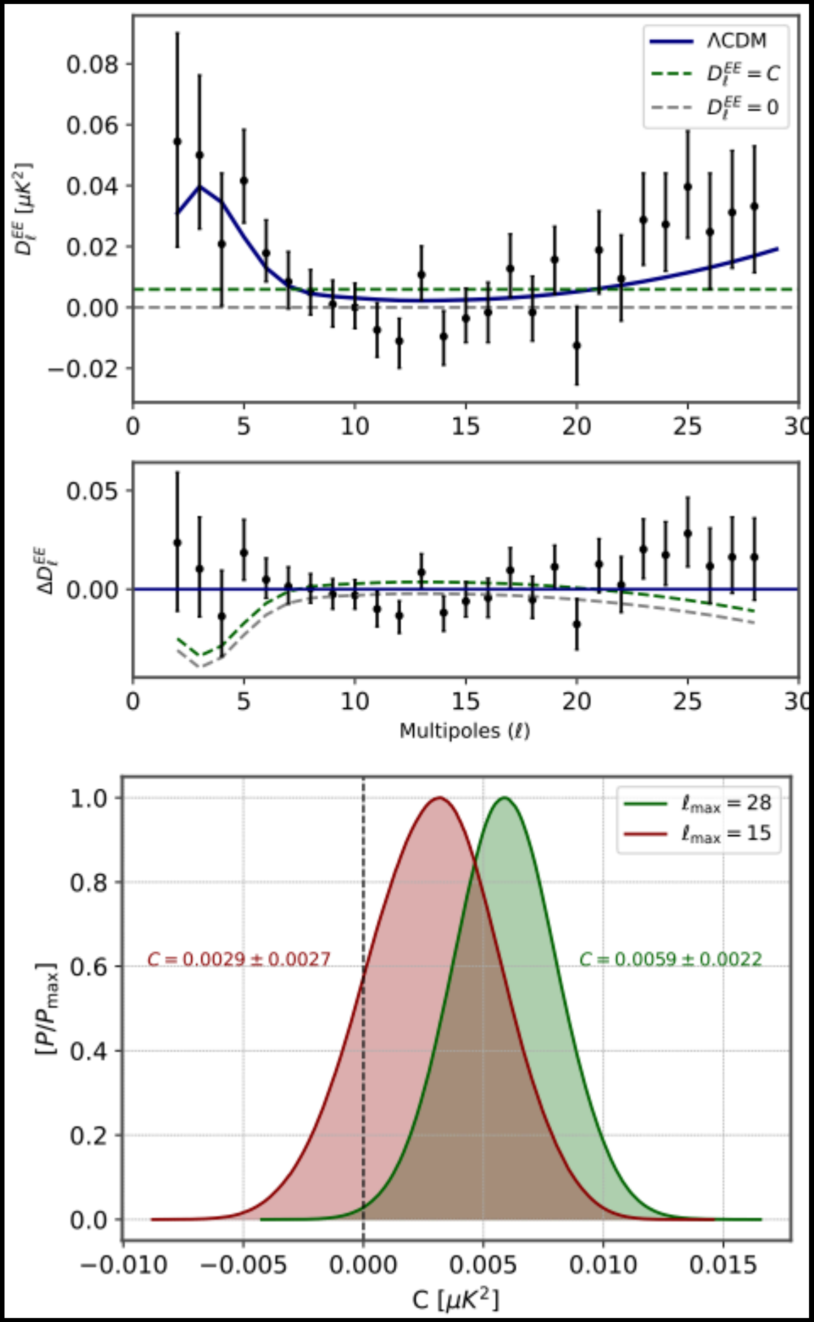

We perform a fit to measurements of the low multipoles EE data assuming a constant instead of the expected reionization bump, and this is compatible with the data with a p-value of p=0.063, above the threshold value typically adopted to reject the hypothesis.

And if we focus only on data-points at $2 \leq l \leq 15$, i.e. those scale that contribute more when determining τ because it is where the reionization bump in polarization manifests itself more prominently, the case C = 0 (i.e., no signal at all) falls basically within the 1σ range.

Therefore we argue the concern that, when dealing with measurements so close to the absence of a signal and experimental sensitivity, any statistical fluctuation or lack of understanding of the foregrounds could be crucial and potentially have implications in the measurement of τ.

Giarè, Di Valentino, Melchiorri, Phys.Rev.D 109 (2024) 10, 103519

Planck new physics depends on the optical depth

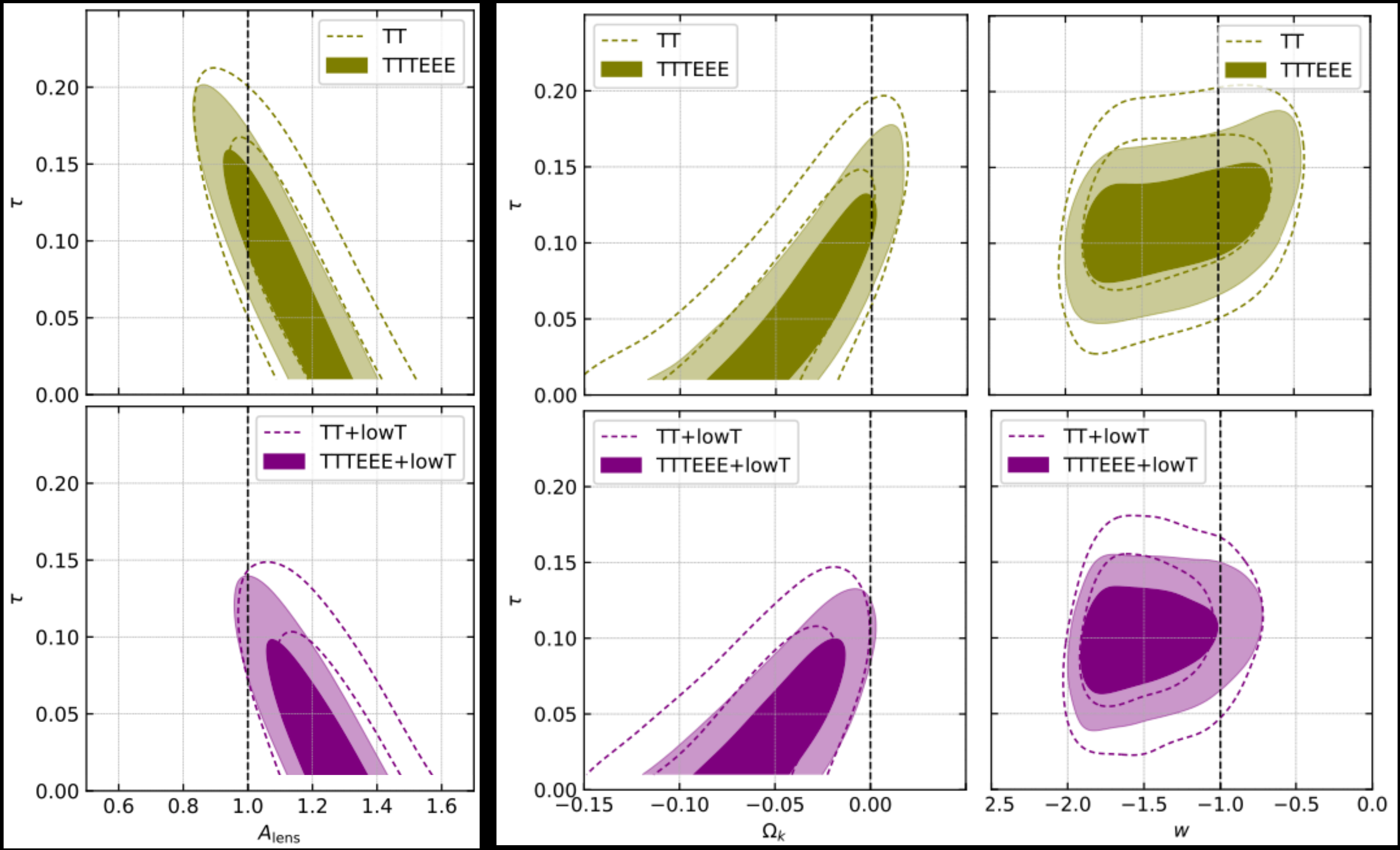

Excluding the lowE data everything is consistent with ΛCDM.

Giarè, Di Valentino, Melchiorri, Phys.Rev.D 109 (2024) 10, 103519

Is it possible to achieve competitive constraints on τ without exclusively relying on large-scale CMB polarization?

lowE independent optical depth

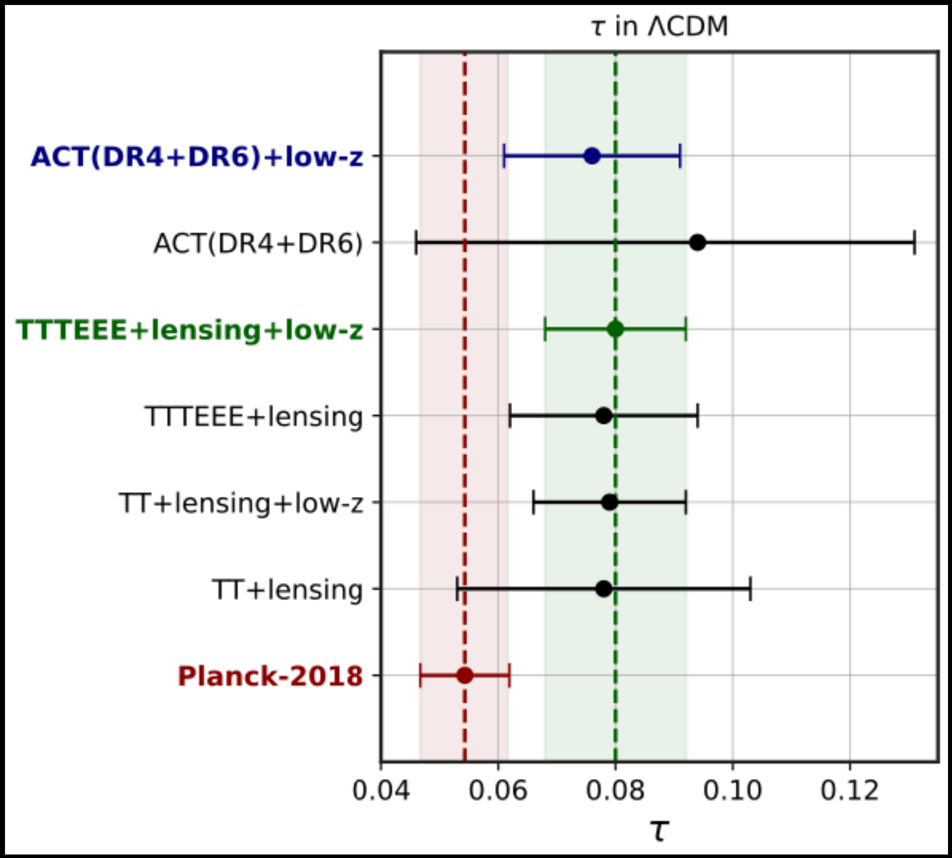

By using different combinations of Planck temperature and polarization data at $l > 30$, ACT and Planck reconstructions of the lensing potential, BAO measurements from BOSS and eBOSS surveys, and Type-Ia supernova data from the Pantheon-Plus sample, we can constrain τ independently.

The most constraining limit $\tau = 0.080 \pm 0.012$ comes from TTTEEE+lensing+low-z.

Using only ACT- based temperature, polarization, and lensing data, from ACT(DR4+DR6)+low-z we got $\tau = 0.076 \pm 0.015$ which is entirely independent of Planck.

Giarè, Di Valentino, Melchiorri, Phys.Rev.D 109 (2024) 10, 103519

lowE independent optical depth

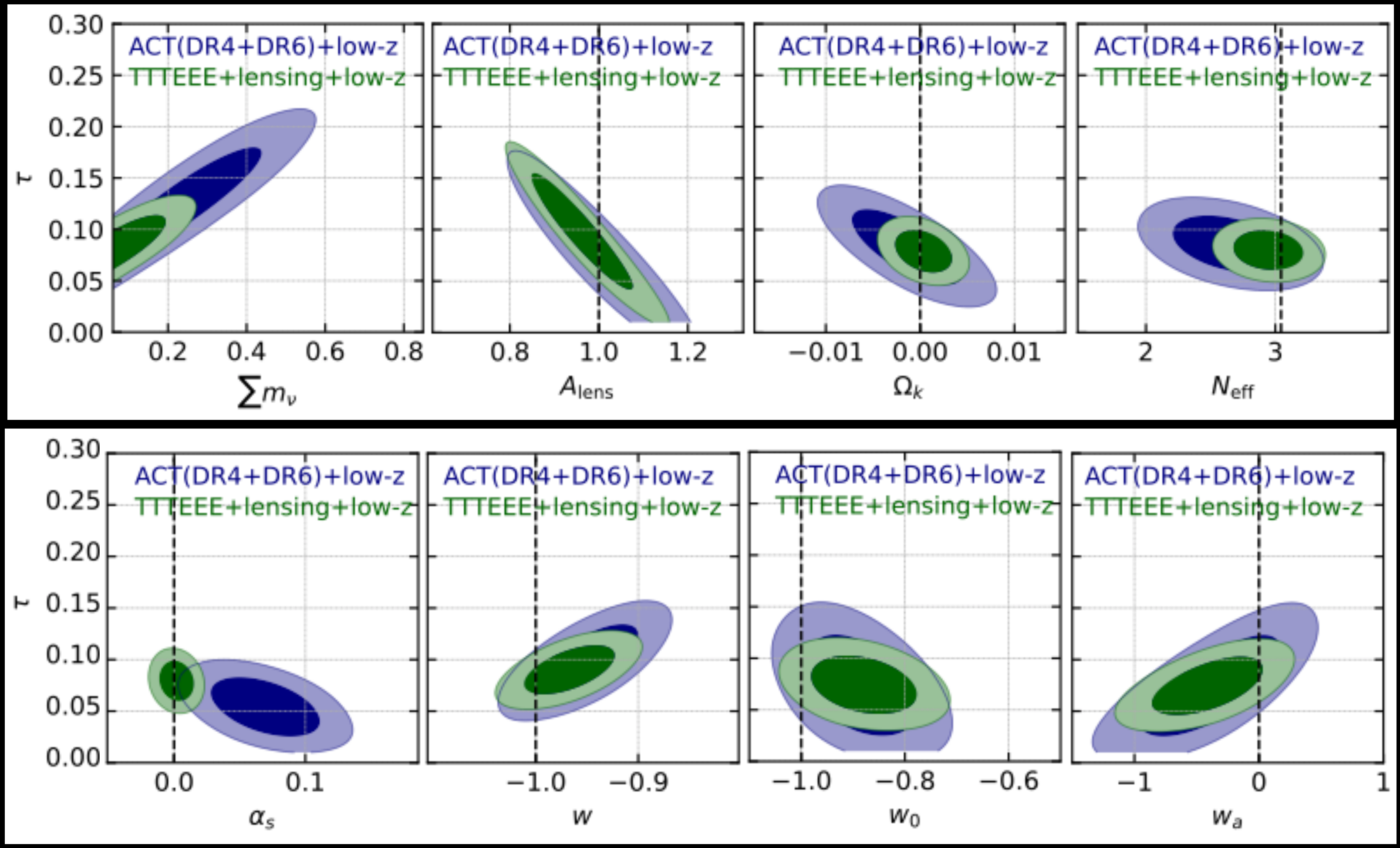

Considering our best combinations to constrain τ the typical ΛCDM extensions are all in agreement with the expected values.

Giarè, Di Valentino, Melchiorri, Phys.Rev.D 109 (2024) 10, 103519

What about the alternative CMB experiments?

Harrison-Zel'dovich scale-invariant spectrum?

Dataset	Scalar Spectral Index (n_s)
	ΛCDM
ACT	1.009 ± 0.015
ACT+BAO (DR12)	1.006 ± 0.013
ACT+BAO (DR16)	1.006 ± 0.014
ACT+DESy1	1.007 ± 0.013
ACT+SPT+BAO (DR12)	0.996 ± 0.012
Planck	0.9649 ± 0.0044
Planck+BAO (DR12)	0.9668 ± 0.0038
Planck+BAO (DR16)	0.9677 ± 0.0037
Planck ($2 \leq \ell \leq 650$)	0.9655 ± 0.0043
Planck ($\ell > 650$)	0.9634 ± 0.0085

Giarè, Renzi, Mena, Di Valentino, and Melchiorri, MNRAS 521 (2023) 2, 2911

ACT shows a preference for a larger spectral index consistent with a Harrison-Zel'dovich scale-invariant spectrum ns=1 of primordial density perturbations introducing a tension with a significance of 2.7σ with the results from the Planck satellite.

Harrison-Zel’dovich scale-invariant spectrum?

Dataset	Scalar Spectral Index (n_s)
	ΛCDM
ACT	1.009 ± 0.015
ACT+BAO (DR12)	1.006 ± 0.013
ACT+BAO (DR16)	1.006 ± 0.014
ACT+DESy1	1.007 ± 0.013

In ACT-DR4 2020, arXiv:2007.07288 [astro-ph.CO] this discrepancy was interpreted as a consequence of the lack of information concerning the first acoustic peak of the temperature power spectrum.

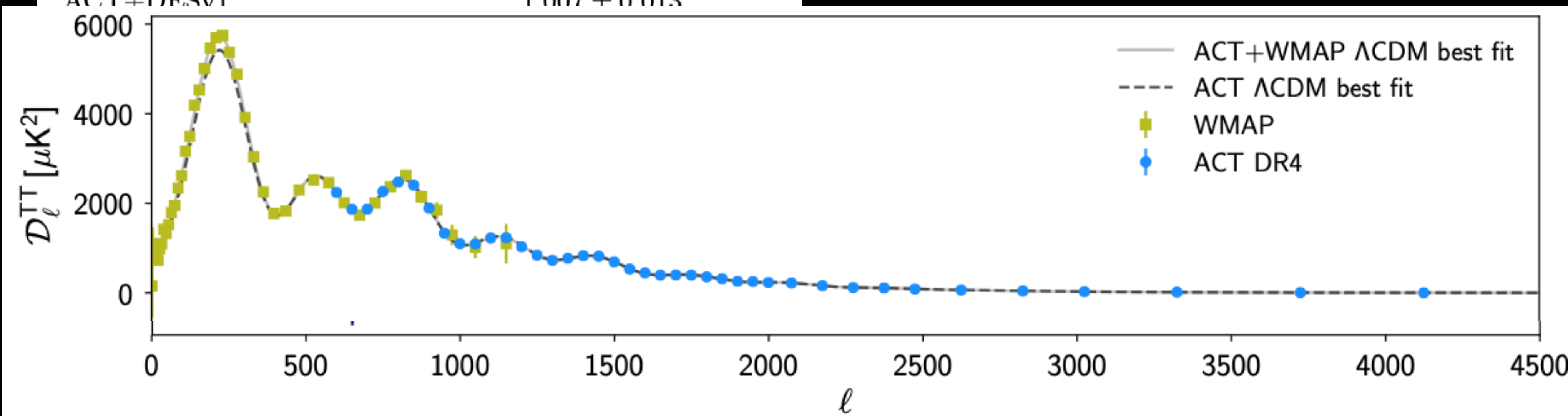

Harrison-Zel'dovich scale-invariant spectrum?

Dataset	Scalar Spectral Index (n_s)
	ΛCDM
ACT	1.009 ± 0.015
ACT+BAO (DR12)	1.006 ± 0.013
ACT+BAO (DR16)	1.006 ± 0.014
ACT+DESy1	1.007 ± 0.013
ACT+SPT+BAO (DR12)	0.996 ± 0.012
Planck	0.9649 ± 0.0044
Planck+BAO (DR12)	0.9668 ± 0.0038
Planck+BAO (DR16)	0.9677 ± 0.0037
Planck ($2 \leq \ell \leq 650$)	0.9655 ± 0.0043
Planck ($\ell > 650$)	0.9634 ± 0.0085

Giarè, Renzi, Mena, Di Valentino, and Melchiorri,
MNRAS 521 (2023) 2, 2911

In ACT-DR4 2020, arXiv:2007.07288 [astro-ph.CO] this discrepancy was interpreted as a consequence of the lack of information concerning the first acoustic peak of the temperature power spectrum.

To verify this origin of the discrepancy in the CMB values of ns, we have performed two separate analyses of the Planck observations, splitting the likelihood into low 2< l < 650 and high l > 650 multipoles. We find that the discrepancy still persists at the level of 3σ (2σ) for low (high) multiple temperature data. Planck data still prefer a value of the scalar spectral index smaller than unity at ~4.3σ when the information about the first acoustic peak is removed.

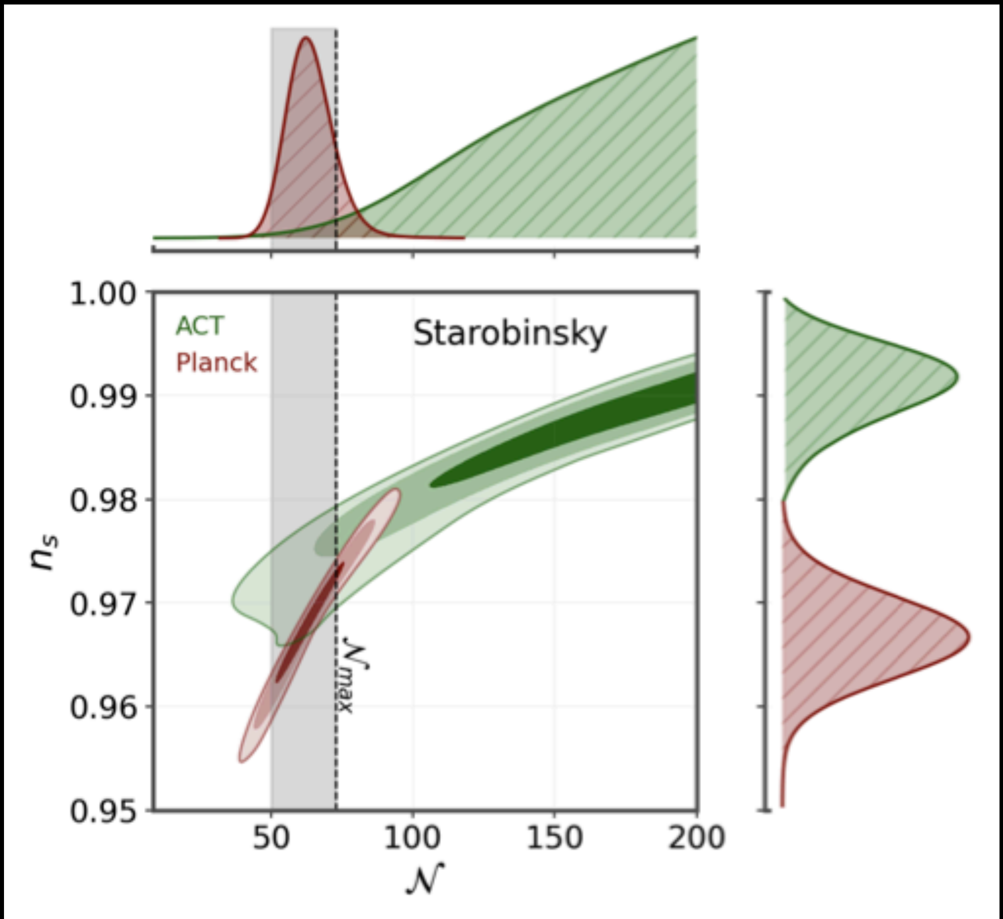

Giarè, Pan, Di Valentino, Yang, de Haro, and Melchiorri, *JCAP* 09 (2023) 019

We tested some models of inflation regarded as well - established benchmark scenarios and found out that they are ruled out by ACT at more than 3σ.

In the plot we show for example the 2D contours at 68%, 95%, and 99% CL and 1D posteriors in the (n_s, N_{efolds}) plane for the Starobinsky model.
The grey vertical band refers to the typical range of folds expansion $N_{efolds} \in [50, N_{max}]$, expected in standard inflation.
The upper limit, $N_{max} \leq 73$, is represented by the black dashed line.

Very similar results are obtained for all the other potentials, and in particular for ACT we find the following values for the number of e-folds at 68% (95%) CL:

- $\mathcal{N} > 138$ ($\mathcal{N} > 92.8$) for the Starobinsky model;
- $\mathcal{N} > 134$ ($\mathcal{N} > 88.6$) for α-Attractor models;
- $\mathcal{N} > 257$ ($\mathcal{N} > 208$) for Polynomial inflation;
- $\mathcal{N} > 177$ ($\mathcal{N} > 105$) for the SUSY potential.

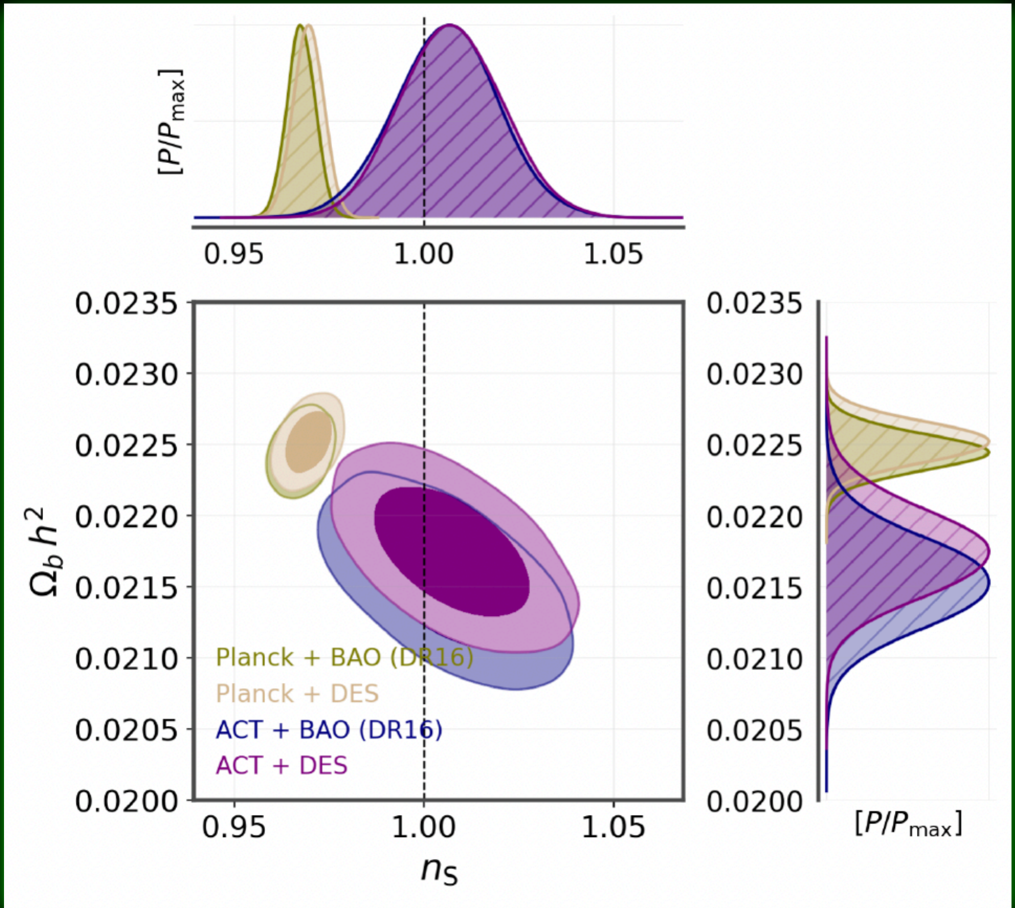

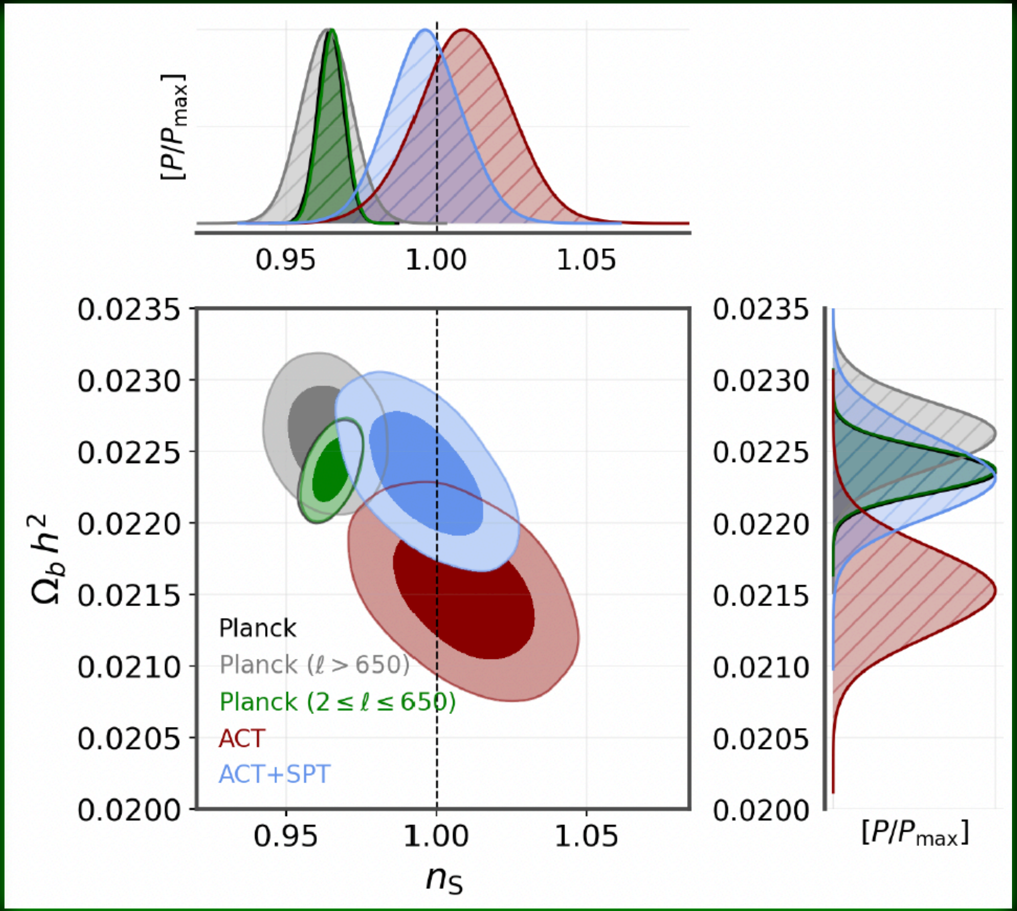

Giarè, Renzi, Mena, Di Valentino, and Melchiorri, MNRAS 521 (2023) 2, 2911

Such preference remains robust under the addition of large scale structure information, and in the two-dimensional plane it can be definitely noted that the direction of the $\Omega_b h^2$ - ns degeneracy is opposite for ACT and Planck, and the disagreement here is significantly exceeding 3σ. This tension is partially driven by the ACT polarization data, as we can see replacing it with the SPT polarization measurements, but while the tension is relaxed in the plane $\Omega_b h^2$ - ns, this combination is still preferring ns=1.

Quantifying global CMB tension

Handley and Lemos, arXiv:2007.08496 [astro-ph.CO]

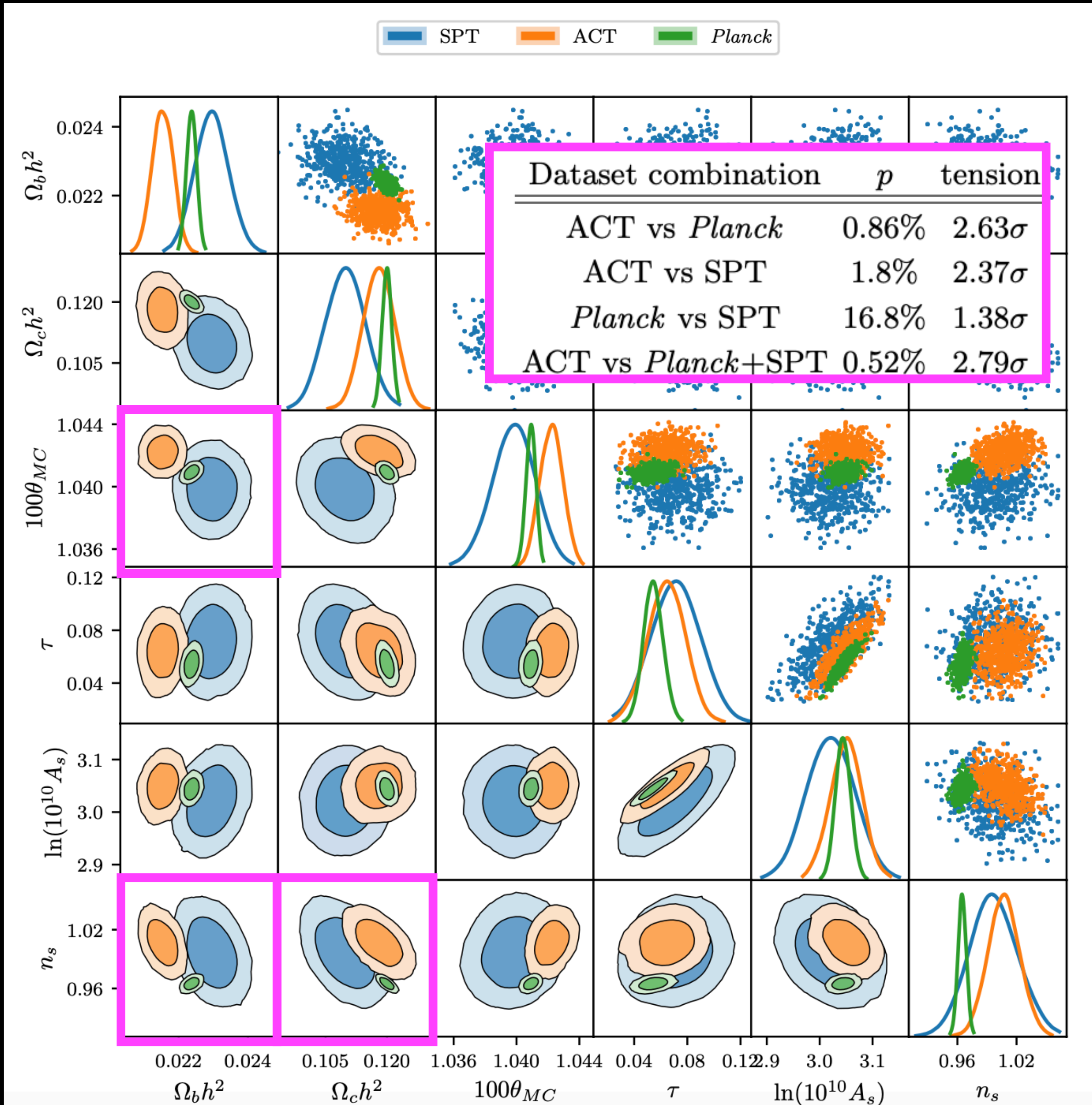

Dataset combination	p	tension
ACT vs *Planck*	0.86%	2.63σ
ACT vs SPT	1.8%	2.37σ
Planck vs SPT	16.8%	1.38σ
ACT vs *Planck*+SPT	0.52%	2.79σ

Global tensions between CMB datasets.

For each pairing of datasets this is the tension probability p that such datasets would be this discordant by (Bayesian) chance, as well as a conversion into a Gaussian-equivalent tension.

Between Planck and ACT there is a 2.6σ tension.

Assuming ΛCDM

ACT-DR4 vs Planck: EDE

Constraints on EDE ($n = 3$)

Parameter	ACT DR4 TT+TE+EE, τ	ACT DR4 TT+TE+EE, *Planck* 2018 TT ($\ell_{\rm max} = 650$), τ	ACT DR4 TT+TE+EE, *Planck* 2018 TT ($\ell_{\rm max} = 650$), *Planck* 2018 lensing, BAO, τ	*Planck* 2018 TT+TE+EE (from Ref. [38])	ACT DR4 TT+TE+EE, *Planck* 2018 TT+TE+EE (no low-ℓ EE), τ
$\boldsymbol{f_{\rm EDE}}$	$0.142^{+0.039}_{-0.072}$	$0.129^{+0.028}_{-0.055}$	$0.091^{+0.020}_{-0.036}$	< 0.087	< 0.124
$\boldsymbol{\log_{10}(z_c)}$	< 3.70	< 3.43	< 3.36	$3.66^{+[illegible]}_{-0.28}$	$3.54^{+[illegible]}_{-0.20}$
$\boldsymbol{\theta_i}$	> 0.24	< 2.89	< 2.82	> 0.36	> 0.51
$\boldsymbol{\Omega_c h^2}$	$0.1307^{+0.0054}_{-0.0120}$	$0.1291^{+0.0051}_{[illegible]}$	$0.1286^{+0.0027}_{[illegible]}$	$0.1234^{+0.0019}_{-0.0038}$	$0.1244^{+0.0025}_{-0.0051}$
H_0 [km/s/Mpc]	$74.5^{+2.5}_{-4.4}$	$74.4^{+2.2}_{-3.0}$	$70.9^{+1.0}_{-2.0}$	$68.29^{+0.73}_{-1.20}$	$69.17^{+0.83}_{-1.70}$
Ω_m	$0.276^{+0.020}_{-0.023}$	0.274 ± 0.017	0.3000 ± 0.0072	0.3145 ± 0.0086	0.3084 ± 0.0084
σ_8	$0.831^{+0.027}_{-0.043}$	$0.827^{+0.029}_{-0.035}$	$0.829^{+0.013}_{-0.021}$	$0.820^{+0.009}_{-0.013}$	$0.838^{+0.013}_{-0.015}$
S_8	0.796 ± 0.049	$0.791^{+0.040}_{-0.046}$	$0.828^{+0.015}_{-0.018}$	0.839 ± 0.018	0.850 ± 0.017

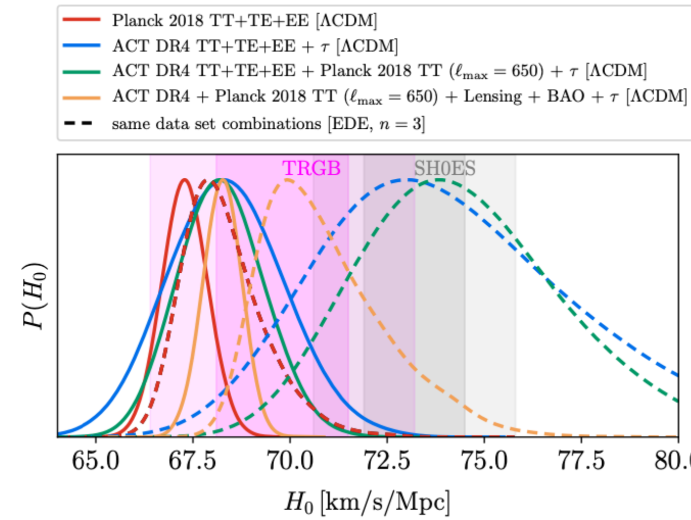

ACT collaboration, Hill et al. arXiv:*2109.04451*

Considering ACT only data or combined with Planck TT up to multipoles 650, there is an evidence for EDE > 3σ, solving completely the Hubble tension. The evidence for EDE > 3σ persists with the inclusion of Planck lensing + BAO data, but shifting H0 towards a lower value. Once the full Planck data are considered, the evidence for EDE disappears and H0 is again in tension with SH0ES.

The Planck damping tail is in disagreement with EDE different from zero.

ACT-DR4 vs Planck: α_s and β_s

Forconi, Giarè, Di Valentino and Melchiorri, *Phys.Rev.D* 104 (2021) 10, 103528

$$\alpha_s \doteq \left[\frac{dn_s}{d\log k}\right]_{k=k_*} \qquad \beta_s \doteq \left[\frac{d\alpha_s}{d\log k}\right]_{k=k_*}$$

Parameter	Planck18	ACTPol + WMAP
$\Omega_b h^2$	0.02235 ± 0.00017	0.02195 ± 0.00025
$\Omega_c h^2$	0.1207 ± 0.0015	0.1190 ± 0.0029
[illegible]	[illegible]1	1.04174 ± 0.00066
[illegible]	[illegible]6	0.061 ± 0.013
$\log(10^{10} A_S)$	3.053 ± 0.018	3.051 ± 0.026
n_s	0.9612 ± 0.0054	0.9680 ± 0.0082
α_s	0.001 ± 0.010	0.035 ± 0.012
β_s	0.012 ± 0.013	0.035 ± 0.013

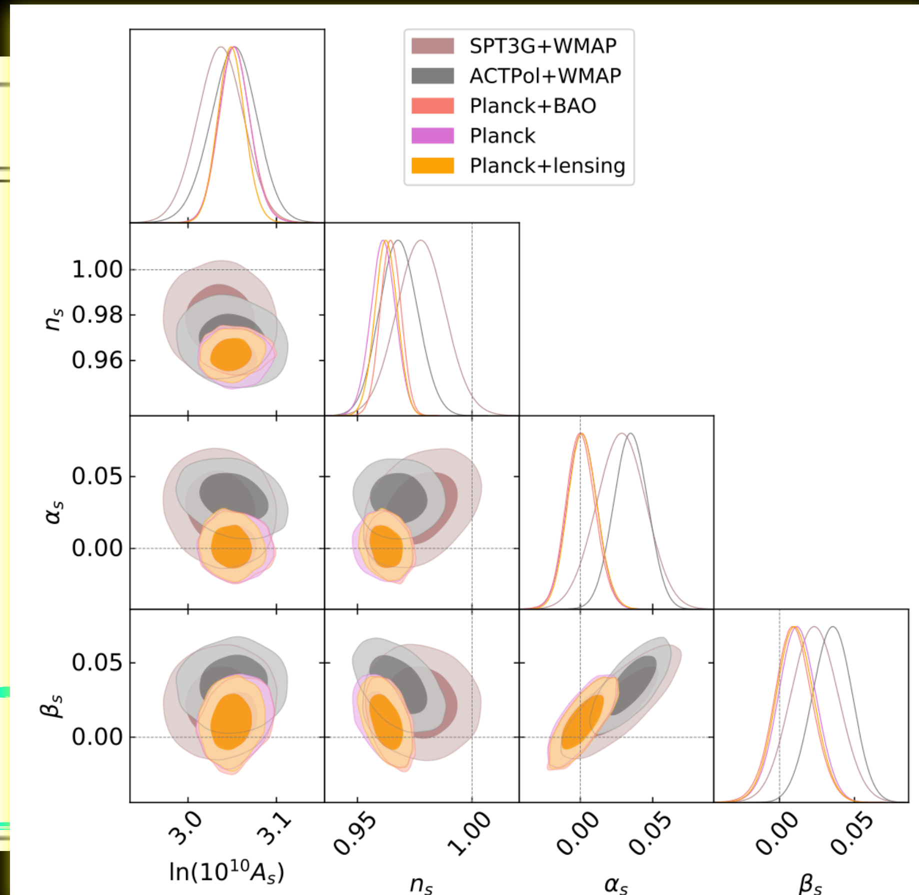

ACT-DR4 and SPT-3G are in agreement one with each other, but in disagreement with Planck, for the value of the running of the scalar spectral index α_s and of the running of the running β_s.
In particular ACT-DR4 + WMAP prefer both a non vanishing running α_s and running of the running β_s at the level of 2.9σ and 2.7σ, respectively.

Alternative CMB vs Planck: Σmν

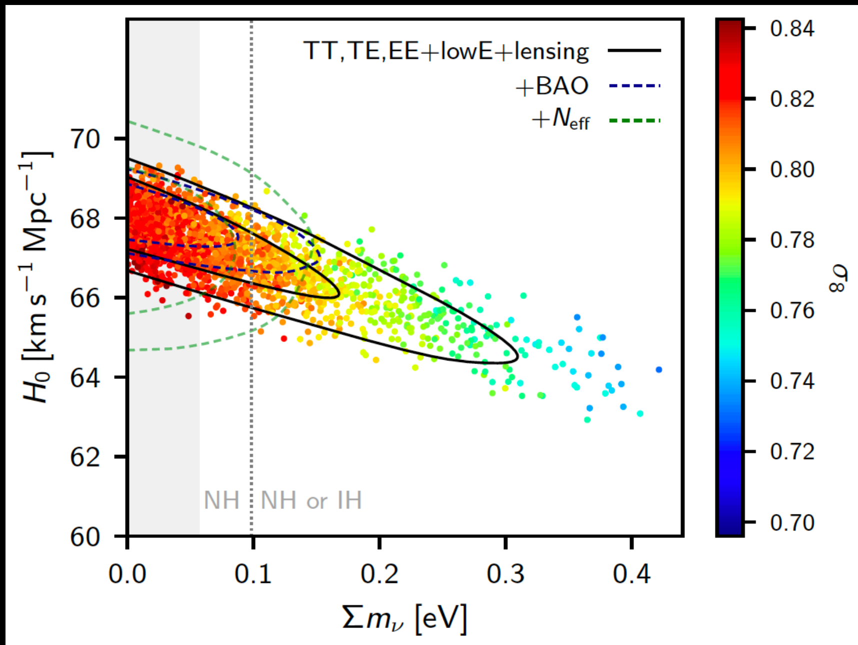

$$\sum m_\nu < 0.24 \text{ eV} \quad (95\,\%,\ \text{TT,TE,EE+lowE+lensing})$$

Planck 2018 collaboration, arXiv:1807.06209 [astro-ph.CO]

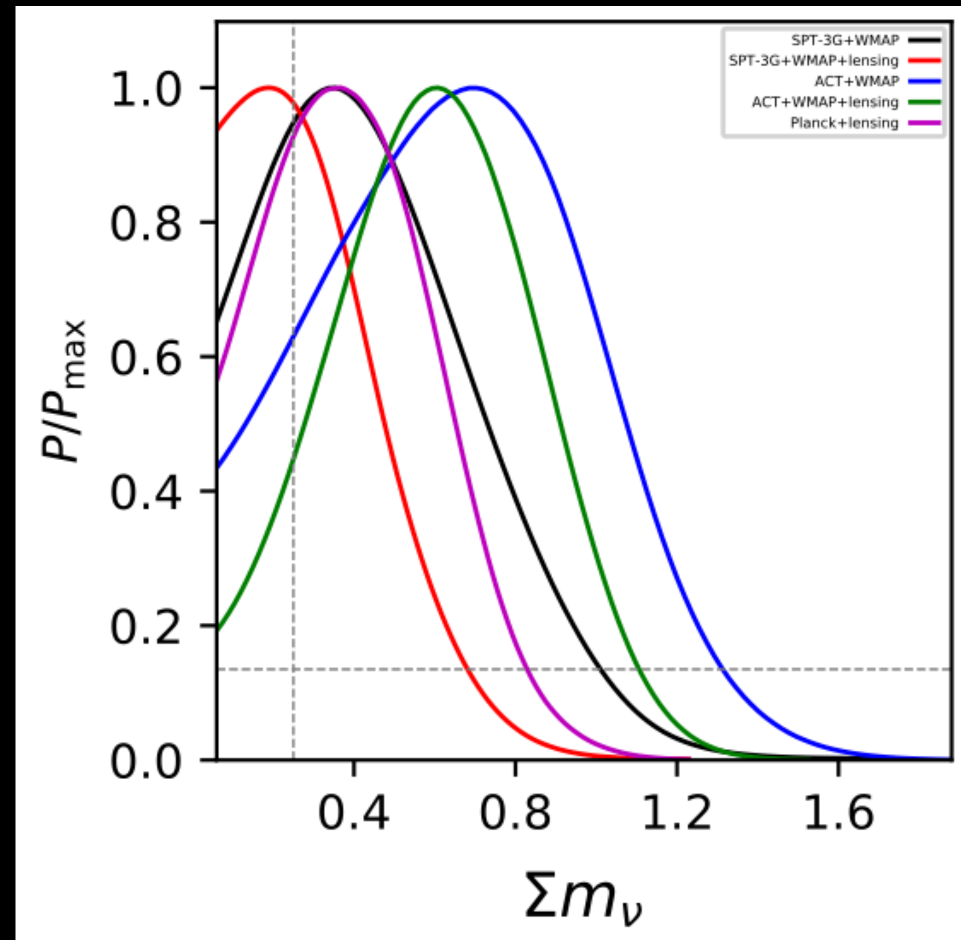

Di Valentino and Melchiorri, 2022 *ApJL* **931** L18

Constraints at 68% CL

Dataset	Σm_ν [eV]
ACT-DR4+WMAP+Lensing	0.60 ± 0.25
Planck+Lensing ($+A_{\rm lens}$)	$0.41^{+0.17}_{-0.25}$

While we have only an upper limit for Planck on the total neutrino mass, ACT-DR4, when combined with WMAP and lensing, prefers a neutrino mass different from zero at more than 95% CL.

Quantifying global CMB tension

Cosmological model	d	χ^2	p	$\log S$	Tension
ΛCDM	6	16.3	0.012	−5.17	$2.51\,\sigma$
$\Lambda\text{CDM} + A_{\text{lens}}$	7	18.5	0.00977	−5.77	$2.58\,\sigma$
$\Lambda\text{CDM} + N_{\text{eff}}$	7	13	0.0719	−3	$1.80\,\sigma$
$\Lambda\text{CDM} + \Omega_k$	7	16.5	0.0209	−4.75	$2.31\,\sigma$
wCDM	7	16.8	0.0187	−4.9	$2.35\,\sigma$
$\Lambda\text{CDM} + \sum m_\nu$	7	20.7	0.00421	−6.86	$2.86\,\sigma$
$\Lambda\text{CDM} + \alpha_s$	7	20.6	0.00448	−6.78	$2.84\,\sigma$
$w\text{CDM} + \Omega_k$	8	17.6	0.0249	−4.78	$2.24\,\sigma$
$\Lambda\text{CDM} + \Omega_k + \sum m_\nu$	8	21.2	0.00651	−6.62	$2.72\,\sigma$
$w\text{CDM} + \Omega_k + \sum m_\nu$	9	19.8	0.0195	−5.38	$2.34\,\sigma$
$w\text{CDM} + \Omega_k + \sum m_\nu + N_{\text{eff}}$	10	18.8	0.0434	−4.38	$2.02\,\sigma$
$w\text{CDM} + \Omega_k + \sum m_\nu + \alpha_s$	10	22	0.015	−6.01	$2.43\,\sigma$
$w\text{CDM} + \Omega_k + N_{\text{eff}} + \alpha_s$	10	20.9	0.0218	−5.45	$2.29\,\sigma$
$w\text{CDM} + \sum m_\nu + N_{\text{eff}} + \alpha_s$	10	31.1	0.000575	−10.5	$3.44\,\sigma$
$w\text{CDM} + \Omega_k + \sum m_\nu + N_{\text{eff}} + \alpha_s$	11	24.7	0.0102	−6.83	$2.57\,\sigma$

Di Valentino et al., MNRAS 520 (2023) 1, 210-215

$\Lambda\text{CDM} + N_{\text{eff}}$	Planck	–	2.92 ± 0.19
	ACT-DR4	–	$2.35^{+0.40}_{-0.47}$

If we now study the global agreement between Planck and ACT in various cosmological models that differ by the inclusion of different combinations of additional parameters, we can use the Suspiciousness statistic, to quantify their global "CMB tension".

We find that the 2.5σ tension within the baseline ΛCDM is reduced at the level of 1.8σ when Neff is significantly less than 3.044, while it ranges between 2.3σ and 3.5σ in all the other extended models.

Concluding

At this point, given the quality of all the analyses at play,
probably these tensions are indicating a problem with the underlying cosmology
and our understanding of the Universe,
rather than the presence of systematic effects.
Therefore, this is presenting a serious limitation to the precision cosmology.

Many models have been proposed to solve the H0 tension.
However, looking for a solution by changing the standard model of cosmology is challenging because of some additional complications:

1. The sound horizon problem
2. The S8 tension
3. The correlation between the parameters and possible fake detection
4. The hidden model dependence of some of the datasets (such as BAO)
5. The Planck AL problem
6. The role of the optical depth
7. The inconsistency between the different CMB experiment

Overall, the new DESI BAO data add an intriguing twist to the situation.

These cosmic discordances
call for new observations and stimulate the investigation of
alternative theoretical models and solutions.

ANOMALIES & TENSIONS IN COSMOLOGY • COSMOVERSE •

MENU

Thank you!

e.divalentino@sheffield.ac.uk

COSMOVERSE • COST ACTION CA21136

Addressing observational tensions in cosmology with systematics and fundamental physics

https://cosmoversetensions.eu/

WG1 – Observational Cosmology and systematics

Unveiling the nature of the existing cosmological tensions and other possible anomalies discovered in the future will require a multi-path approach involving a wide range of cosmological probes, various multiwavelength observations and diverse strategies for data analysis.

READ MORE

WG2 – Data Analysis in Cosmology

Presently, cosmological models are largely tested by using well-established methods, such as Bayesian approaches, that are usually combined with Monte Carlo Markov Chain (MCMC) methods as a standard tool to provide parameter constraints.

READ MORE

WG3 – Fundamental Physics

Given the observational tensions among different data sets, and the unknown quantities on which the model is based, alternative scenarios should be considered.

READ MORE

Latest H0 measurements

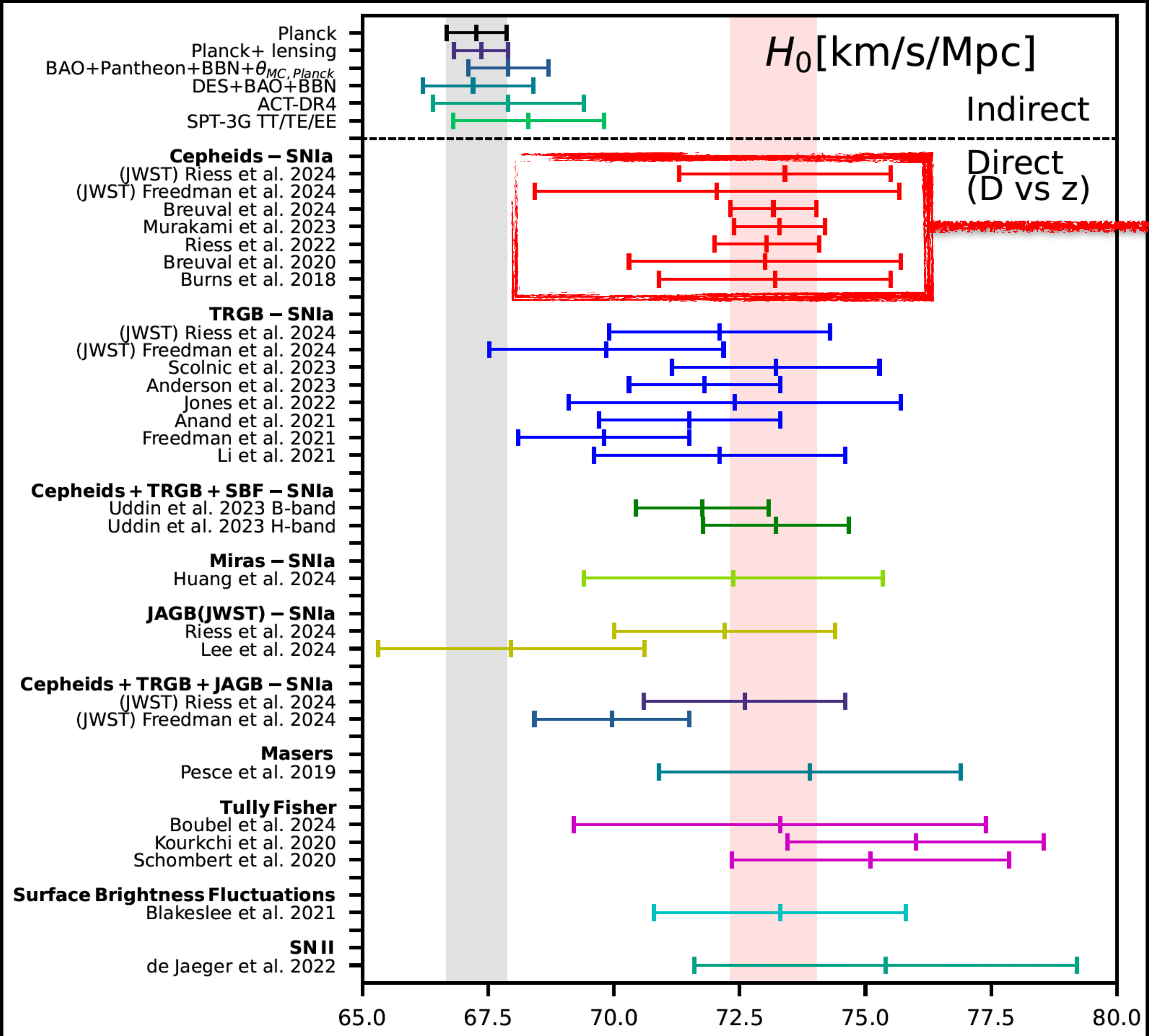

Cepheids-SN Ia:

H0 = 74.3 ± 2.1 km/s/Mpc

Riess et al., arXiv: *2408.11770*

H0 = 72.05 ± 3.62 km/s/Mpc

Freedman et al., arXiv:*2408.06153*

H0 = 73.17 ± 0.86 km/s/Mpc

Breuval et al., arXiv:*2404.08038*

H0 = 73.29 ± 0.90 km/s/Mpc

Murakami et al., arXiv:*2306.00070*

H0 = 73.04 ± 1.04 km/s/Mpc

Riess et al., arXiv:*2112.04510*

Di Valentino, *MNRAS* 502 (2021) 2, 2065-2073

Latest H0 measurements

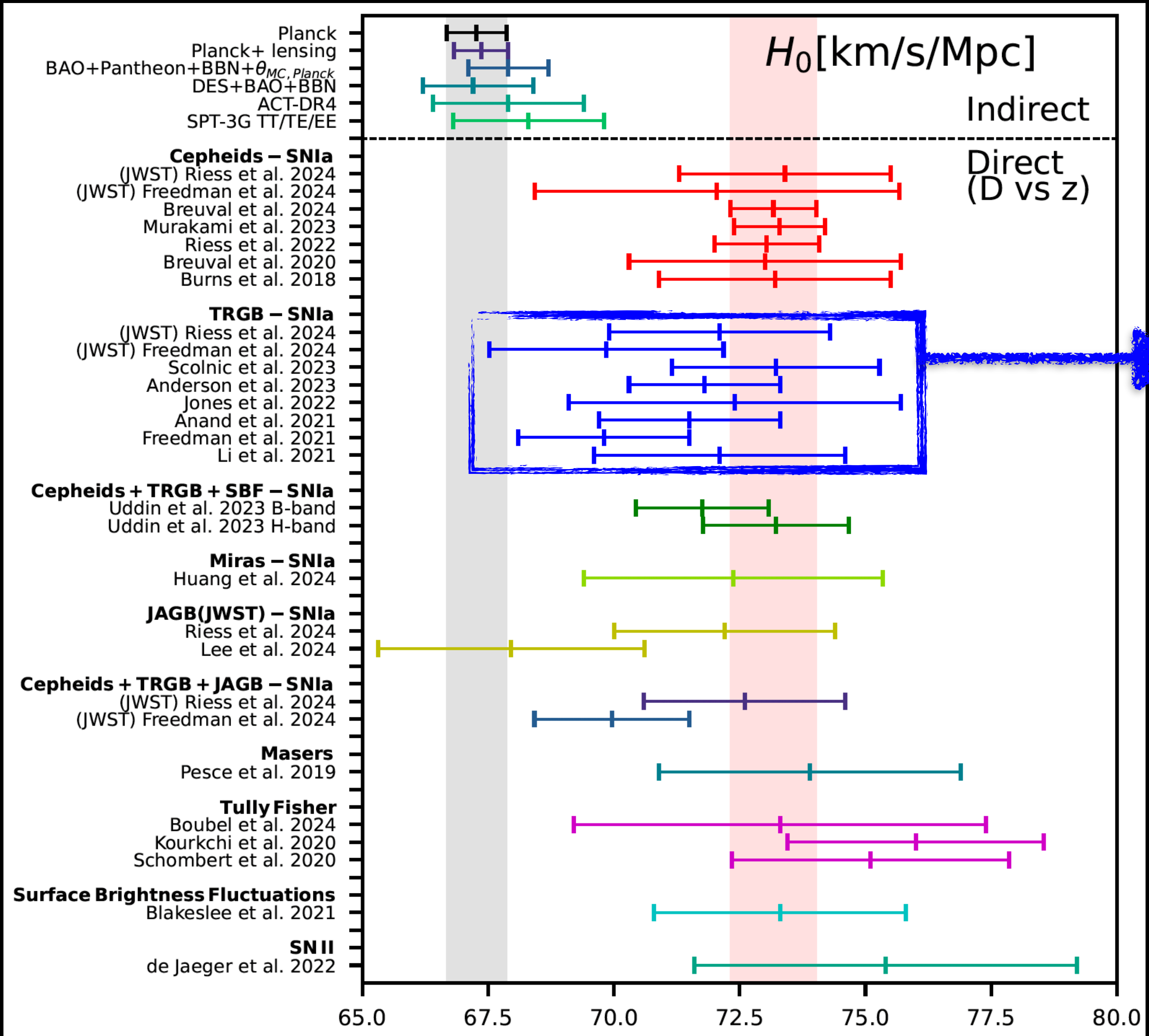

The Tip of the Red Giant Branch (TRGB) is the peak brightness reached by red giant stars after they stop using hydrogen and begin fusing helium in their core.

H0 = 72.1 ± 2.2 km/s/Mpc

Riess et al., arXiv: *2408.11770*

H0 = 69.85 ± 2.33 km/s/Mpc

Freedman et al., arXiv:*2408.06153*

H0 = 73.22±2.06 km/s/Mpc

Scolnic et al., arXiv:2304.06693

H0 = 71.8±1.5 km/s/Mpc

Anderson et al., arXiv:2303.04790

H0 = 69.8±1.7 km/s/Mpc

Freedman, arXiv:2106.15656

Di Valentino, *MNRAS* 502 (2021) 2, 2065-2073

Latest H0 measurements

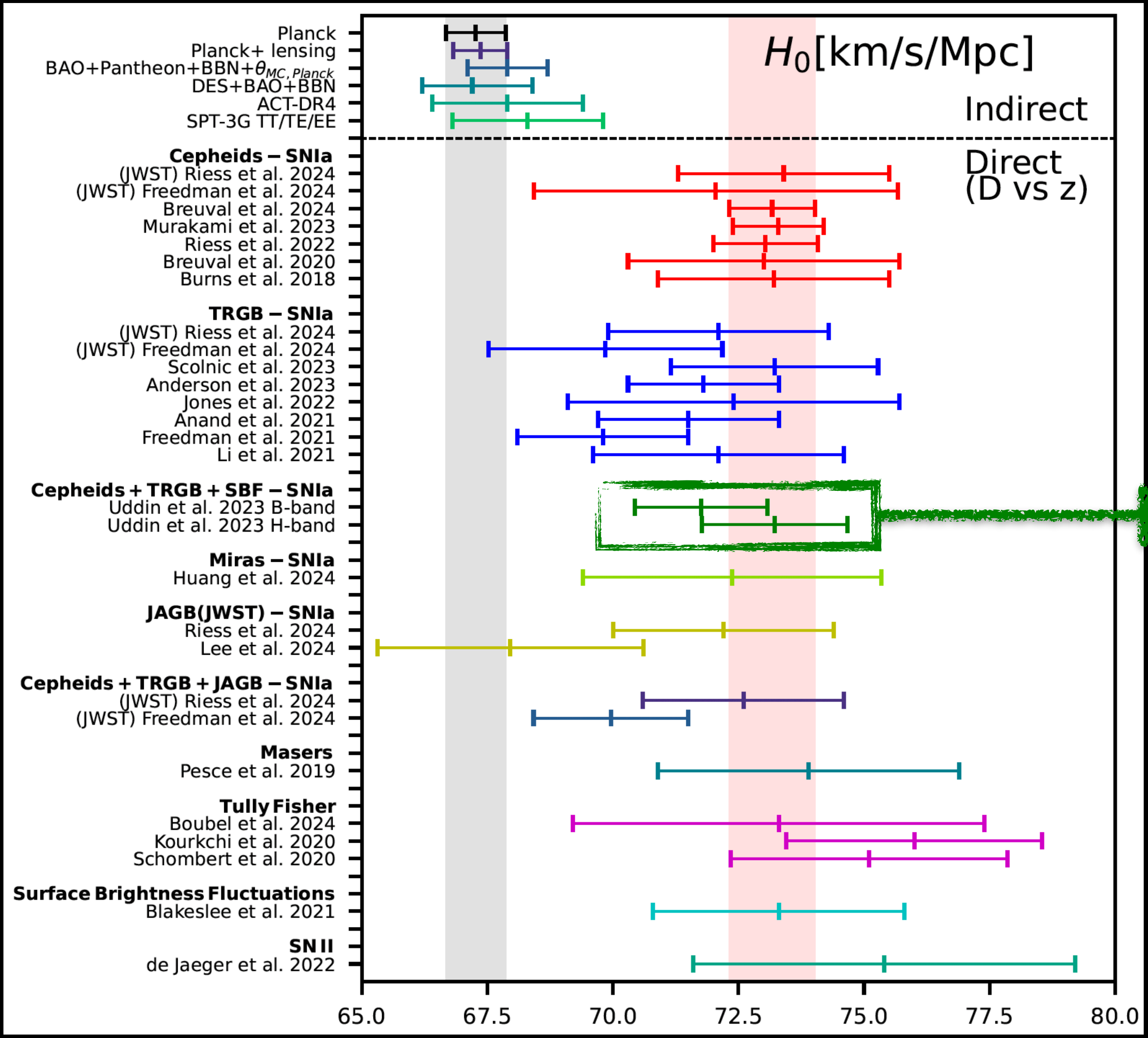

Carnegie Supernova Project:

Measurements of H0 using Cepheids, TRGB, and SBF Distance Calibration to Type Ia Supernovae

H0 = 71.76 ± 1.32 km/s/Mpc

H0 = 73.22 ± 1.45 km/s/Mpc

Uddin et al., arXiv:2308.01875

Di Valentino, *MNRAS* 502 (2021) 2, 2065-2073

Latest H0 measurements

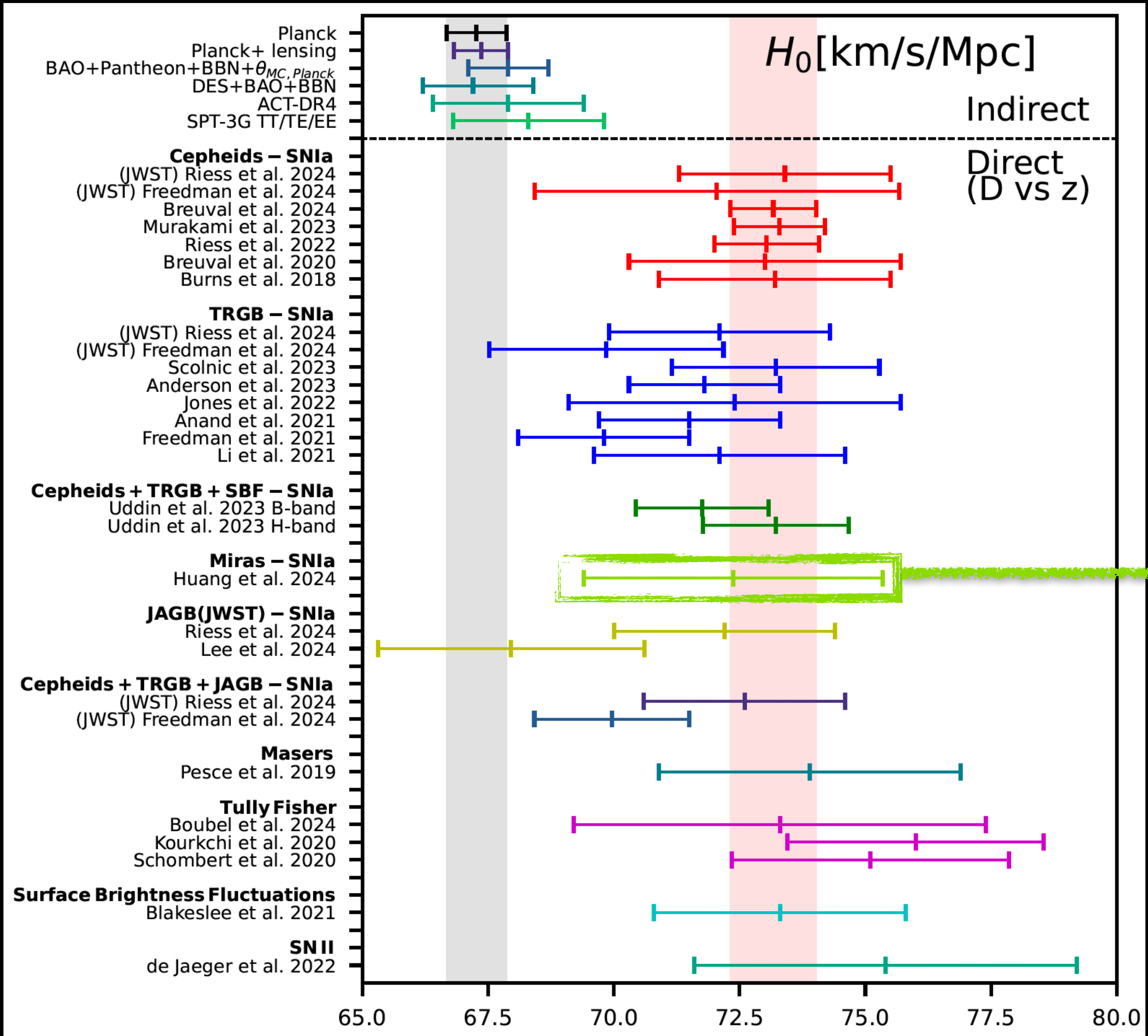

MIRAS
variable red giant stars from older stellar populations

H0 = 72.37 ± 2.97 km/s/Mpc

Huang et al., arXiv:2312.08423]

Di Valentino, *MNRAS* 502 (2021) 2, 2065-2073

Latest H0 measurements

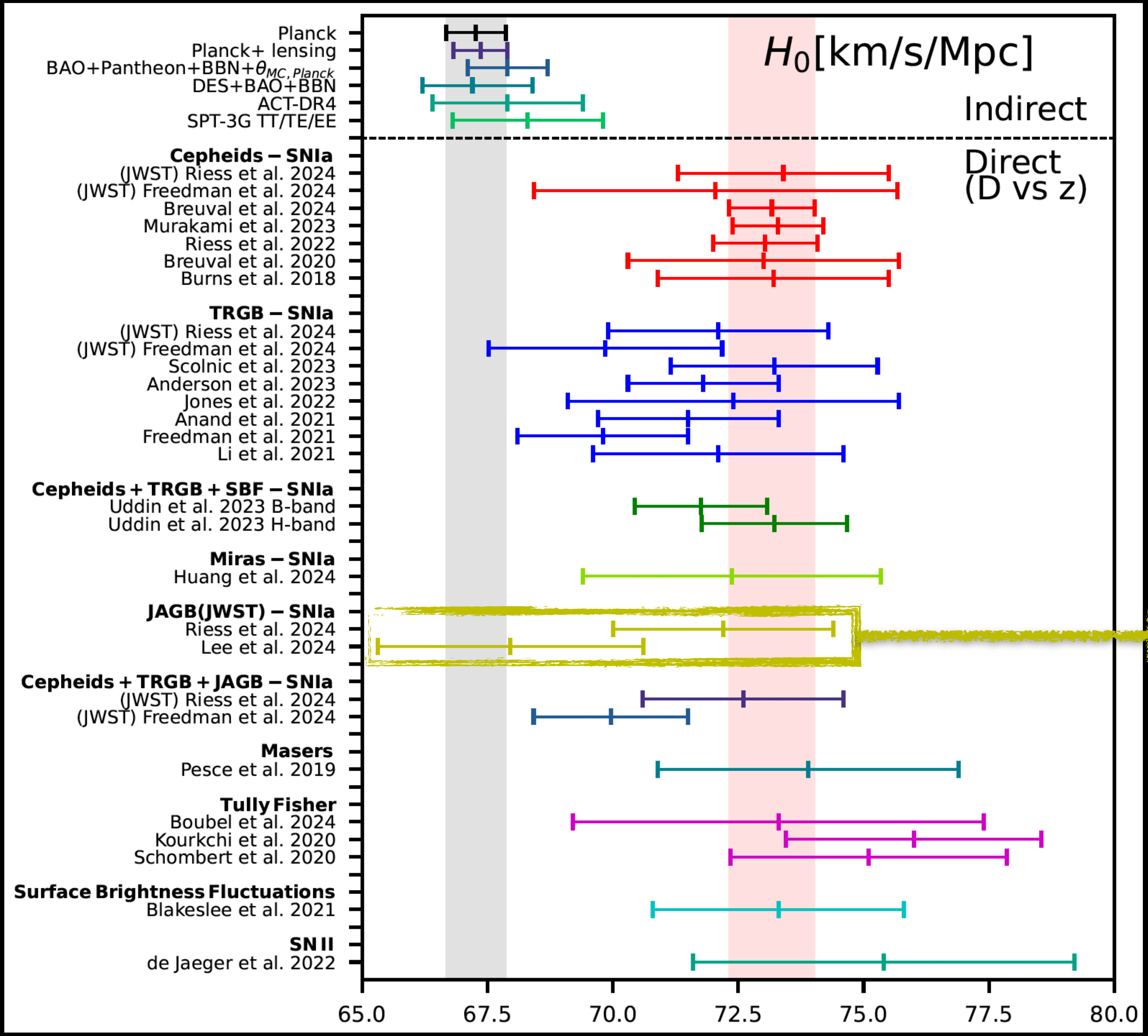

JAGB
The J-regions of the Asymptotic Giant Branch is expected from stellar theory to be populated by thermally-pulsing carbon-rich dust-producing asymptotic giant branch stars.

H0 = 72.2 ± 2.2 km/s/Mpc

Riess et al., arXiv: *2408.11770*

H0 = 67.96 ± 2.65 km/s/Mpc

Lee et al., arXiv:2408.03474

Di Valentino, *MNRAS* 502 (2021) 2, 2065-2073

Latest H0 measurements

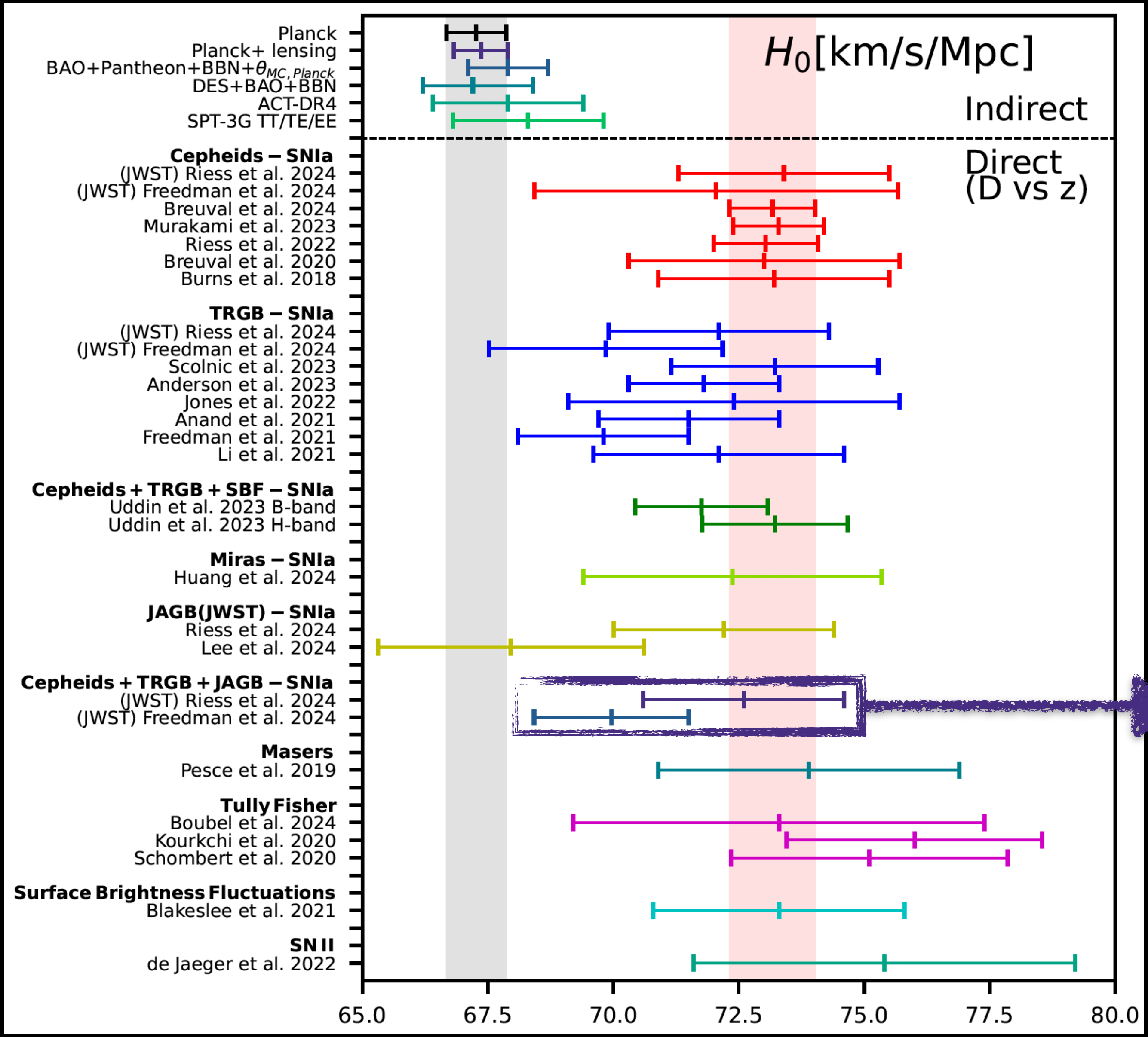

Measurements of H0 using Cepheids, TRGB, and JAGB Distance Calibration to Type Ia Supernovae from JWST

H0 = 72.6 ± 2.0 km/s/Mpc

Riess et al., arXiv: *2408.11770*

H0 = 69.96 ± 1.54 km/s/Mpc

Freedman et al., arXiv:*2408.06153*

Di Valentino, *MNRAS* 502 (2021) 2, 2065-2073

Latest H0 measurements

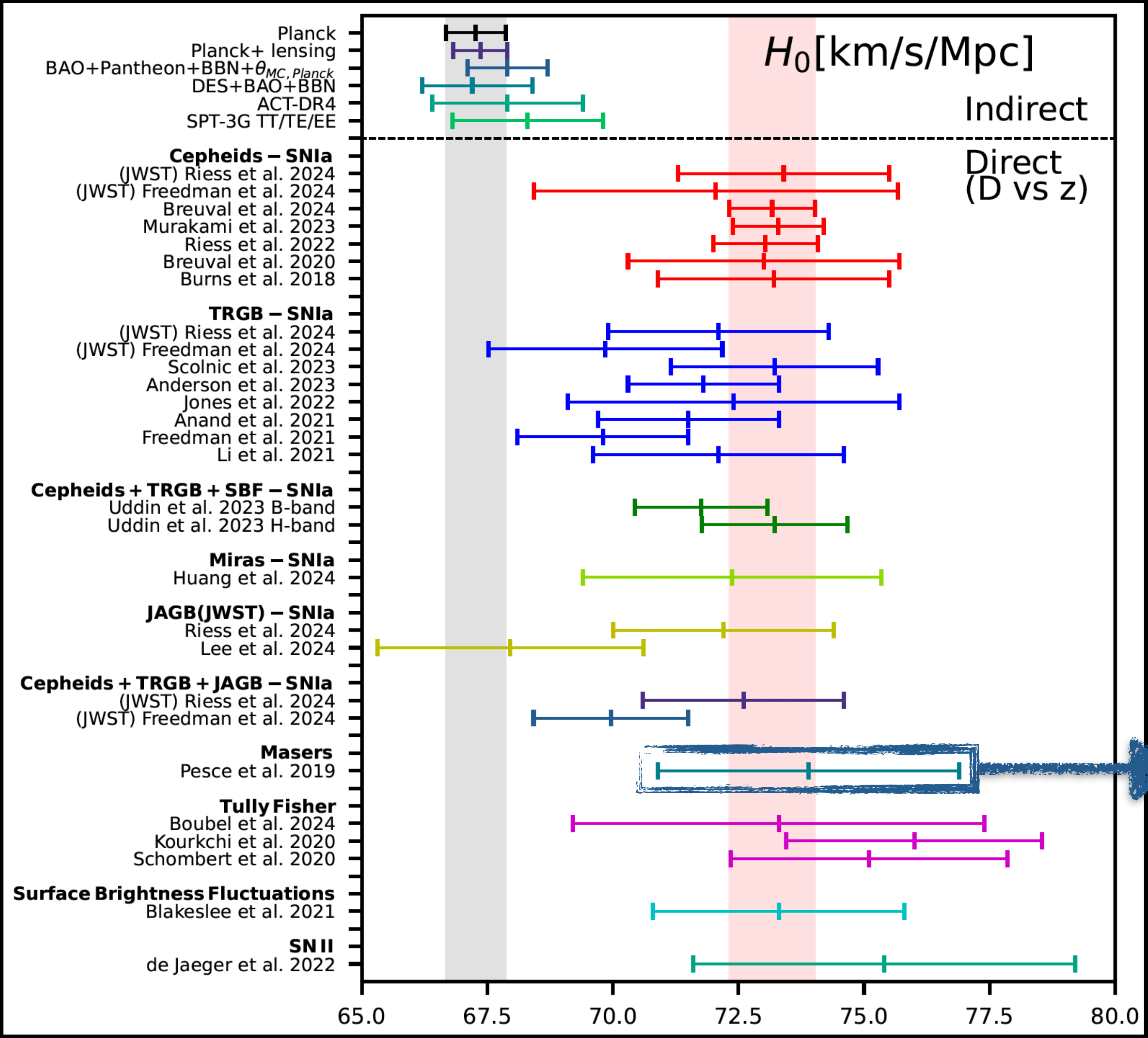

Di Valentino, *MNRAS* 502 (2021) 2, 2065-2073

H0 = 73.9 ± 3.0 km/s/Mpc

Pesce et al. arXiv:2001.09213

The Megamaser Cosmology Project measures H0 using geometric distance measurements to six Megamaser - hosting galaxies. This approach avoids any distance ladder by providing geometric distance directly into the Hubble flow.

Latest H0 measurements

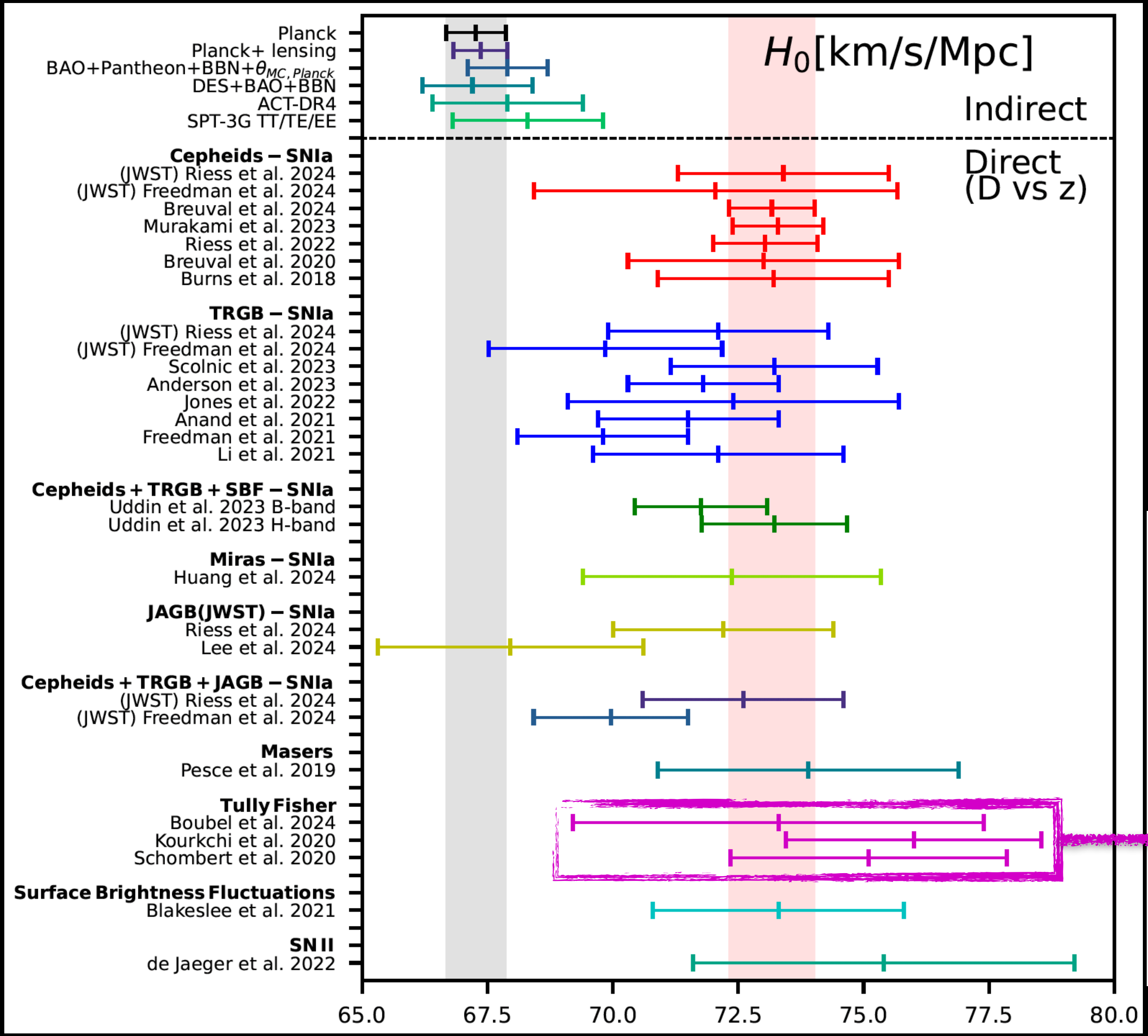

H0 = 73.3 ± 4.1 km/s/Mpc
Boubel et al. arXiv:2408.03660

H0 = 76.00 ± 2.55 km/s/Mpc
Kourkchi et al. arXiv:2004.14499

H0 = 75.10 ± 2.75 km/s/Mpc
Schombert et al. arXiv:2006.08615

Tully-Fisher Relation (based on the correlation between the rotation rate of spiral galaxies and their absolute luminosity or total baryonic mass, and using as calibrators Cepheids and TRGB)

Di Valentino, *MNRAS* 502 (2021) 2, 2065-2073

Latest H0 measurements

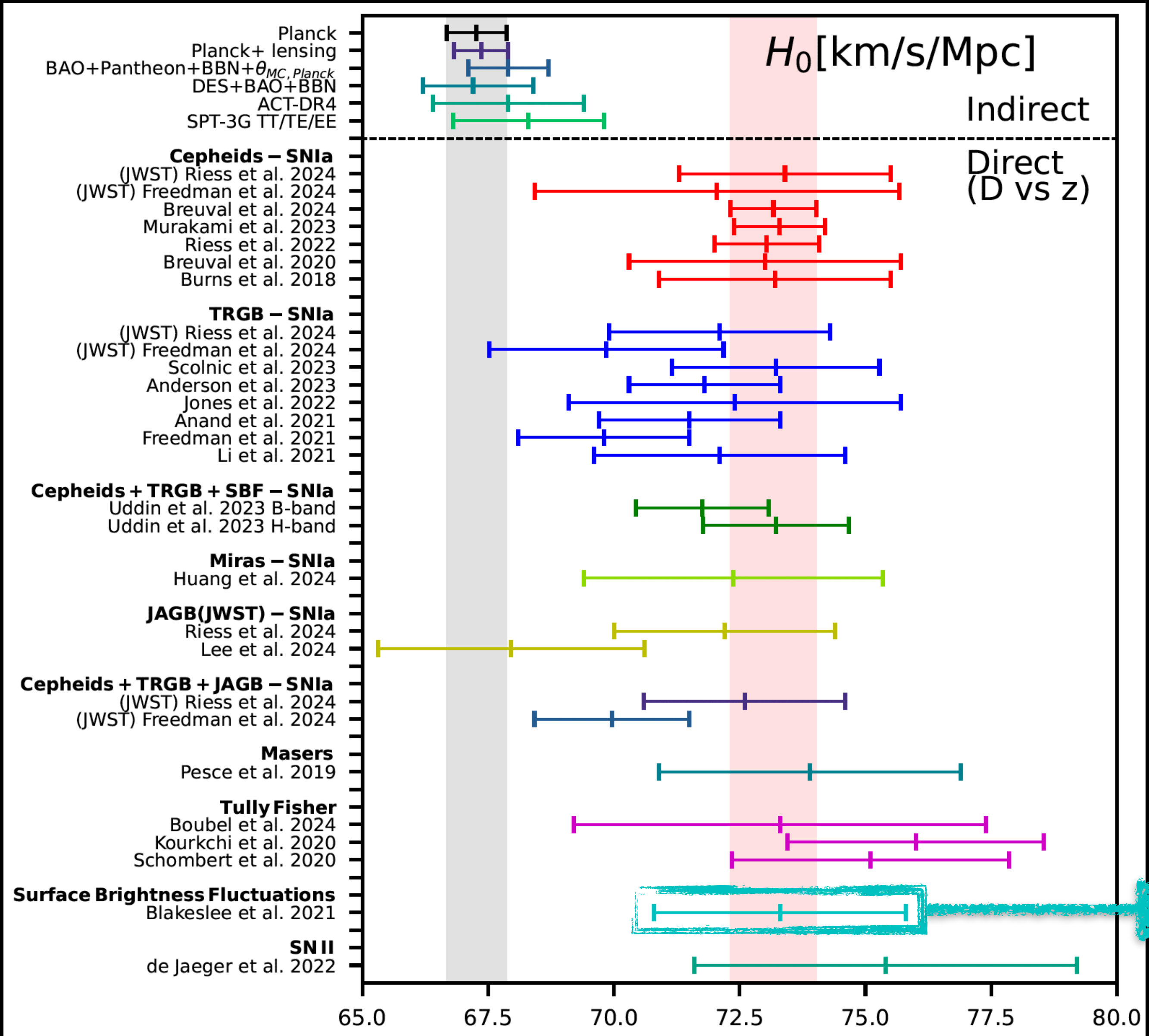

H0 = 73.3 ± 2.5 km/s/Mpc

Blakeslee et al., arXiv:2101.02221

Surface Brightness Fluctuations (substitutive distance ladder for long range indicator, calibrated by both Cepheids and TRGB)

Di Valentino, *MNRAS* 502 (2021) 2, 2065-2073

Latest H0 measurements

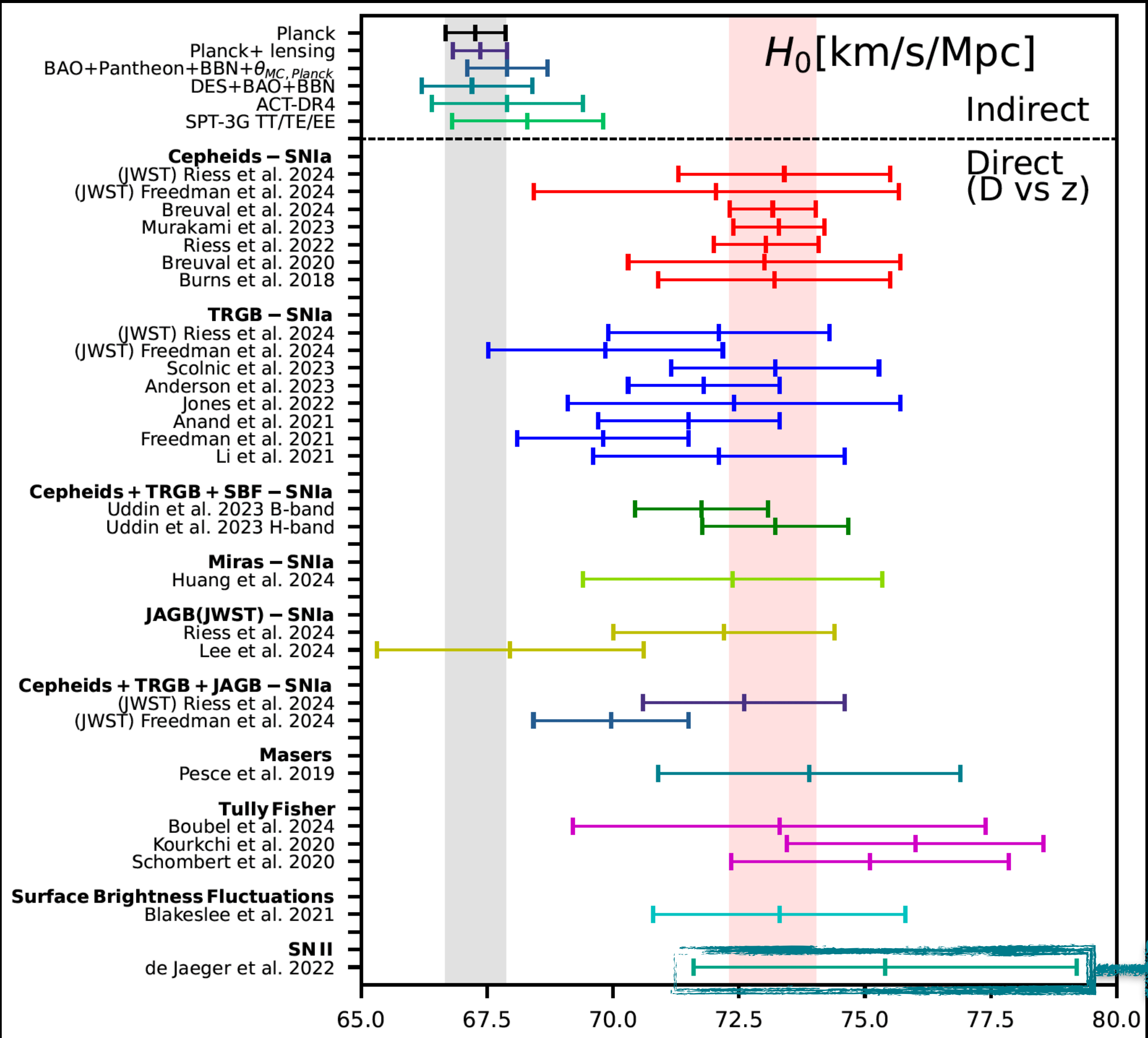

$H0 = 75.4^{+3.8}_{-3.7}$ km/s/Mpc

de Jaeger et al., arXiv:2203.08974

Type II supernovae used as standardisable candles and calibrated by both Cepheids and TRGB

Di Valentino, *MNRAS* 502 (2021) 2, 2065-2073

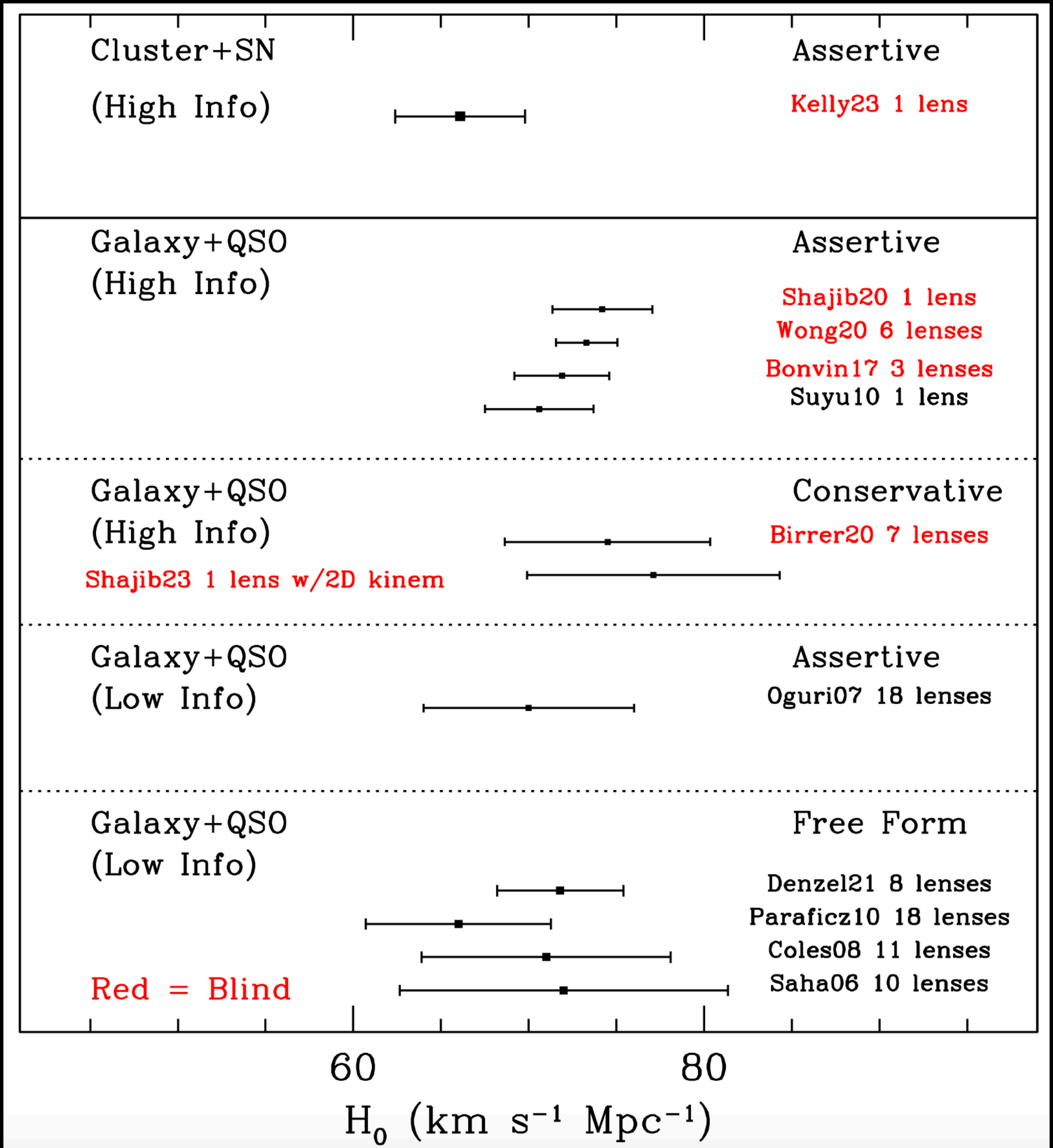

Treu and Shajib, arXiv:2307.05714

Measurements of the time delays of multiple images of quasar or SN systems caused by the strong gravitational lensing from a foreground galaxy.
Uncertainties coming from the lens mass profile.

Astrophysical model dependent

Late universe measurements since 2020

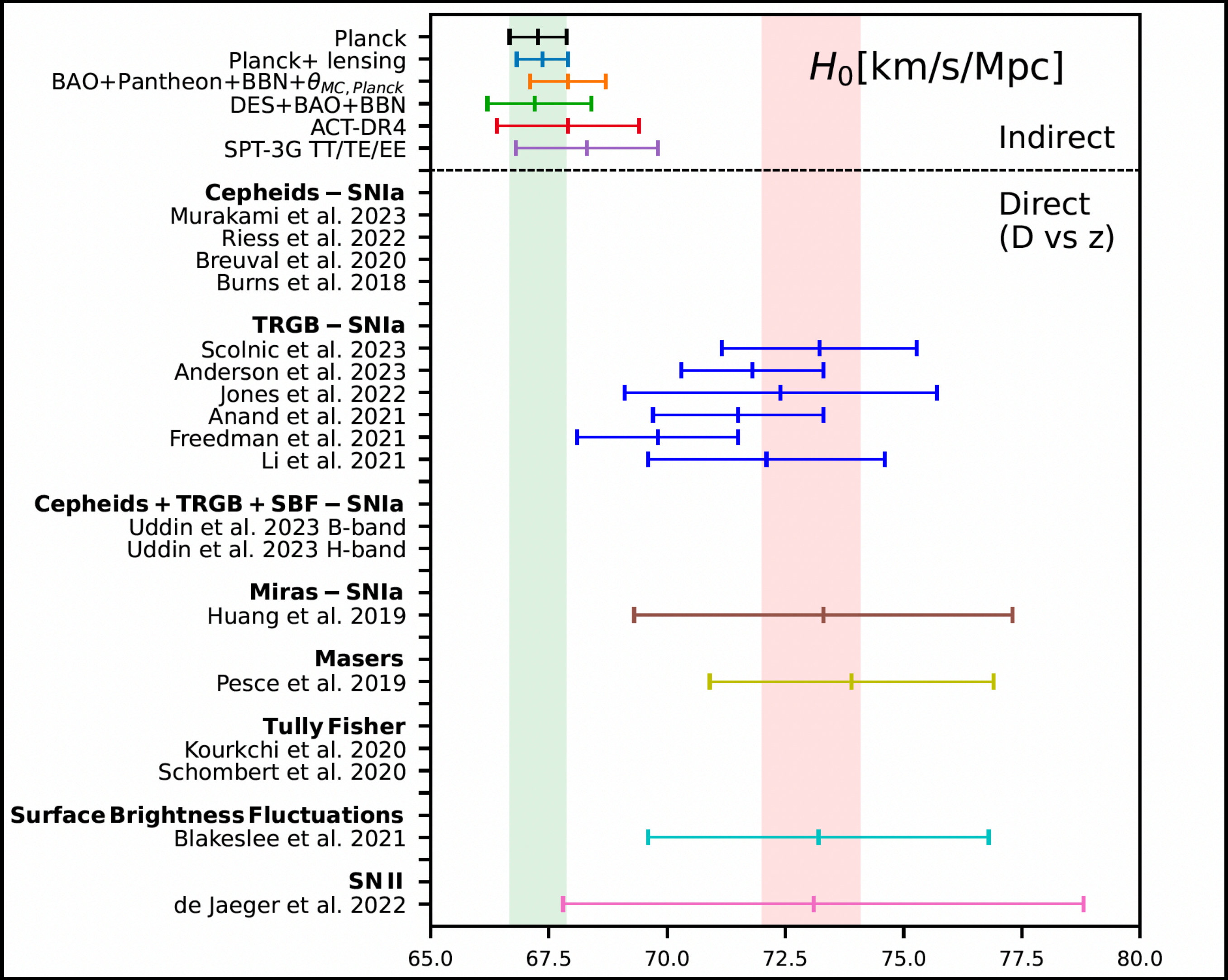

Cepheids independent

DES Y1 + KiDS-1000 from peak count statistics

4.1σ disagreement

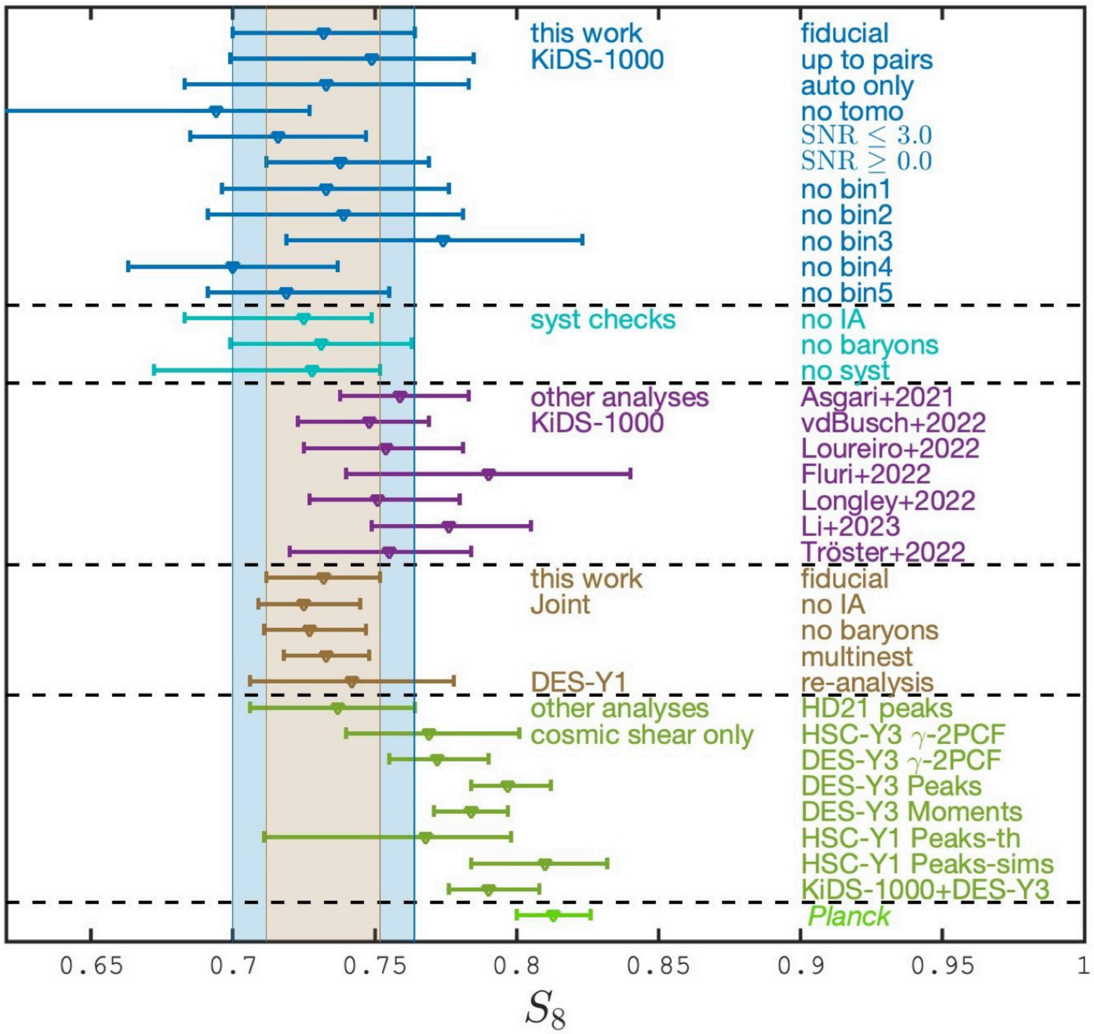

Figure 10. Summary of S_8 constraints from this work, from recent cosmic shear data analyses and from *Planck*. This figure shows the projected 1σ errors.

Harnois-Deraps et al., arXiv:2405.10312 [astro-ph.CO]

BAO measurements

To simplify let's consider an ensemble of galaxy pairs at a specific redshift z.

When the pairs are oriented across the line-of-sight,
a preferred angular separation of galaxies Δθ can be observed.
This allows us to measure the comoving distance DM(z) = rd/Δθ to this redshift,
which is an integrated quantity of the expansion rate of the universe.

$$D_{\mathrm{M}}(z) = \frac{c}{H_0} \int_0^z \mathrm{d}z' \frac{H_0}{H(z')}$$

The angular diameter distance will be DA(z) = DM(z)/(1 + z).

Conversely, when the pairs are aligned along the line-of-sight, a preferred redshift separation Δz can be observed. This measures a comoving distance interval that, for small values, provides a redshift dependent measurement of the Hubble parameter, represented by the equivalent distance variable DH(z) = c/H(z) = rd/Δz.

Hence BAO measurements constrain the quantities DM(z)/rd and DH(z)/rd.
This interpretation holds under standard assumptions and models similar to ΛCDM.
For measurements in redshift bins with low signal-to-noise ratios,
the angle-averaged quantity DV(z)/rd can be constrained,
where DV(z) is the angle-average distance that represents the average of the distances measured along and perpendicular to the line-of-sight.

$$D_{\mathrm{V}}(z) = \left(z D_{\mathrm{M}}(z)^2 D_H(z)\right)^{1/3}$$

DESI collaboration, arXiv:2404.03002